

---

# **Type IIb Kähler Moduli: Inflationary Phenomenology**

**Duncan Buck**



The University of  
**Nottingham**

Thesis submitted to the University of Nottingham  
for the degree of Doctor of Philosophy, January 2010

---

**Supervisor:** Prof. Edmund Copeland

**Examiners:** Dr. Beatriz de Carlos  
Dr. Paul Saffin

# Abstract

The inflationary paradigm of standard big bang cosmology provides a mechanism to generate primordial curvature perturbations and explain the large scale homogeneity and isotropy of the observable universe. This is achieved through requiring a period of accelerated expansion during the early universe and requires a deep understanding of particle physics for its correct formulation. With the emergence of string theory as a potential description of a fundamental laws of nature provides a the natural framework in which we can construct realistic models of inflation seems plausible. A common feature of string theories is the requirement of extra dimensions and, in the absence of a complete formulation of the theory, it is necessary to dimensionally reduce the theories to give a 4d effective theory. String compactifications provide a promising approach through which this can be done. However compactifications lead to the generation of a large number of massless scalar fields (moduli) which would mediate unobserved 'fifth forces'. Methods of stabilising these fields give rise to exponentially flat potentials which provide the means of obtaining inflation quite naturally. In the introductory chapters a review of Type IIb flux compactifications gives methods to stabilise the complex structure moduli and dilaton through the use of fluxes. In order to stabilise the Kähler moduli additional non perturbative corrections to the superpotential are required. We introduce the well know class of meta stable de Sitter string vacua obtained when such corrections are included. An additional class vacua at large volume are discussed, these are found when leading order perturbative corrections to the Kähler potential are also considered. The large volume vacua are then shown to give rise to a model of inflaton using a Kähler modulus as an inflaton field. We show that there exists a large class of inflationary solutions corresponding to a constant volume  $\mathcal{V}$  of the compactification manifold. In a second chapter on this inflationary model

the existence of a basin of attraction for inflation with a constant volume is described. We also find a larger class of inflationary solutions when we evolve the axionic components of the Kähler moduli and the phenomenological aspects are discussed. We finally review the standard slow roll analysis and discuss its use in multiple field inflationary models. We introduce two multiple field extensions to the standard single field slow roll approach. We proceed with an investigation into the suitability of the multiple field slow roll approaches in predicting the slow roll footprint of Supergravity models of inflation. This is achieved through comparing the results with single field results and numerical simulation data when more complex models are considered.

# Acknowledgements

First and foremost I am extremely grateful to my supervisor Edmund Copeland for the guidance and support he has shown me. His insight and passion for physics has helped encourage and inspire me throughout, and without him this thesis would not have been possible. I thank my collaborators Jose Blanco-Pillado, Marta Gomez-Reino and in particular Nelson Nunes for their detailed explanations, time and patience. I extend my thanks to all the physicists that I have had emailed, the time you spent clarifying my understanding of physics is greatly appreciated. I am thankful to my colleagues Graeme Candlish, Mark Brook, Rob Chuter and John Omotani for accompanying me throughout the PhD. In particular I would like to thank Ian Whiley and Mitsuo Tsumagari for their help on many issues but most of all their friendship.

Finally, my love and thanks goes to my family and friends. To my friends Freya, Ana and Charlie who have kept me inspired and smiling, I can not thank you enough for everything we have done together. Special thanks to my parents Mum and Stuart, and my sister Bryony your love has been a constant to which I can always turn to.

# Contents

<b>List of Figures</b>	<b>iii</b>
<b>List of Tables</b>	<b>v</b>
<b>TypeIIB Kähler Moduli: Inflationary Phenomenology</b>	
<b>1 Introduction</b>	<b>2</b>
1.1 Introduction and motivation . . . . .	2
<b>2 Moduli Stabilisation</b>	<b>9</b>
2.1 Introduction . . . . .	9
2.2 String Compactifications . . . . .	11
2.3 Flux Compactifications . . . . .	16
2.3.1 Type IIB orientifold compactifications . . . . .	17
2.4 Kähler Moduli Stabilisation . . . . .	20
2.5 KKLT . . . . .	23
2.6 Large Volume scenarios . . . . .	28
<b>3 Kähler Moduli Inflation</b>	<b>33</b>
3.1 Introduction . . . . .	33
3.2 The Kähler moduli potential . . . . .	35
3.3 Revisiting Kähler Moduli Inflation . . . . .	36
3.4 Single Field Kähler Moduli Inflation . . . . .	38
3.5 Full Kähler Moduli inflation . . . . .	41
3.5.1 Numerical evolution . . . . .	42
3.5.2 Example 1 . . . . .	43
3.5.3 Example 2 . . . . .	46
3.5.4 Example 3 . . . . .	48

3.5.5	Example 4 . . . . .	50
3.6	Conclusions . . . . .	52
<b>4</b>	<b>Basin of Attraction</b>	<b>54</b>
4.1	Basin of attraction . . . . .	54
4.1.1	Variation of parameters . . . . .	56
4.2	Evolving the Axions . . . . .	62
4.2.1	Comparison of Bond and Full Kähler Moduli Analysis . . . . .	63
4.3	Conclusions . . . . .	70
<b>5</b>	<b>Extended Slow Roll</b>	<b>72</b>
5.1	Introduction . . . . .	72
5.2	Standard Inflationary Cosmology . . . . .	74
5.3	Supergravity models . . . . .	78
5.3.1	Slow roll formalisms . . . . .	85
5.4	Comparative study of multiple field methods of slow roll inflation . . . . .	86
5.4.1	Chaotic Inflation in Supergravity . . . . .	87
5.4.2	Comparisons in Kähler Moduli Inflation . . . . .	94
5.5	Conclusions . . . . .	107
<b>6</b>	<b>Conclusion</b>	<b>113</b>
<b>Appendices</b>		
<b>A</b>	<b>Phase plane analysis</b>	<b>118</b>
<b>B</b>	<b>Slow Roll Conventions</b>	<b>123</b>
B.1	Kähler Metrics and Complex fields . . . . .	123
B.1.1	$\xi^2$ . . . . .	126
B.2	Supergravity models: Spectral index . . . . .	127
	<b>Bibliography</b>	<b>129</b>

# List of Figures

3.1	Evolution of the $\tau_2$ field in the last few e-folds in Example 1. . . . .	45
3.2	Evolution of the different moduli fields in the last few e-folds in Example 2. (a) Evolution of the field $\tau_1$ . (b) Evolution of the field $\tau_3$ . . . . .	47
3.3	(a) Evolution of the moduli field $\tau_2$ (the inflaton) in the last few e-folds in Ex- ample 2. (b) Amplitude of the density perturbations in the 10 observationally relevant e-foldings.. . . .	47
3.4	Evolution of the different moduli fields in the last few e-folds in Example 3. (a) Evolution of the field $\tau_1$ . (b) Evolution of the field $\tau_2$ . . . . .	49
3.5	Evolution of the different moduli fields in the last few e-folds in Example 3. (a) Evolution of the field $\tau_3$ . (b) Evolution of the field $\mathcal{V}$ . . . . .	50
3.6	Evolution of the different moduli fields in the last few e-folds in Example 4. (a) Evolution of the field $\tau_1$ . (b) Evolution of the field $\tau_3$ . . . . .	51
3.7	Evolution of the different moduli fields in the last few e-folds in Example 4. (a) Evolution of the field $\tau_2$ (the inflaton). (b) Evolution of the field $\mathcal{V}$ . . . .	52
4.1	Contour plot of the scalar potential $V$ in the $(\tau_1, \tau_2)$ plane for fixed $\tau_3 =$ $\tau_3^{\text{local}}$ , for example 1 of chapter 3. The dashed line shows the trajectory which maintains volume $\mathcal{V}$ constant at this fixed $\tau_3$ . The trajectories plotted are $\theta_2^i = \theta_{2_{min}}$ (blue solid line) and $\theta_2^i \neq \theta_{2_{min}}$ (red dashed line). . . . .	57
4.2	Contour plot of the scalar potential $V$ in the $(\tau_1, \tau_2)$ plane for fixed $\tau_3 =$ $\tau_3^{\text{local}}$ , for example 2 of chapter 3. The dashed line shows the trajectory which maintains volume $\mathcal{V}$ constant at this fixed $\tau_3$ . The trajectories plotted are $\theta_2^i = \theta_{2_{min}}$ (blue solid line) and $\theta_2^i \neq \theta_{2_{min}}$ (red dashed line). . . . .	58
4.3	Contour plot of the scalar potential $V$ in the $(\tau_1, \tau_2)$ plane for fixed $\tau_3 =$ $\tau_3^{\text{local}}$ , for example 3 of chapter 3. The dashed line shows the trajectory which maintains volume $\mathcal{V}$ constant at this fixed $\tau_3$ . The trajectories plotted are $\theta_2^i = \theta_{2_{min}}$ (blue solid line) and $\theta_2^i \neq \theta_{2_{min}}$ (red dashed line). . . . .	59
4.4	Contour plot of the scalar potential $V$ in the $(\tau_1, \tau_2)$ plane for fixed $\tau_3 =$ $\tau_3^{\text{local}}$ , for example 4 of chapter 3. The dashed line shows the trajectory which maintains volume $\mathcal{V}$ constant at this fixed $\tau_3$ . In this example, the inflationary trajectory is essentially given by a combination of two fields. The trajectories plotted are $\theta_2^i = \theta_{2_{min}}$ (blue solid line) and $\theta_2^i \neq \theta_{2_{min}}$ (red dashed line). . .	60

- 
- 4.5 Comparison of Bond et al. analysis (dashed lines) and Full analysis (solid lines) for  $\tau_{2i} = 0.45$  and  $\theta_{2i} = (1/11, 1/12, 1/14)$  for the red, green and blue trajectories respectively. Trajectories using Bond style analysis.  $T_1$  and  $T_3$  fields are not evolved with all fields set to the global minimum values except for the initial displacement of the  $\tau_2$  and  $\theta_2$  fields. Allowing all the moduli fields to evolve in the full analysis we find significantly different trajectories. 64
- 4.6  $T_2$  plane for simulations using the full dynamical analysis of chapter 3 with an initially non-zero axionic component,  $\theta_{2i} = 1/13$ . Shown are trajectories with a variation of  $\tau_{2i} = (0.45, 0.46, 0.47, 0.48)$ . . . . . 65
- 4.7  $T_1$  plane for a number of simulations with an initially non-zero axionic component,  $\theta_{2i} = 1/13$ . This shows the variation of the trajectories for  $\tau_{2i} = (0.45, 0.46, 0.47, 0.48)$  . . . . . 66
- 4.8  $T_3$  plane for a number of simulations with an initially non-zero axionic component,  $\theta_{2i} = 1/13$ . This shows the variation of the trajectories with a variation of  $\tau_{2i} = (0.45, 0.46, 0.47, 0.48)$  . . . . . 67

# List of Tables

4.1	Location of the global minimum of the scalar potential and the order of the basin of attraction under variation of the flux generated superpotential term, $W_0$ . Tuning $W_0$ can lift the scale of the potential. The variation between the two volume scales $\delta\mathcal{V}$ is left unchanged $\delta\mathcal{V} \sim 23\%$ , since the overall volume at its minimum $\mathcal{V}_{min}$ and in the basin $\mathcal{V}_{basin}$ both scale similarly. . . . .	62
4.2	Location of the global minimum of the scalar potential (3.4) and the order of the basin of attraction under variation of leading order $\alpha'$ -correction $\xi$ and $A_2$ . . . . .	62
4.3	Location of the global minimum of the scalar potential (3.4) and the order of the basin of attraction under variation of $a_2$ . The separation of the inflationary basin and the global minimum can be significantly tuned with the value of $a_2$ . The uplift parameter $\beta$ required to obtain a dS vacua is roughly the same in each scenario. . . . .	63
5.1	Slow roll parameters for Kähler moduli inflation examples of chapter 3 obtained through single field, eigenvalue and extended formalisms. The eigenvalue formalism obtains predictions remarkably similar to the single field approximations for $\eta$ and $n_s$ whilst $\epsilon$ and $\frac{dn_s}{dln\kappa}$ are consistently larger, the latter resulting from the larger magnitude. The extended formalism gives inconsistent predictions with the requirement of removing 'heavy' fields from the calculations and is found to break down for example 4 for which the inflaton trajectory is highly curved in field space, and so the $\xi^2$ and $\frac{dn_s}{dln\kappa}$ terms have not been calculated for this particular example. . . . .	108

# **Kähler Moduli: Inflationary Phenomenology**

# Chapter 1

## Introduction

### 1.1 Introduction and motivation

What is the history of the universe? The realistic answer is that, in the absence of a fundamental theory of particle physics, prior to the era of Nucleosynthesis we can only speculate on the answer. However the observable universe provides us with many signposts to help us along the way. Our universe on scales larger than  $\sim 100Mpc$  is observed to be homogeneous and isotropic. This feature is useful as it suggests that our observations of the universe are roughly representative of the universe as a whole. However the universe on small scales constrains inhomogeneities such as galaxies and clusters. The cosmic microwave background (CMB), the imprint of the universe from a time when the universe was roughly 10000 times smaller than it is today also reveals these features. It is seen on the large scales to be homogenous and isotropic with a mean temperature of  $T_{cmb} \sim 2.7K$  whilst it reveals small scale anisotropies in the temperature distribution at the order of  $\sim 10^{-5}$ .

We arrive now at another question: what can give rise to the large scale homogeneity and isotropy in the universe? The most widely believed explanation is that the universe underwent a period of accelerated expansion in the early universe caused by a repulsive force, this is commonly referred to as a period of inflation. To understand the attractive qualities of inflation let us consider a universe that is homogenous and isotropic. We

can then use the Robertson Walker metric to describe the geometry of spacetime,

$$ds^2 = -dt^2 + a(t)^2 \left[ \frac{dr^2}{1 - \kappa r^2} + r^2 (d\theta^2 + \sin^2\theta d\phi^2) \right] \quad (1.1)$$

where  $a(t)$  is the scale factor, and  $\kappa$  is a constant and depends on the spatial curvature of the universe. Substituting the metric (1.1) into the Einstein equations,

$$R_{\alpha\beta} - \frac{1}{2}Rg_{\alpha\beta} = 8\pi GT_{\alpha\beta}, \quad (1.2)$$

where  $\alpha, \beta = 0, \dots, 3$  and  $R$  is the Ricci tensor, we arrive at the Friedmann equations

$$\left( \frac{\dot{a}}{a} \right)^2 = \frac{8\pi G\rho}{3} - \frac{\kappa}{a^2}, \quad (1.3)$$

$$\frac{\ddot{a}}{a} = -\frac{4\pi G}{3}(\rho + 3p). \quad (1.4)$$

The observable universe is measured experimentally to be spatially flat. Given (1.3) we arrive at the relation

$$\frac{\kappa}{a^2 H^2} = \frac{8\pi G}{3H^2} - 1 \equiv \Omega - 1, \quad (1.5)$$

where  $\Omega$  is the critical energy density and  $H = \frac{\dot{a}}{a}$  is the Hubble parameter. Assuming that the scale factor grows as a power law with time,  $a \sim t^p$  with  $p$  dependent on the matter dominating the evolution of the universe, we see that  $|\Omega - 1|$  diverges at late times, and so  $\Omega$  must have been extremely close to unity in the early universe. In a period of accelerated expansion we have  $\dot{a}(t) > \dot{a}_i$  for  $t > t_i$  which leads us to conclude that  $\Omega \rightarrow 1$  as  $t \rightarrow \infty$ . Inflation then provides an explanation for the observed spatial flatness. Let us now turn to the observed homogeneity and isotropy. For a light-like radial trajectory,  $dr = a(t)dt$  the maximum distance that can be covered over a time period defines the horizon,

$$d_H(t) = a(t) \int_{t_i}^t \frac{dt}{a} = a(t) \int_{a(t_i)}^{a_H} \frac{da}{\dot{a}H}. \quad (1.6)$$

This defines the maximum distance of regions of space which are causally connected. The horizon grows with time and so at the era of last scattering observations its homogeneity suggests the universe was causally connected on scales many orders of magnitude larger than the horizon. This issue is commonly referred to as the horizon problem. Inflation again provides a mechanism to solve this problem, since in an accelerated universe the horizon, after a period of inflation, is comparable to the causally

connected domain. The resolution of these two problems through a period of accelerated expansion is encouraging. Conversely a period of inflation requires the assumption that the universe underwent a period of accelerated expansion,  $\ddot{a} > 0$  caused by a repulsive force. Gravity however is an attractive force, causing the decelerated expansion of the universe. What then can be used to drive inflation? From (1.4) this can be satisfied when the equation of state is constrained to be,

$$p < -\frac{1}{3}\rho. \quad (1.7)$$

Clearly this can be achieved through a cosmological constant which has  $p = -\rho$ . However this is found to lead to eternal inflation since at late times the cosmological constant dominates and we have a late time accelerated expansion of the universe. Perhaps a more encouraging solution arises when we consider a scalar field,  $\phi$ . The action of a scalar field coupled to gravity is given by

$$S_\phi = \int d^4x \sqrt{-g} \left( \frac{1}{2} \partial^\alpha \phi \partial_\alpha \phi - V(\phi) \right). \quad (1.8)$$

Assuming we have a metric given by (1.1) we find the homogeneous scalar field to be a perfect fluid with energy density and pressure given by

$$\rho = \frac{1}{2} \dot{\phi}^2 + V(\phi), \quad (1.9)$$

$$p = \frac{1}{2} \dot{\phi}^2 - V(\phi). \quad (1.10)$$

With an appropriate choice of  $V(\phi)$  the conditions for a successful period of inflation (1.7) can then be satisfied. The simplicity of realising inflation with a scalar field with a suitable potential prompted the construction of many inflationary scenarios<sup>1</sup>. During its infancy there was significant freedom to create exotic potentials that could explain observable phenomena. Today we are presented with proposals for fundamental theories of particle physics which have significantly changed the inflationary cosmologist's approach to the model building.

The twentieth century gave rise to two major breakthroughs in our understanding of fundamental physics through the formulation of general relativity and quantum mechanics. These theories give us a description of physics in the large scale through general relativity which with its unification of space and time gives an elegant description

---

<sup>1</sup>For details on the history of inflation the reader is directed to some reviews on the subject of inflation [58, 59, 60].

of the gravitational force through the curvature of a dynamical spacetime. Quantum mechanics, on the other hand, describes the small scales of the universe and provides the framework in which macroscopic physics can be understood. Developments in the field of relativistic quantum mechanics (quantum field theories) have provided remarkable understanding of the fundamental forces of; electromagnetism, through quantum electrodynamics (QED) and the strong and weak nuclear forces through the theory of quantum chromodynamics (QCD). Quantum field theories remove the classical notion of particles describing them as fundamental excitations of fields. These obey specific symmetries and how each transforms determines the particle states their quanta describe. They can be either bosonic (integer spin fields) or fermionic (half integer spin fields) in type. On the bosonic side, the spin-0 field is a scalar field, a spin-1 is a vector field (gauge field) and a spin-2 requires a second rank tensor field. On the fermionic side, the half-integer-spin particles are described by spinors fields. They, however, have representations dependent on the properties of particles and space-time dimension of the theory. A spin-1/2 particle is described using a Lorentz/Dirac Spinor Field, these are 4-component spinors which describe the fermionic fields whilst for higher half-integer spin particles one requires more specific representations. Through QCD and QED we have a macroscopic understanding of three of the four fundamental forces of nature which can be grouped together to form the Standard Model which can be described by the  $SU(3) \times SU(2) \times U(1)$  gauge theory. However the standard model lacks the means to describe the gravitational force and our understanding of the laws of nature on a macroscopic level is incomplete and will continue to be so until a macroscopic theory of gravity can be found. A theoretical model of physics describing the physics of fundamental one dimensional extended objects has risen as a potential quantum theory of gravity. String theory was originally conceived as a macroscopic theory of the strong interaction, however through the development of QCD in the early 1970s and its success in describing the strong interaction, string theory was no longer required. This was in part due to the the technical problems associated with string theory; it required that there exist additional spatial dimensions and contained a massless spin two particle as the fundamental excitation of the string which experimental observations of the strong interaction did not observe. String theory was once again picked up by theorists as a potential quantum theory of gravity exactly for the existence of a massless spin

two particle which could be interpreted as the graviton. It has turned out that string theory can be even more than this and is thought to be a quantum theory which provides a unified description of all the fundamental forces. Whilst it is a promising candidate for a fundamental theory there is still a significant lack of understanding of the full theory. One signal of an incomplete theory was the discovery of 5 distinct string theories, each existing in 10 space-time dimensions. A curious type are called the "heterotic" string theories, which use a 26 dimensional bosonic string formalism for the left-moving string modes and a 10 dimensional supersymmetric string (superstring) formalism for the right-moving modes. The dimensional inconsistency between the left and right string modes leads to heterotic string theories containing only closed strings (a string with no end points, topologically closed strings are equivalent to a circle) whilst the other types can also contain open strings. The extra 16 dimensions of the left moving modes must be compactified on a specific torus, of which there are only two examples, corresponding to the Lie algebras,  $SO(32)$  and  $E_8 \times E_8$ , this choice leads to two distinct heterotic string theories. The remaining three types of string theories used the superstring formalism for both the left and right moving modes. This construction introduces the possibility of a 'handedness' or chirality to the theory, and gives rise to the two possibilities, type IIa where the left-moving and right-moving string modes are symmetric (the modes have the opposite handedness) and type IIb which is left-right asymmetric (same handedness). The final theory is found by modding out the left-right handedness symmetry of type II theories, leading to an unoriented string theory, called type I. It was later realised that these could all be related through various dualities of string theories, and in fact, there is a suggestion that the separate theories are unified in some as yet unknown 11 dimensional theory. We however take the view that in principle string theory will eventually overcome these obstacles and provide a complete understanding of particle physics and cosmology. Taking this approach we see the need for connecting the physics of string theory with the observable universe, or trying to come as close as possible. An obvious testing ground is through cosmology. More specifically through the formulation of string models of inflation. In fact the success of inflationary cosmology has been in its natural resolution of problems faced with the initial conditions in a decelerating universe which stem from the lack of understanding of the fundamental physics which gives rise to these initial conditions. In addition,

the inflationary paradigm gives a mechanism for the generation of the primordial inhomogeneities. The presence of which are essential in the explanation of the large scale structure in the universe. Through expansion, vacuum fluctuations of the scalar field responsible for inflation, the inflaton<sup>2</sup>, are stretched and become classical perturbations of the inflaton field on scales less than the Hubble radius [83]. It is clear that we should use a macroscopic picture to describe these fluctuations, since corrections arising from string theory will be translated into cosmological fluctuations. We will see in this thesis that string theory has many natural candidates for an inflaton field, the problems faced when constructing models of inflation, and the issues of obtaining suitable control of them.

In the second chapter, we will introduce the procedure of dimensional compactification, allowing us to dimensionally reduce the 10d string theories and give rise to 4d effective theories. Although compactifications leads to theories which have a greater connection to the observable universe, they will be shown to come with a large number of undetermined scalar fields which require stabilising. We review the methods which can achieve this, namely that of flux compactifications and by the introduction of perturbative and non-perturbative corrections. The resulting vacua that are obtained through these techniques are then discussed. In the third chapter, having developed the background framework that leads to de Sitter vacua in an 4d effective theory, we introduce a model of inflation where the candidate inflaton field is one of the scalar fields resulting from compactification. This model is studied in detail and is found to give rise to a class of quite general inflationary solutions. We extend this analysis further in chapter 4 and find the existence of an island of stability for inflationary trajectories which corresponds to a constant volume of the compactified space. Through displacement of axionic fields we find an additional class of inflationary trajectories. We conclude with a discussion on the phenomenological implications of this inflationary model. The work contained in chapters 3 and 4 is based on the paper [54] given in the references. In chapter 5 we discuss the validity of the standard slow roll formalism in the context of supergravity models of inflation. We then present two multiple

---

<sup>2</sup>The component responsible is not restricted to scalar fields, and could easily be vector fields [135], spinor fields [136] or something more exotic (see for example [137]). However the simplest choice is that of a scalar field.

field slow roll formalisms present in the current literature. Since there is no general consensus on which method of analysis is preferable, we proceed to carry out a comparative study of the two approaches. This is first investigated in a simple model of multiple field inflation and then is extended to the model of Kähler moduli inflation that plays a central role in both chapters 3 and 4. We find our results favour the eigenvalue formalism of [73]. We present in appendix A the procedure of determining the scaling solutions of a model through an autonomous phase plane analysis carried out by [77]. We illustrate the application of this procedure to supergravity models, which could provide a possible future project and a means to further understand the basin of attraction discovered in chapter 4. In appendix B we provide the conventions used in the slow roll formalisms of chapter 5.

# Chapter 2

## Compactifications, Moduli and Fluxes

This chapter reviews the basic concepts of string geometry and flux compactifications that provide a background to any modern string construction. Particular emphasis will be placed on the development of Large Volume string compactifications. The reader is guided to the valuable sources on string geometry [6, 7, 8], flux compactifications [10, 11] and models of string inflation [58, 60].

### 2.1 Type IIB string theory

Perturbative supersymmetric string theories all exist in a critical space-time dimension of 10, however observation of the world around us suggest that we only have 4 large dimensions and so it is clear there exists some disparity between the exotic world of string theory and the 'everyday' physics of the 4 dimensional standard model. The notion of additional dimensions to the 3 spatial and one temporal of our observable universe is often difficult to comprehend outside the world of mathematics and theoretical physics. However armed only with insight into the world we live in, one easily understands that these dimensions simply are not observed. From this the concept of removing these dimensions from low energy physics stems, with the notion of compactification arising as one possible solution. Compactifying higher dimensional theories is not something new arising from string theory, but was introduced through the 5 dimensional theory of Kaluza and Klein, see [2] for a modern perspective on these ideas. Kaluza first identified that one could unify two of the fundamental the-

ories of Nature, Einstein's relativity with Maxwell's theory of Electro Magnetism if one accepted flexibility in the dimensionality of spacetime and an additional spatial dimension was introduced [1]. All fields are independent of the additional dimension (this was later extended through the work of Klein to include dependence on the additional dimension) and the 5d space time is viewed as the product space  $M^4 \times S^1$ . The additional dimension,  $y$ , is made periodic,  $y = y + 2\pi$ , identifying this dimension topologically as a circle. Since all physics in  $M^4$  is independent of the additional dimension the observable universe does not 'see' it. Essential to the approach is the compactness condition of the additional dimension, allowing the 5d fields to be expanded in a Fourier series,

$$g_{\mu\nu}(x, y) = \sum_{n=-\infty}^{n=\infty} g_{\mu\nu}(x) e^{iny/l}, A_\mu(x, y) = \sum_{n=-\infty}^{n=\infty} A_\mu(x) e^{iny/l},$$

$$\phi(x, y) = \sum_{n=-\infty}^{n=\infty} \phi(x) e^{iny/l}, \quad (2.1)$$

where  $l$  is the size (or length) of  $y$  and  $n$  is the Fourier mode. If  $l$  is sufficiently small, in the low energy limit only the  $n = 0$  mode is retained in the expansion<sup>1</sup>. From these assumptions, taking additionally the scalar  $\phi = \text{constant}$ , one recovers 4d relativity interacting with electromagnetism,

$$g_{mn} = \begin{pmatrix} g_{\mu\nu} + A_\mu A_\nu & \phi^2 A_\mu \\ \phi^2 A_\nu & \phi^2 \end{pmatrix}. \quad (2.2)$$

We are then drawn to applying these ideas to the extra dimensions of string theory with the aim to somehow reduce the number of spatial dimensions of the theory to some product space,  $M_{10} = M_4 \times M_6$  in which a 4d effective theory can live,  $M_4$  representing our visible space with some decoupled physics theory residing in the compactification manifold,  $M_6$ . Compactification of the extra dimensions is not the only viable method, these extra dimensions could be large with our known universe existing on a bound surface in a higher dimensions bulk. Such scenarios are known as Braneworlds and we direct the reader to some reviews on the topic [129, 85].

One interesting consequence of this form of compactification, is the preservation of the supersymmetry of string theory. Supersymmetry is a symmetry which if true dictates

<sup>1</sup>This effectively imposes the assumptions of the four dimensional fields being independent of  $y$ .

that every boson should have at least one fermionic partner and vice-versa. One of the main theoretical motivations behind supersymmetry is that it leads to unification of the gauge couplings at  $\sim 10^{16} GeV$ . The desirable qualities of supersymmetry have led to the development of supersymmetric extensions to the standard model which involve  $\mathcal{N} = 1$  supersymmetry, where  $\mathcal{N}$  is the number of gravitinos in the theory, one such theory is the minimal supersymmetric standard model (MSSM). However the absence of any signature of supersymmetry in current particle experiments suggests that the energy scale of supersymmetry lies somewhere above the experimental bounds on the lightest supersymmetric particle,  $M_{LSP} > 100 GeV$ , [130, 131]. One therefore requires that compactifications of string theories both preserve supersymmetry allowing for simplifications to the theory associated with obtaining the well understood supergravity theories and a means in which supersymmetry can be broken. Ideally a complete theory would identify the exact compactification required to recover the low energy physics of the standard model, however there exist a number of ways to compactify the different string theories in order to obtain the desired  $\mathcal{N} = \infty$  Supergravity in 4d Minkowski space, or of particular interest for this thesis in Type IIB string theories compactified on Calabi Yau manifolds.

## 2.2 Calabi-Yau compactifications

Compactifications provide the sufficiently controlled procedure for obtaining effective 4d supersymmetric theories from string theory. Supersymmetry is only preserved after compactification if the internal manifold is in fact complex, Kähler and Ricci-flat [5] and in the absence of any flux. We will later require flux to stabilise scalar fields present in the theory, the presence of flux has been shown to break the  $SU(3)$  structure of the Calabi Yau manifold. This fact has led to recent work concentrating on compactifications on generalised Calabi Yau manifolds [138] and more complex G-structure manifolds [139], we will not go discuss these further in this thesis. The supersymmetric preserving properties we are interested in are met by Calabi Yau manifolds,  $\mathcal{M}$

defined, commonly through [7, 8],

$$c_1 = 0 \tag{2.3}$$

$$R_{mn} = 0 \tag{2.4}$$

$$dJ = 0 \tag{2.5}$$

where  $m, n = 1, \dots, 6$  are the coordinates in the Calabi Yau space,  $c_1$  is the first Chern class,  $R_{\mu\nu}$  the Ricci tensor and  $J$  is the almost complex structure on the manifold  $M$ , where  $g_{mn} = J_m^l J_n^k g_{lk}$ <sup>2</sup>. The fact that supersymmetry is conserved on Calabi Yau spaces is a strong statement since it tells us that we have a covariantly constant spinor  $\nabla_m \eta = 0$ , where  $m$  are the coordinates on the internal manifold. The existence of such a spinor causes the vacuum values of the supersymmetry transformations to vanish and preserves supersymmetry after compactification [5]. It is found that, for each covariantly constant spinor present on the compactification manifold, there is one conserved supersymmetry in 4 dimensions. A Calabi Yau manifold has the property that it admits only one covariantly constant spinor [5]. Calabi Yau spaces are therefore natural manifolds on which to compactify string theories due to these properties, and Type II theories compactified on Calabi Yau 3-folds lead to preserving  $\mathcal{N} = 1$  supersymmetry [12].

Compactifications however come at a price, with a compactification giving rise to a number of massless scalar fields called Moduli, these are deformations of the compactification which leave the 4d effective theory invariant. Moduli are present in all generic compactifications and typically are of order  $10^{120}$  in number [38]. There are a number of different types of moduli; brane moduli, these are fields parametrising quantities such as the radial distance separating branes, metric moduli and axions. In addition to the moduli fields, string compactifications also always contain the dilaton,  $e^\phi$  a massless scalar field which is the remnant of the 10D worldsheet. It is the metric moduli that we will eventually use as a candidate inflaton and use throughout this thesis so let us study these in detail. The moduli correspond to fluctuations of the metric on the internal space and can be studied by infinitesimally perturbing the metric  $g_{mn} \rightarrow g_{mn} + \delta g_{mn}$ . Constraining the deformations to result in a new manifold which is

<sup>2</sup>This condition on the metric implies the metric is Hermitian, whilst the property that  $J$  is closed defines it as Kähler where  $J$  is the Kähler form.

still Calabi Yau corresponds to imposing that the manifold retains Ricci flatness under these deformations,

$$R_{mn}(g + \delta g) = 0. \quad (2.6)$$

Expanding this to first order, and imposing  $\delta g_{mn} = 0$ , we obtain the Lichnerowicz equation describing the solutions to all possible deformations  $\delta g$ ,

$$\nabla^l \nabla_l \delta g_{mn} - [\nabla^l, \nabla_m] \delta g_{ln} - [\nabla^l, \nabla_n] \delta g_{lm} = 0. \quad (2.7)$$

The solutions to this equation decouple into deformations of two types of Kähler manifolds; those of pure type  $\delta g_{\mu\nu}$  (or  $\delta g_{\bar{\mu}\bar{\nu}}$ ) and those of mixed type  $\delta g_{\mu\bar{\nu}}$ , where  $z^\mu, \bar{z}^{\bar{\mu}}$ , where  $\mu, \bar{\mu}$  take values 1, 2, 3 and  $\bar{1}, \bar{2}, \bar{3}$  and are the complex holomorphic co-ordinates of the Calabi Yau manifold,  $\mathcal{M}$  and their conjugates respectively with,

$$\delta g = \delta g_{\mu\nu} dz^\mu dz^\nu + \delta g_{\mu\bar{\nu}} dz^\mu d\bar{z}^{\bar{\nu}} + c.c. \quad (2.8)$$

Deformations associated with the mixed type correspond exactly with the harmonic (1,1) forms of the Calabi Yau,

$$\delta g_{\mu\bar{\nu}} \leftrightarrow \delta g_{\mu\bar{\nu}} dz^\mu \wedge d\bar{z}^{\bar{\nu}}, \quad (2.9)$$

and correspond to deformations of the Kähler form  $J$  of the manifold,

$$J = i g_{\mu\bar{\nu}} dz^\mu \wedge d\bar{z}^{\bar{\nu}} \longrightarrow i (g_{\mu\bar{\nu}} + \delta g_{\mu\bar{\nu}}) dz^\mu \wedge d\bar{z}^{\bar{\nu}}. \quad (2.10)$$

For this reason they are defined as Kähler moduli. We can expand the deformations of the Kähler form in the basis of harmonic 2-forms,  $\omega_i$ , where  $i = 1, \dots, h^{(1,1)}$ ,

$$J_{\mu\bar{\nu}} = t^i (\omega_i)_{\mu\bar{\nu}} \quad (2.11)$$

In compactifications of this type the parameters  $t^i$  are 4d scalars with their value giving the Kähler form  $J$  of the Calabi Yau manifold  $\mathcal{M}$ . In chapter 1 it was briefly mentioned that there exists 5 different string theories, in each of these there is an antisymmetric 2-form field  $B_2$  which arises in string compactifications [5]. After compactification this gives rise to a (1,1)-form  $B_{\mu\bar{\nu}}$  on the internal manifold  $\mathcal{M}$ . This has  $h^{(1,1)}$  zero modes and naturally combines with the Kähler form,  $J$  to give a complexified Kähler form  $\mathcal{J} = B + iJ$ . We can expand  $B$  in a similar basis of 2-forms,  $B = b^i \omega_i$  where

in the 4d theory  $b^i$  corresponds to  $h^{(1,1)}$  real scalar fields called axions in string theory. There are now  $h^{(1,1)}$  complex Kähler moduli fields which parameterise a Kähler cone, these are given by,

$$\rho^i = b^i + it^i. \quad (2.12)$$

Deformations of pure type are not so easily understood since the properties of the Calabi Yau ensures there are no (2,0) harmonic forms in which we can expand these deformations and, more simply, the symmetry of  $g_{\mu\nu}$  ensures this. If we then consider a pure deformation  $\delta g_{\mu\nu}$ , followed by a coordinate transformation  $f^m$  which causes the deformation to vanish then we have,

$$\delta g_{\mu\nu} = \frac{\partial \bar{f}^{\bar{\mu}}}{\partial z^\mu} g_{\bar{\mu}\nu} + \frac{\partial \bar{f}^{\bar{\mu}}}{\partial z^\nu} g_{\bar{\mu}\mu}. \quad (2.13)$$

This deformation leads to no new physics and cannot alter the pure coordinates of the metric  $g_{\mu\nu}$  which suggests that the coordinate transformation  $f^m$  can not be holomorphic. A non-holomorphic coordinate change would correspond to altering the complex structure of the Calabi Yau, and so deformations of the pure type are called complex structure moduli. These deformations are associated with complex harmonic (2,1) forms as,

$$\delta g_{\bar{\mu}\bar{\nu}} \leftrightarrow \bar{\Omega}_{\gamma\delta}^{\bar{\mu}} \delta g_{\bar{\mu}\bar{\nu}} dz^\gamma \wedge dz^\delta \wedge d\bar{z}^{\bar{\nu}}, \quad (2.14)$$

where  $\Omega_{\gamma\delta}^{\bar{\mu}} = g^{\bar{\mu}\nu} \Omega_{\gamma\delta\nu}$  an  $\Omega$  is a nowhere vanishing harmonic (3,0) form.

We can introduce a basis which will help describe the complex structure deformations in greater detail, defining the homology basis of 3-cycles,  $A^a, B_b$  and the dual cohomology basis by the 3-forms  $\alpha_a, \beta_b$ , where  $a, b = 1, \dots, h^{2,1} + 1$  and we have

$$\int_{A^b} \alpha_a = - \int_{B_a} \beta^b = \delta_a^b, \quad (2.15)$$

$$\int_{\mathcal{M}} \alpha_a \wedge \beta^b = - \int_{\mathcal{M}} \beta^b \wedge \alpha_a = \delta_a^b. \quad (2.16)$$

It is possible to define a set of coordinates on the moduli space by considering the integral of the holomorphic three form over the 3-cycle basis. This gives the periods

$$z^a = \int_{A^a} \Omega, \quad F_b = \int_{B_b} \Omega, \quad (2.17)$$

where the function  $F(z)$  is commonly known as the prepotential and is a function of the coordinates  $z^a$ ,  $F_b = \partial_a F$ , with the prepotential determining the Kähler potential and therefore the Kähler metric on the complex structure moduli space. This particular geometry is known as special geometry [8]. The coordinates  $z^a$  describe one direction more than the number  $h^{(2,1)}$ , however since they are defined only up to a complex rescaling of the holomorphic  $(3, 0)$ -form  $\Omega \rightarrow f(\phi_i)\Omega$  which can remove the additional coordinate. It follows from (2.17) that the complex structure moduli are described by these periods and  $\Omega$  can be expanded in terms of them,

$$\Omega = z^a \alpha_a - F_b \beta^b. \quad (2.18)$$

The parameter space of continuous deformations of the Calabi Yau manifold is called the moduli space and we have seen this is generated by a set of  $h^{(1,1)} + 2h^{(2,1)}$  real parameters, where  $h^{(p,q)} = \dim H^{p,q}(\mathcal{M})$  are the Hodge numbers of a manifold  $\mathcal{M}$  where  $H^{p,q}$  are the cohomology classes of the manifold [6]. We then see that since the moduli are in one-to-one correspondence with the harmonic forms on the Calabi Yau the number of geometric moduli in a compactification is completely determined by the cohomology of the manifold.

We have seen that compactifying string theory to a product space manifold where the internal manifold is a Calabi Yau is motivated through the phenomenologically attractive quality that such a manifold can preserve supersymmetry after compactification. Calabi Yaus therefore seem a natural space in which to formulate string theories with the hope that after compactification we are left with a low workable low energy aspects 4d  $\mathcal{N} = 1$  supergravity action. However there is no uniquely defined Calabi Yau manifold on which to compactify, and the moduli space of deformations associated with these compactifications is problematic due to the undesirably large number of moduli parameterising the space of continuous deformations which preserve Ricci flatness that come arise from these compactifications. These moduli are free scalar fields in the effective 4d theory, and if one couples with at least gravitational strength to the matter sector the theory would contain observable "fifth" forces at a range  $\sim \frac{1}{m_\phi}$ , where  $m_\phi$  is the mass of a typical moduli field. Experiments have so far tested the inverse square law down to the submillimeter scale with no observational evidence of its violation [3] requiring moduli to have masses  $m_\phi > 10^{-3}$ . Giving a vacuum expectation value to

these moduli would solve this problem, lifting the flat directions of the moduli space, and generating large masses for the moduli fields. We will see that fixing the masses of the moduli fields generically leads to the breaking of supersymmetry through a non vanishing superpotential term,  $W \neq 0$ , at the stabilised minimum. One could even use quantum corrections to the superpotential to do this and we will expand on this issue later in this chapter. One method of giving these moduli a vacuum expectation values is the process of flux compactifications, which we shall see generates terms in the 4d effective theory which can fix some of the moduli fields introduced in this section.

## 2.3 Flux Compactifications

Recent developments in string theory have focussed on the issue of using flux fields in string theory as a means of constructing flux vacua [19, 31, 12]. This involves moving to a warped background geometry in which there exists non-vanishing  $(p + 1)$ -form fields, where  $p = 1, 3, 5$  for Type II string theories. It is possible to construct string vacua through manipulation of the associated field strengths,  $F^{p+2}$  and compactifying on a manifold with non-trivial  $(p+2)$  cycles,  $\Sigma$ . Through identifying and wrapping the fluxes over cycles in the internal manifold there is an energetic cost which depends on the precise structure of the Calabi Yau metric leading to the generation of a potential for the complex structure moduli introduced in the previous section. From the 4d perspective, the generation of a potential dependent on the moduli allows these fields to be fixed and integrated out of the theory, alleviating the problems characteristic of allowing these fields to evolve. The use of fluxes in compactifications has been a fruitful area of research with the inclusion of sources such as branes leading to the violation of the no-go theorems of [19] which had found that Type IIb string theory compactified on a compact and non-singular manifolds can never lead to de Sitter or Minkowski space (The case where  $p = 1$  or  $p = D - 1$  is allowed, where  $D$  is the spacetime dimension, however this gives a constant cosmological constant). In this section we will outline the use of fluxes in methods of compactification and will follow the IIb orientifold compactifications of Giddings et al [12]. A development of the basic framework of flux compactifications will provide insight into the mechanisms which lead to the stabilisation of the complex structure moduli and dilaton. From this we will

see the need for additional mechanisms through which the remaining Kähler moduli of the previous section can also be stabilised.

### 2.3.1 Type IIB orientifold compactifications

The no go theorems of Maldacena-Nunez mean that we are unable to work with the simple string theory action but instead must consider the case including orientifold limits. The orientifold compactifications of Giddings et al [12] provide a consistent solution to 10d supergravity with local sources which through a Kaluza-Klein type reduction allows for both a 10d or 4d effective theory perspective. This is an attractive feature of this construction, since the low energy description removes some of the problems associated with our understanding of the full 10d theory. Progress can then be made in significantly simpler and well understood model. The action of the 10d Type IIB string theory in the Einstein frame is

$$S_{IIB} = \frac{1}{2\kappa_{10}^2} \int d^{10}x \sqrt{-g} e^{-2S} \left( \mathcal{R} - \frac{\partial_\mu \tau \partial^\mu \tau}{2(\text{Im}\tau)^2} - \frac{G_3 \cdot \bar{G}_3}{12\text{Im}\tau} - \frac{\tilde{F}_5^2}{4 \times 5} \right) + S_{CS} + S_{loc} \quad (2.19)$$

where  $S_{CS}$ ,  $S_{loc}$  are respectively the Chern Simons term and contributions from additional sources.  $\kappa_{10}^2 = (2\pi)^7 \alpha'^4$  is the 10 dimensional Newton's constant. The combined three form flux is  $G_3 = F_3 + \tau H_3$  with  $H_3$  the Neveu-Schwarz field strength with potential  $B_2$  and the Ramond-Ramond field strengths are  $F_{1,3,5}$  with corresponding potentials  $C_{0,2,4}$ . The axion dilaton is given by  $\tau = C_0 + ie^{-\Phi}$ . The five form flux field,

$$\tilde{F}^5 = F_5 - \frac{1}{2} C_2 \wedge H_3 + \frac{1}{2} B_2 \wedge F_3, \quad (2.20)$$

is self dual and the constraint,  $*\tilde{F}_5 = \tilde{F}_5$  has to be imposed by hand in order to obtain a complete set of equations of motion. Identifying the fluxes with the co-ordinates of 3-cycles,  $\Sigma_{a,b}$  of the Calabi Yau leads to quantisation of the Flux given by,

$$\frac{1}{(2\pi)^2 \alpha'} \int_{A_a} F_3 = n_a \in \mathbb{Z} \quad , \quad \frac{1}{(2\pi)^2 \alpha'} \int_{B_b} H_3 = m_b \in \mathbb{Z} \quad (2.21)$$

In order to compactify the theory to four dimensions the Einstein frame metric takes the form of a warped product of flat 4d Minkowski space and a conformally flat Calabi Yau orientifold,

$$ds_{10}^2 = e^{2A(y)} \eta_{\alpha\beta} dx^\alpha dx^\beta + e^{-2A(y)} \tilde{g}_{mn} dy^m dy^n, \quad (2.22)$$

where  $\alpha, \beta = 0, \dots, 3$  and  $m, n = 4, \dots, 9$  and  $\tilde{g}_{mn}$  is the metric of the internal compactification manifold. This form is similar to the idea of KK compactification, where here we allow for the possibility of a warp factor  $A(y)$ . We impose the conditions  $\tau = \tau(y)$  and  $\tilde{F}_5 = (1 + *)d(e^{A(y)}) \wedge dx^0 \wedge dx^1 \wedge dx^2 \wedge dx^3$  which relates the warp factor to the 5-form flux on the Calabi Yau orientifold. The Bianchi identity for  $\tilde{F}_5$  gives the constraint

$$d\tilde{F}_5 = H_3 \wedge F_3 + 2\kappa_{10}^2 T_3 \rho_3^{\text{loc}}, \quad (2.23)$$

which when integrated over the internal manifold  $\mathcal{M}$  leads to the tadpole cancellation condition

$$\frac{1}{2\kappa_{10}^2 T_3} \int_{\mathcal{M}} H_3 \wedge F_3 + Q_3^{\text{loc}} = 0, \quad (2.24)$$

where  $Q_3^{\text{loc}}$  is the total D3 charge coming from all localised sources. There are however additional sources to the D3 charge, in particular negative D3 charge and D7 branes, [11]. In F-theory compactifications, [18, 17] on a 4fold,  $X$ , it is found that the charge of these additional sources is related to the Euler characteristics<sup>3</sup>,  $\chi(X)$  and we then have, [4]

$$\frac{1}{2\kappa_{10}^2 T_3} \int_{\mathcal{M}} H_3 \wedge F_3 + N_{D3} - N_{\bar{D}3} = \frac{\chi(X)}{24}. \quad (2.25)$$

It is then seen that the number of  $D3$  branes present,  $N_{D3}$  may be varied dependent on the choice of discrete flux specified by (2.21), and this leads to a large choice of possible vacua. One may then over saturate the tadpole condition with the inclusion of localised sources on the background such as D-branes and orientifold planes. These localised sources invalidate the no go theorem since there is an associated energy momentum tensor which gives a negative contribution to the total energy momentum. We have introduced the basics of the 10d constructions of [12], these have been shown to restrict the form of compactification manifold through the tadpole condition (2.25). This result is an important one since the fluxes are related to the complex structure moduli through the  $G_3$  flux which is imaginary self dual,  $*_6 G_3 = iG_3$ . Supersymmetric solutions to this are harmonic (2,1)-forms [11], which we saw in section 2.2

<sup>3</sup>The Euler characteristic is a topological invariant of a manifold which in the case of a Calabi Yau is given by  $\chi(X) = 2(h^{(1,1)} - h^{(2,1)})$ .

correspond to the complex structure moduli. In the following chapters we will work in the low energy effective 4d,  $\mathcal{N} = 1$  supergravity description which results from compactification described above. In this perspective the fluxes generate a superpotential of Gukov-Vafa-Witten form [9].

$$W = \frac{1}{(2\pi)^2 \alpha'} \int_{\mathcal{M}} G_3 \wedge \Omega, \quad (2.26)$$

where  $\mathcal{M}$  is the internal manifold,  $G_3 = F_3 + \tau H_3$ ,  $\tau$  is the dilaton-axion  $\tau = C_0 + ie^\Phi$  and  $\Omega$  is the holomorphic  $(3, 0)$  form of the Calabi-Yau. It was seen earlier in this chapter that the complex structure moduli are completely determined by the periods of the holomorphic 3-form integrated over 3-cycles, (2.17) and we could expand  $\Omega$  in terms of the these periods. Since the complex structure moduli are identified with the  $h^{(2,1)}$  coordinates of  $z^a$  it is clear then that the generated superpotential depends on all of the complex structure moduli. There is an additional the axion-dilaton  $\tau$  dependence arising through  $G_3$ . The superpotential (2.26) however is independent of the Kähler moduli, present in all such compactifications suggesting they will remain unfixed. The Kähler potential is given as the sum of the contributions from the massless fields,  $\mathcal{K} = \mathcal{K}_T + \mathcal{K}_{CS} + \mathcal{K}_S$  which can be determined from the metric of moduli space deformations described in the previous section. This is given by the tree level Kähler potential [12],

$$\mathcal{K} = -2\ln[\mathcal{V}] - \ln[-i \int_{\mathcal{M}} \Omega \wedge \bar{\Omega}] - \ln(S + \bar{S}) \quad (2.27)$$

with the three terms arising from the Kähler moduli, the complex structure moduli and the dilation-axion respectively, and we have defined the dilaton field as  $S = i\tau$ .  $\mathcal{V}$  is the internal volume of the Calabi-Yau  $\mathcal{M}$ ,

$$\mathcal{V} = \int_{\mathcal{M}} J \wedge J \wedge J = \frac{1}{6} \kappa_{ijk} t^i t^j t^k \quad (2.28)$$

written in terms of the triple intersection number  $\kappa_{ijk}$  and the Kähler form, and where  $t_i, i = 1, \dots, h_{1,1}$  are the 2-cycle volumes introduced earlier in (2.11) which are related to the Kähler moduli  $T_i \equiv -i\rho^i \equiv \tau_i + i\theta_i$  through  $\tau_i$  the volume of 4-cycles

$$\tau_i = \frac{\partial \mathcal{V}}{\partial t^i} = \frac{1}{2} \kappa_{ijk} t^j t^k. \quad (2.29)$$

The standard  $N = 1$  supergravity potential is given by [10],

$$V = e^{\mathcal{K}} \left( \mathcal{K}^{i\bar{j}} D_i W D_{\bar{j}} \bar{W} - 3|W|^2 \right), \quad (2.30)$$

where  $i, j$  run over all moduli fields and  $D_i W = \partial_i W + (\partial_i \mathcal{K})W$ . Since in the flux compactification scenario of [12] the superpotential as we have noted has no dependence on the Kähler moduli,  $V$  becomes of no-scale type (i.e.  $\mathcal{K}^{T_i \bar{T}_j} \mathcal{K}_{T_i} \mathcal{K}_{\bar{T}_j} = 3$ ) then the scalar potential reduces to

$$V_{ns} = e^{\mathcal{K}} \left( \sum_{a, \bar{b}} \mathcal{K}^{a \bar{b}} D_a W D_{\bar{b}} \bar{W} \right), \quad (2.31)$$

where  $a, b$  run over the dilaton and complex structure moduli only. It follows that the scalar potential is now positive-definite with a global minimum at zero, and all fields expect for the Kähler moduli are fixed by the condition that the covariant derivative of the superpotential be zero,  $D_a W = 0$ . Solving these equations will lead to the stabilisation of the complex structure moduli and the dilaton. This can be achieved for a generic choice of fluxes through the use of the tadpole cancelation condition (2.25). Note that the minimum will be supersymmetric only if the contribution from the Kähler moduli is  $D_{T_i} W = W = 0$ , since non-zero contributions would lead to a ground state with negative energy. These results are encouraging, with the flux compactifications providing methods that lead to the stabilisation of a large set of moduli arising from string compactifications. However the Kähler moduli so far are still undetermined by flux compactifications at tree level and still require fixing. In the next section non perturbative corrections to the superpotential will be introduced which can lead to the successful stabilisation of the Kähler moduli.

## 2.4 Kähler Moduli Stabilisation

We saw in the previous section that through utilising fluxes and the compactification methods of [12] it is possible to stabilise the complex structure moduli through the generation of a superpotential of Gukov-Witten type (2.26). This generates terms in the scalar potential (2.30) dependent on these fields and it is then possible to integrate out these fields from the theory, giving them vacuum expectation values. Therefore providing a mechanism for stabilising a significant number of the moduli fields. Noticeably absent from the perturbative terms in the superpotential were the Kähler moduli fields, presenting a problem of how to stabilize these fields. Leaving these moduli undeter-

mined is a significant hinderance to string phenomenology since geometrically we have seen they correspond to the overall volume  $\mathcal{V}$  of the Calabi Yau manifold (2.28). This determines fundamentally important quantities such as the gravitino mass,  $m_{3/2} \sim \frac{M_p}{\mathcal{V}}$  and the string scale  $m_s \sim \frac{M_p}{\sqrt{\mathcal{V}}}$  [48]. The Kähler moduli are not stabilised at tree level since the conditions for unbroken supersymmetry are invariant under rescalings of the internal volume  $\mathcal{V}$  by a constant [68]<sup>4</sup>. Since the Kähler moduli at tree level are absent from the superpotential which is not renormalised in perturbative theory it is understood that Kähler moduli can only appear, and fortunately do appear at the nonperturbative level.

Recent progress has shown that non-perturbative effects like gaugino condensation<sup>5</sup> or D3-brane instantons can generate terms in the superpotential dependent on the Kähler moduli therefore providing a method of stabilization [23, 22]. The contribution to the superpotential is of the form  $\sum_{i=2}^n A_i e^{ia_i T_i}$ , where  $n = h^{(1,1)}$  is the number of Kähler moduli fields. One example of such a model where this type of construction is used is that due to Kachru, Kallosh, Linde and Trivedi [31], in which the inflaton is the moduli associated with the  $D3-\bar{D}3$  interaction potential. In such constructions the non-perturbative contributions to the superpotential breaks the no-scale form of the potential and, for general solutions, the scalar potential has a negative minimum. This is expected to give rise to a supersymmetric AdS Vacuum (as it corresponds to a negative cosmological constant). Thus it is common to add in additional terms that will 'uplift' the potential to a dS vacuum. One common way to do this is by adding in  $\bar{D}3$ -branes which generate potential terms that scale inversely with the internal volume of the Calabi-Yau (and therefore have some modular dependence).

The introduction of non perturbative effects will break the interesting property of the no-scale potential, namely that at  $V = 0$  at the supersymmetric minimum,  $D_i W = W = 0$  giving a vanishing cosmological constant. Generally since  $W \neq 0$  at the

---

<sup>4</sup>More specifically there is an exact shift symmetry in the axionic modes of the Kähler moduli for the classical action.

<sup>5</sup>An effect where the product of the gaugino fields  $\langle \lambda\lambda \rangle$  acquires a vacuum expectation value due to their strong coupling, this generally leads to breaking of the chiral symmetry, and can lead to breaking of the Supersymmetry. Gaugino condensation is similar to that of the quark-antiquark condensates of QCD [22].

minimum  $D_\rho \neq 0$  is non vanishing. This gives a mechanism for breaking supersymmetry whilst not generating a large cosmological constant. Ideally though the vacua constructed would not have any remaining flat directions due to unstabilised moduli. Non-perturbative effects can in fact lead to corrections to the superpotential which depend on the Kähler moduli and the currently known methods for generating the effects are through gaugino condensation on wrapped D7-branes in the presence of 3-form flux on 4-cycles [20, 21, 22] or through Euclidean D3-brane instantons, both generating corrections to the 4d superpotential of the form  $W_{np} \sim e^{-aT_i}$ , where  $T_i$  are the Kähler moduli introduced earlier and  $A_i, a_i$  are model dependent constants [16]. Gaugino condensation assumes the fluxes have fixed the moduli space in the region of the wrapping. If we consider a stack of  $N$  coincident branes wrapping one of the 4-cycles in the 4d theory we have a  $SU(N)$  Yang-Mills theory where the gauge couplings are dependant on the Kähler moduli [31]. If the gauginos live on these branes and undergo gaugino condensation in the groundstate, the resulting superpotential is [22]

$$W_{gc} = Ae^{-\frac{2\pi T}{N}}. \quad (2.32)$$

The coefficient  $A = N\Lambda^3$  is determined by the UV cutoff energy scale  $\Lambda^3$  below which the supersymmetric QCD theory becomes valid and the number of stacked D7-branes wrapping the 4-cycle,  $N$  [16]. Euclidean D3 brane instantons [23] can also lead to corrections to the superpotential of the form

$$W_{inst} = T(z^i)e^{-2\pi T} \quad (2.33)$$

which arises from the action of Euclidean D3 branes wrapping a 4-cycle in the compactification manifold. The use of instanton corrections are tightly constrained and requires exactly two fermionic zero modes, in order to generate a contribution to the superpotential [24]. In general every holomorphic cycle gives rise to an instanton term which requires topological restrictions to be imposed in order to ensure a non zero amplitude. A comprehensive review on the applications of instantons in type IIB compactifications see [24]. Both methods of producing Kähler moduli dependent terms for the superpotential give similar contributions and in general we will assume that the Kähler moduli appear as exponential terms in the superpotential.

In the Type IIB limit of weak coupling the leading order expansion of the Kähler moduli contribution to the Kähler potential is an expansion in terms of the inverse volume

[118, 44, 45]. These corrections to all orders are not well defined in string theory and are significantly less constrained than the corrections to the superpotential. We then run into a problem through the inclusion of non-perturbative corrections of the superpotential, as we should now theoretically include the perturbative terms as well. This is a common issue of theoretical physics called the Dine-Seiberg problem [46] which we will briefly outline to highlight this issue. Considering a typical modulus  $\phi$  such as the volume modulus or the inverse string coupling,  $g_s = e^{-\phi}$ , in the limit  $\phi \rightarrow \infty$  this corresponds to the weakly coupled limit and the tree level action may be trusted, whilst corrections to the modulus are expected to generate a potential term of the form

$$\lim_{\phi \rightarrow \infty} V(\phi) = 0 \quad (2.34)$$

which allows  $V$  to approach zero from above or below. If  $V(\phi) > 0$  then there is a runaway direction as  $\phi \rightarrow \infty$  whilst if  $V(\phi) < 0$  in this region then the modulus is pulled towards the strongly coupled limit. In order to fix these problems and generate a local minimum higher order corrections must be included. Since the corrections are required to significantly alter the form of  $V(\phi)$  they must be calculated in the strong coupling limit where all corrections may give significant contributions. Therefore in order to justify the inclusion of the nonperturbative superpotential contributions there are two possible ways of proceeding. The first, is to check the necessity of including corrections to all orders which we will come to shortly and provides the basic motivation for a class of Large Volume string vacua [44] which will be studied in the later chapters of this thesis. The second and that followed by the infamous construction of Kachru, Kallosh, Linde and Trivedi [31] is to allow control over the form of the Kähler potential through an appropriate tuning of parameter space for which the perturbative corrections can be ignored. We now turn our attention to that example.

## 2.5 The vacua of KKLT

In the model of Kachru, Kallosh, Linde and Trivedi [31] (KKLT) a method for constructing metastable de Sitter vacua is proposed. This is achieved through application of all the techniques reviewed so far in this chapter. Flux compactifications and non-

perturbative corrections to the superpotential are used to first stabilise all the moduli fields in a supersymmetric Anti de Sitter vacua in a controlled manner. The introduction of additional sources then provides a means to successfully break supersymmetry and obtain de Sitter vacua. The model first considers the superpotential generated through the flux compactifications of [12] studied in section 2.3 given by (2.26). The non-perturbative contribution to (2.26) is considered to be small compared to the tree-level flux term allowing us to integrate out the complex structure and dilaton fields through solving  $D_a W = 0$ . The complex structure moduli are then frozen out and receive typical masses of the order  $m_{cs} \sim \mathcal{O}(\frac{m_s}{\sqrt{V}})$ , [16]. Since the Kähler moduli are massless at tree level it is consistent to integrate out the complex structure moduli. Setting them to their vacuum expectation values allows us to investigate the low-energy effective theory where only the unfixed Kähler moduli need be considered. Considering only one Kähler modulus,  $T$  describing the overall volume  $\mathcal{V} = (T + \bar{T})^{3/2}$ , the superpotential is then given by

$$W = W_{flux} + W_{np} = W_0 + Ae^{-aT}, \quad (2.35)$$

with  $W_{flux} = W_0 = \text{constant}$  and  $A, a$  are constants dependent on the mechanism used to generate the non-perturbative corrections. Absorbing the complex structure and dilaton contributions to the Kähler potential given by (2.27) as  $\mathcal{K}_{cs} = \text{constant}$  leaves us with a Kähler potential which is still of no-scale type,

$$\mathcal{K} = \mathcal{K}_{cs} - 3\ln(T + \bar{T}). \quad (2.36)$$

The supersymmetric minimum of the potential (2.30) is found by solving  $D_T W = \partial_T W + \partial_T \mathcal{K} W = 0$ , from which the location of the minimum is given by

$$-aAe^{-aT} - \frac{3}{T + \bar{T}}(W_0 + Ae^{-aT}) = 0. \quad (2.37)$$

The non-perturbative contributions to  $W$  break the interesting property that the supersymmetric minimum lies at  $V = 0$ , which corresponds to a vanishing cosmological constant. The  $V = 0$  supersymmetric minimum suggests a conceivable way of breaking supersymmetry whilst generating the almost vanishing cosmological constant. However the non-perturbative corrections break the no-scale structure (2.31) of the potential, and the supersymmetric minimum corresponds to an anti de Sitter vacuum, with negative vacuum energy density. The potential at the minimum is given

by,

$$V_{AdS} = -3e^{\mathcal{K}}|W|^2 = -\frac{a^2 A^2}{6T}e^{-2aT}. \quad (2.38)$$

From this we can take a few important ideas. The inclusion of the non perturbative corrections provides a mechanism to stabilise the Kähler moduli however the resulting susy minimum is AdS. This AdS minimum is quite generic [31], with perturbative corrections to the Kähler potential still giving a SUSY minimum that solves (2.37). Looking at (2.37) the volume modulus is stabilised at  $Re(T) \sim -\frac{1}{a}\log(W_0)$ . For the supergravity approximation to remain valid  $T \gg 1$ , which can be easily achieved if  $W_0$  is taken to be small. Since  $W_0$  is dependant on the choice of fluxes used to stabilise the complex structure moduli it is possible to 'find' such a low value of  $W_0$  in the landscape of choices. The authors of [38, 39] have quantified a method of counting the landscape of possible solutions, giving equal weight to each specific choice of flux. It is then seen that typically  $W_0 \sim \mathcal{O}(1)$ . Since this is the case the KKLТ construction requires some level of tuning in order to achieve the limit  $W_0 \ll 1$ , with typical values of  $W_0 \sim 10^{-5}$  being required in order to neglect the perturbative corrections. This is in order to meet the conditions that the volume modulus is stabilised at values large compared to the string scale. In this limit the corrections to the Kähler potential can be ignored. The minimum is negative and corresponds to a supersymmetric AdS vacua. In order to break supersymmetry the potential must be uplifted by additional effects. This is done by reconsidering the tadpole cancellation condition (2.25),

$$N_{D3} + \frac{1}{2\kappa_{10}^2 T_3} \int_{\mathcal{M}} H_3 \wedge F_3 = \frac{\chi(X)}{24}, \quad (2.39)$$

where  $T_3$  is the tension of the D3 Branes,  $N_{D3}$  is the net number of  $(D3 - \bar{D}3)$  branes and  $H_3, F_3$  are the three form fluxes. One can over saturate the tadpole condition by turning on excess flux; in turn this then requires the additional presence of  $\bar{D}3$  branes in order to saturate (2.39) once more [31]. The additional energy density from the excess flux and  $\bar{D}3$  brane generates additional contributions to the scalar potential of the form

$$V_{uplift} = \frac{\beta}{(T + \bar{T})^n}, \quad (2.40)$$

where commonly  $n = 3$  and is determined by the uplift mechanism used. The uplift parameter  $\beta$  is related to the number of additional branes introduced and their location

in the internal space, because of this we have the freedom to finely tune  $\beta$ . With a suitable choice of  $\beta$  we can uplift the AdS minima given by (2.38) to a dS minimum with a sufficiently small positive energy [31]. The uplifting method is the least robust step in this construction and there exists a number of other possible methods of lifting to a dS minimum [28, 29, 25, 30]. Additionally the uplift term leads to the breaking of supersymmetry since the the superpotential with non perturbative corrections of the form (2.35) is only gauge invariant when  $W_0 = 0$  or  $A = 0$ , [25]. The breaking of supersymmetry at the vacuum complicates the analysis and moves us away from the well understood supergravity approximation. The authors of [101] found that by turning on fluxes associated with gauge fields living on D7 branes there is a contribution to the potential, which can cause an uplift to dS vacua without breaking SUSY. This type of uplifting mechanism has D-term uplift terms generated by turning on fluxes on D7 branes. Such uplifting terms give positive contribution to the scalar potential and can lead to supersymmetric dS vacua, [28]. These methods have been criticised since issues arise since once the KKLT potential is fixed at its supersymmetric AdS minimum,  $D_{T_i}W$ ,  $W \neq 0$  the F-terms and D-terms are related, leading to the vanishing of the D-term uplift contribution. This issue however can be overcome through considering gauge invariance [30] and these appealing uplift methods provide a means of gaining extra control when constructing string vacua. Non-geometric compactifications have also been proposed and shown to give 4d AdS and Minkowski vacua [26, 27]. The KKLT construction [31] however provides the first hope of obtaining realistic cosmologies from string theory through overcoming the no-go theorems of [19] through proposing a mechanism to obtain dS vacua and successfully stabilise all the geometric moduli in a controlled manner using the flux compactification models of [12] discussed in section 2.3 and the inclusion of non perturbative corrections to the superpotential (2.35) discussed in section (2.4) which broke the no-scale structure of the scalar potential (2.31) leading to a AdS minimum. In order to consistently include the non-perturbative contributions to the superpotential whilst neglecting the perturbative  $\alpha'$  corrections to the Kähler potential the model was confined to the limit  $W_0 \ll 1$  representing a significant tuning of the model, since the analysis of the distribution of flux vacua by [38] has shown that typically  $W_0 \sim \mathcal{O}(1)$ .

Let us outline the issues raised through the inclusion of corrections in more detail. The

Kähler potential receives corrections at every order in the perturbation theory through a series of  $\alpha'$  terms arising from higher derivative terms in the 10D supergravity action in addition to non perturbative corrections. The superpotential conversely is not renormalised at any level in perturbation theory and only receives the non-perturbative corrections [11] and so we have,

$$\mathcal{K} = \mathcal{K}_0 + \mathcal{K}_p + \mathcal{K}_{np} \quad (2.41)$$

$$W = W_0 + W_{np} \quad (2.42)$$

where the subscripts  $p$  and  $np$  represent the perturbative and non-perturbative corrections discussed above. Using the scalar potential

$$V = e^k (K^{i\bar{j}} D_i W D_{\bar{j}} \bar{W} - 3W\bar{W}), \quad (2.43)$$

we have  $V = V_0 + V_{\mathcal{K}_p} + V_{W_{np}} \dots$  with

$$V_0 \sim W_0^2, \quad V_{\mathcal{K}_p} \sim \mathcal{K}_p W_0^2, \quad V_{W_{np}} \sim W_{np}^2 + W_0 W_{np}. \quad (2.44)$$

In the scenario where we have a flat direction along which  $V_0$  is constant, then the structure of the potential will be determined by the corrections. In the low energy supergravity arising from the flux compactifications of [12] the non-perturbative corrections of the superpotential  $W_{np}$  are well known in comparison to the perturbative Kähler corrections,  $\mathcal{K}_p$  therefore it is sensible to look for a regime where  $\mathcal{K}_p$  can be neglected, as was the done in the KKLT model [31]. From the relations in (2.44) this occurs if  $W_0$  vanishes, giving the leading order correction to the potential  $V$  proportional to  $W_{np}$ . Similarly if we have  $W_0 \ll 1$ , we have

$$V_{W_{np}} \sim W_{np}^2 \gg W_{np}^2 \mathcal{K}_p \sim V_{\mathcal{K}_p}. \quad (2.45)$$

So we see that only when the tree level superpotential  $W_0$  is zero or of the same order of magnitude as  $W_{np}$  can we neglect the perturbative effects to the superpotential. However the distribution of the flux vacua is uniform [38] and so a naturally small  $W_0$  represents a significant fine tuning. We see also that perturbative effects are dominant and must be included when  $\frac{W_{np}}{\mathcal{K}_p} < W_0 \ll 1$ . This motivates us now to work in the limit where we include the perturbative corrections to the Kähler potential  $\mathcal{K}_p$  to which we now turn.

## 2.6 Large Volume scenarios

Having shown that the non perturbative contributions to the superpotential can lead to Kähler moduli stabilisation and dS vacua [31], following the work of KKLT it was then argued that these vacua be restricted to the finely tuned limit  $W_0 \ll 1$  so that the perturbative corrections to the Kähler potential need not be considered. However, as shown above and argued in detail in [44], the  $\alpha'$  corrections can only be neglected in a few very special cases. In this section we will present the  $\alpha'$  corrected Kähler potential determined in [118] and introduce the large volume class of vacua of Conlon et al [44] that arise when we include the the perturbative corrections to the Kähler potential. The work of [44, 43, 107] will be followed closely, in particular the reader is directed to [44] for a more detailed understanding of the Large Volume framework. The leading order corrections to the Kähler potential (2.27) have been calculated previously and lead to the  $\alpha'$  corrected Kähler potential of the form [118],

$$\mathcal{K} = -2\ln\left(\mathcal{V} + \xi\left(\frac{-i(\tau - \bar{\tau})}{2}\right)^{3/2}\right) - \ln(i(\tau - \bar{\tau})) - \ln\left(-i \int_{\mathcal{M}} \Omega \wedge \bar{\Omega}\right), \quad (2.46)$$

where  $\xi = \frac{-\chi(\mathcal{M})\zeta(3)}{2(2\pi)^3}$ ,  $\tau = -iS$  and  $\chi(\mathcal{M})$  are the Euler characteristics of the internal manifold. The internal volume  $\mathcal{V}$  of the Calabi Yau is given in equation (2.28). The super potential is

$$W = \int_{\mathcal{M}} G_3 \wedge \Omega + \sum_{i=2}^n A_i e^{-\frac{a_i T_i}{g_s}}. \quad (2.47)$$

We write here the explicit dependence of the theory on the complex structure moduli and the dilaton. In order to stabilise these fields we follow the flux compactification techniques of [12] outlined in section 2.3 and 'integrate out' the dependence by solving the covariant derivative,  $D_s W = 0$  and setting the fields at these fixed values. After this has been done we are left with a dependence only on the Kähler moduli, which are now fixed by the minimum of the scalar potential specified by the new Kähler and superpotentials

$$\mathcal{K} = \mathcal{K}_{cs} - 2\ln\left(\mathcal{V} + \frac{\xi}{2}\right), \quad (2.48)$$

$$W = W_0 + \sum A_i e^{-\frac{a_i T_i}{g_s}}. \quad (2.49)$$

The minimum of this model is in fact that of the KKLT solution [31], in the limit of  $W_0 \ll 1$ . As discussed previously, in this limit the perturbative corrections  $\xi$  to the

Kähler potential are negligible and can be ignored with the superpotential receiving non-perturbative corrections which stabilise the Kähler moduli. However the Kähler potential and superpotential here define the model entirely in the large volume limit  $\mathcal{V} \rightarrow \infty$ , since the leading order  $\alpha'$  correction can be seen to be an expansion in inverse volume [43]. This can be seen by looking at the Kähler potential (2.46) in this limit,

$$e^{\mathcal{K}} \sim \frac{e^{\mathcal{K}_{cs}}}{\mathcal{V}^2} + \mathcal{O}\left(\frac{1}{\mathcal{V}^3}\right). \quad (2.50)$$

The consequence of this being that we can consistently include only the leading order  $\alpha'$  correction in the large volume limit  $\mathcal{V} \rightarrow \infty$  which was shown in [43, 44]. The scalar potential (2.30) specified by the Kähler and superpotentials in equation (2.48) is given by [43],

$$\begin{aligned} V &\equiv V_{np1} + V_{np2} + V_{\alpha'}, \\ V_{np1} &= e^{\mathcal{K}} \mathcal{K}^{i\bar{j}} (a_i A_i a_{\bar{j}} \bar{A}_{\bar{j}} e^{-(a_i T_i - a_{\bar{j}} \bar{T}_{\bar{j}})}), \\ V_{np2} &= e^{\mathcal{K}} (a_i A_i e^{-a_i T_i} \bar{W} \partial_{\bar{T}_{\bar{j}}} \mathcal{K} + a_{\bar{j}} \bar{A}_{\bar{j}} e^{-a_{\bar{j}} \bar{T}_{\bar{j}}} W \partial_{T_i} \mathcal{K}) \\ V_{\alpha'} &= +e^{\mathcal{K}} 3\xi \frac{(\xi^2 + 7\xi\mathcal{V} + \mathcal{V}^2)}{(\mathcal{V} - \xi)(2\mathcal{V} + \xi)^2} |W|^2. \end{aligned} \quad (2.51)$$

Let us consider the general form of each of these terms individually in order to understand the behaviour of this potential as we go to the  $\mathcal{V} \rightarrow \infty$  limit. To do this we now follow closely the work of [43]. The leading order perturbative correction comes from  $V_{\alpha'}$ , and using the form of the Kähler potential in the large volume limit (2.50) we have,

$$V_{\alpha'} \sim \frac{3\xi}{4\mathcal{V}^3} e^{\mathcal{K}_{cs}} |W|^2 + \mathcal{O}\left(\frac{1}{\mathcal{V}^4}\right). \quad (2.52)$$

Requiring that there be more complex structure than Kähler moduli we have  $\xi = 2(h^{(1,1)} - h^{(2,1)}) > 0$ . This term is then always positive,  $V_{\alpha'} > 0$  and tends to zero as we go to the large volume limit,  $\mathcal{V} \rightarrow \infty$ .  $V_{np1}$  and  $V_{np2}$  both depend on the Kähler moduli which requires us to consider the limit  $\mathcal{V}$  more carefully. We follow [43] and take the limit in which all but one of the 4-cycle volumes  $\tau_l \rightarrow \infty$ . In this limit all  $\tau_l$  dependent terms in  $V_{np1}$  are exponentially suppressed. The remaining moduli,  $\tau_s$  then gives a contribution of,

$$V_{np1} = e^{\mathcal{K}} \mathcal{K}^{ss} (a_s A_s)^2 e^{-2a_s \tau_s}. \quad (2.53)$$

The sign of this term is determined by that of the inverse Kähler metric  $\mathcal{K}^{i\bar{j}}$  which is given by [43],

$$\mathcal{K}^{i\bar{j}} = -\frac{2}{9}(\mathcal{V} + \xi)\kappa_{i\bar{j}k}t^k + \frac{4\mathcal{V} - \xi}{\mathcal{V} - \xi}\tau_i\tau_{\bar{j}} \quad (2.54)$$

Where  $\kappa_{i\bar{j}k}$  is the triple intersection number given in (2.28). In the limit described above considering the  $\tau_s$  term this reduces to,

$$\mathcal{K}^{s\bar{s}} \sim -\frac{4}{9}\mathcal{V}\kappa_{s\bar{s}k}t^k + \mathcal{O}(1), \quad (2.55)$$

and so (2.53) becomes,

$$V_{np1} \sim \frac{4}{9} \frac{e^{\mathcal{K}_{cs}}(-\kappa_{s\bar{s}k}t^k)(a_s A_s)^2 e^{-2a_s \tau_s}}{\mathcal{V}} + \mathcal{O}\left(\frac{1}{\mathcal{V}^2}\right). \quad (2.56)$$

This term is positive for the limit described, as the term  $(-\kappa_{s\bar{s}k}t^k)$  is positive due to the Kähler metric  $\mathcal{K}^{i\bar{j}}$  being positive definite [43]. The term  $V_{np2}$  defined in (2.51) in the limit we have described takes the form,

$$V_{np2} = -e^{\mathcal{K}} \left[ \mathcal{K}^{s\bar{j}} a_s A_s e^{-a_s T_s} \bar{W} \partial_{\bar{j}} \mathcal{K} + \mathcal{K}^{i\bar{s}} a_{\bar{s}} \bar{A}_{\bar{s}} e^{-a_{\bar{s}} \bar{T}_{\bar{s}}} \bar{W} \partial_{\bar{s}} \mathcal{K} \right]. \quad (2.57)$$

Determining the contribution this has on the potential requires some more work. From the definition of the Kähler potential (2.48) we have,

$$\partial_{T_k} \mathcal{K} = \frac{t^k}{\mathcal{V} + \frac{\xi}{2}}, \quad (2.58)$$

whilst considering the symmetry of the inverse Kähler metric (2.54),  $\mathcal{K}^{i\bar{s}} = \mathcal{K}^{s\bar{i}}$  and noting the leading order contribution to the superpotential in the large volume limit is  $W \sim W_0 + \mathcal{O}\left(\frac{1}{\mathcal{V}}\right)$ . Using these results we can simplify (2.57) to give,

$$V_{np2} \sim e^{\mathcal{K}} a_s A_s W e^{-a_s \tau_s} \mathcal{K}^{s\bar{j}} \frac{t^j}{\mathcal{V} + \frac{\xi}{2}} \cos(a_s \theta_s) + \mathcal{O}\left(\frac{e^{-a_s \tau_s}}{\mathcal{V}^2}\right), \quad (2.59)$$

where we have expanded the Kähler moduli,  $T_i = \tau_i + i\theta_i$ . The axions  $\theta_i$  appear in the potential in the term and we can set the axion  $\theta_s$  to its minimum,  $\cos a_s \theta_s = -1$  which changes the overall sign of the  $V_{np2}$  contribution to the potential. Using the large volume limit of the inverse Kähler metric (2.54) once more we obtain,

$$V_{np2} \sim -e^{\mathcal{K}_{cs}} a_s A_s W e^{-a_s \tau_s} \frac{-\frac{8}{9}\mathcal{V}\tau_s + 4\tau_s \tau_j t^j}{\mathcal{V}^3} + \mathcal{O}\left(\frac{e^{-a_s \tau_s}}{\mathcal{V}^3}\right). \quad (2.60)$$

Finally noticing from the definition (2.29) that  $\tau_j t^j \propto \mathcal{V}$  we can collect the contributions (2.52), (2.56) and (2.60) together to give the the full potential in this limit,

$$V \sim e^{\mathcal{K}_{cs}} \left[ \frac{(-\kappa_{ssk} t^k)(a_s A_s)^2 e^{-2a_s \tau_s}}{\mathcal{V}} - \frac{a_s A_s W \kappa_{sjk} t^j t^k e^{-a_s \tau_s}}{\mathcal{V}^2} + \frac{\xi |W|^2}{\mathcal{V}^3} \right], \quad (2.61)$$

where we used equation (2.29) to replace the  $\tau_s$  in the second term and have dropped the numerical coefficients. In the limit  $\mathcal{V} \rightarrow \infty$  and  $a_s \tau_s = \ln \mathcal{V}$  all three terms have a volume dependence of  $\frac{1}{\mathcal{V}^3}$ . However in the limit where all the moduli blow up,  $\tau_i \rightarrow \infty$  we can identify the scaling of the three terms through the presence of the 2cycle volumes,  $t^i$  in the numerators, these are given as  $\frac{\sqrt{\ln \mathcal{V}}}{\mathcal{V}^3}$ ,  $\frac{\ln \mathcal{V}}{\mathcal{V}^3}$  and  $\frac{1}{\mathcal{V}^3}$  respectively [24]. Therefore the contribution  $V_{np2}$  given by (2.60) dominates in this limit, since we have argued that this term is negative we conclude that the full potential (2.61) tends to zero from below in large volume limit. At smaller volumes the dominate contribution to the potential comes from one of the two positive terms,  $V_{\alpha'}$  or  $V_{np1}$ . From this is was concluded by [24] that there exists an AdS minimum at large volumes. The arguments followed so far for a minimum at Large volumes have only considered the Kähler moduli contributions and one may wonder if the minimum we have identified is the global minimum of the full potential (2.30) when the complex structure and dilaton contributions are also included. In which case the full potential is given by,

$$V = e^{\mathcal{K}_{ab}} (\mathcal{K}^{a\bar{b}} D_a W D_{\bar{b}} \bar{W} + \mathcal{K}_{s\bar{s}} \mathcal{K}^{s\bar{s}} D_s W D_{\bar{s}} \bar{W}) + V_{\alpha'} + V_{np1} + V_{np2} \quad (2.62)$$

The additional two contributions from the complex structure moduli and the dilaton both vanish at the Supersymmetric minimum  $D_a W = D_s W = 0$  with deviations from this leading to positive definite contributions which from the Kähler potential at large volumes (2.50) we find are of order  $\mathcal{O}(\frac{1}{\mathcal{V}^2})$ . As we have shown above the Kähler moduli contributions are of order  $\mathcal{O}(\frac{1}{\mathcal{V}^3})$ . The positive contribution wins over and the potential is lifted. It is then concluded that the Large volume minimum of the Kähler moduli is a minimum of the full potential since [24]. The crux of the Large volume class of minima lies in the inclusion of the  $\alpha'$  corrections which dominant the form of the potential in the large volume limit. Since these were not included in the KKLT construction [31] the class of minimas are restricted to the  $W_0 \ll 1$  regime of moduli space. The Large volume class is not limited to a regime where the perturbative corrections can be ignored and so can take natural values of  $W_0$ . Additionally the large volume models coexist with the KKLT when  $W_0 \ll 1$  since here the  $\alpha'$  corrections

give negligible contribution to the potential, this is obvious since the KKLT class of vacua are a good approximation in this limit. The absence of tuning in the large volume models is encouraging since the exponentially large volumes relative to the string scale can generate large hierarchies as the gravitino mass is given by  $m_{3/2} = e^{\mathcal{K}}W \sim \frac{W_0}{\mathcal{V}}$  [48], a phenomenologically desirable gravitino mass of  $m_{3/2}$  at the TeV scale can be obtained with a stabilised volume of  $\mathcal{V} \sim 10^{15}l_s^6$ , where  $l_s = (2\pi)\sqrt{\alpha'}$  is the string length scale. A full analysis of the spectrum of moduli masses and couplings can be found in [48, 127], whilst the role of the gravitino mass and its cosmological implications will be returned to in chapter 4. We now have a consistent framework in which non perturbative effects, introduced in [31] to stabilise the Kähler moduli, can be used alongside perturbative corrections to construct AdS vacua. This class of vacua can be lifted to dS vacua through the uplifting potential (2.40) generated by the introduction of additional sources as we saw was done in the construction of [31]. Looking again at the Kähler moduli fields  $T_i$  present in the potential (2.51) we see that they appear along exponentially flat directions. It is then natural to ask if the Large volume potential can be used to construct an inflationary model from the moduli fields arising in string compactifications. This in fact can and has been done in the model of Kähler moduli inflation of [47] which we will study throughout the rest of this thesis.

# Chapter 3

## Kähler Moduli Inflation

The work in this chapter is based on the paper given by reference [54].

### 3.1 Introduction

The theory of inflation has been very successful in resolving many of the most important puzzles in early universe cosmology. However, there is, at the moment, no compelling evidence as to what could actually produce this period of accelerated expansion. It is therefore interesting to look for ways to understand this period of cosmic evolution within the framework provided by a fundamental theory. String theory is, at present, one of the most promising candidates for a fundamental theory and has inspired many attempts to embed inflation within it (for reviews see [84, 85, 86, 87, 88, 89, 90]). One of the most important challenges that has faced string phenomenology for a long time has been the issue of moduli stabilization [40, 80, 12, 31]. Any successful model of low energy string theory should, somehow, be able to fix all the moduli such that it would be compatible with our current experimental constraints from fifth force experiments [3] requiring a typical modulus,  $\phi$ , to have mass,  $m_\phi > 10^{-3}$ . On the other hand, the universe is not a static place but dynamical, so one is also interested in learning how we reached this low energy state, making other regions of the moduli space, and not only the final minimum, important in order to confront theory with cosmological observations. Taking this into account it is not surprising that recent developments of general methods of moduli stabilisation [12], and in particular sta-

bilisation techniques of KKLT [31], have led to a large number of new inflationary scenarios using either the open string moduli related to the position of a mobile D-brane [91, 92, 93, 94, 95, 96, 97, 98] or the closed string moduli coming from the compactification [99, 73, 100, 101, 102, 103, 104, 105, 106, 47, 53] as the relevant scalar fields.

This plethora of models should not be taken as a sign that inflation is easy to achieve within string theory. In fact, it is probably safe to say that it is just the opposite since most of these models have some degree of fine tuning in them. Indeed some of these problems were already encountered in the early models of modular inflation [113, 40, 114]. The main reason for these difficulties is the fact that the majority of these models are based on  $\mathcal{N} = 1$  supergravity theories, if they are to satisfy the slow roll conditions necessary to have a successful inflationary model, they must overcome the so-called  $\eta$  problem [116]. This is, the parameter  $\eta \equiv \frac{V''}{V}$ , where primes denote derivatives with respect to a canonical scalar field  $\Phi$ , is naturally of order one in supergravity theories due to the exponential factor,  $e^{\mathcal{K}}$ , in (2.30). We can see this clearly if we take the Kähler potential as  $\mathcal{K} = |\Phi|^2$ , where  $\Phi$  is a complex scalar field with canonical kinetic term. The potential (2.30) can be written as  $V = e^{\mathcal{K}}\tilde{V}$ , and we see through expanding the exponential to first order

$$V \sim (1 + |\Phi|^2 + \dots)\tilde{V}, \quad (3.1)$$

the scalar field then picks up a mass term of order  $\tilde{V}$ ,

$$V'' \sim \tilde{V}, \quad (3.2)$$

due to the scalar field dependence of the Kähler potential. This means that the contribution to  $\eta$  is typically of order one. We will look at the parameter  $\eta$  in more detail throughout the rest of this thesis, in particular chapter 5. These problems are quite generic and it is therefore of interest to look for inflationary models based within string theory that can somehow alleviate or ameliorate these difficulties.

In this chapter we will focus on a particular model of modular inflation that makes use of the special form of the potential for the Kähler moduli [47] enabling it to avoid the  $\eta$ -problem. The model is embedded within the Large Volume scenario developed in [44, 43, 128, 48] something that, as we will show, turns out to be an important ingredient for

the arguments presented in [47]. These Large Volume Models have been extensively studied in the last few years, due to their phenomenological interest as an explicit example within string theory of the large extra dimensional scenarios envisioned by [117]. It is therefore very interesting to study the cosmological implications of these type of models since they could provide us with a way to select the correct properties of the compactification scenario that we would like to have.

The purpose of this chapter is two fold. Firstly we demonstrate that there are inflationary solutions consistent with current observational data even when all of the moduli fields are allowed to vary during the cosmological evolution. Secondly, we show with explicit examples that the set of initial conditions that lead to a stable evolution, i.e., that avoid a runaway in the decompactification direction, is fairly wide. This property results from the existence of a basin of attraction in field space which we will explore with detail in more detail in the next chapter. There is an overlap in places between our work and that of Bond et al. [53], and where appropriate we will compare our results with theirs.

## 3.2 The Kähler moduli potential

Our inflationary scenario can be obtained within a class of Type IIB flux compactification models on a Calabi-Yau orientifold introduced in the previous chapter. In this context it has been shown in [12, 31] that the superpotentials generated by background fluxes and by non-perturbative effects like instantons or gaugino condensation may generate a scalar potential that stabilizes all the geometric moduli coming from the compactification. More concretely, it was seen in section 2.3 that the introduction of background fluxes in the model induces a superpotential that freezes the dilaton as well as the complex structure moduli to their values at their supersymmetric minimum [12]. The remaining moduli, that is, the Kähler moduli, could be then stabilized by non-perturbative contributions to the superpotential [31] (section 2.4). The resulting effective 4D description of the Kähler moduli  $T_i$  is an  $\mathcal{N} = 1$  supergravity theory with a superpotential of the type,

$$W = W_0 + \sum_{i=2}^n A_i e^{-a_i T_i} . \quad (3.3)$$

In this formula  $W_0$  is the perturbative contribution coming from the fluxes, which depends only on the frozen dilaton and the complex structure moduli, and therefore we will take to be a constant. There is also a non-perturbative piece depending on the Kähler moduli  $T_i$  where  $A_i$  and  $a_i$  are model dependent constants.

The  $F$ -term scalar potential is then given by the standard  $\mathcal{N} = 1$  formula

$$V(T_i) = e^{\mathcal{K}} [\mathcal{K}^{i\bar{j}} D_i W D_{\bar{j}} \bar{W} - 3|W|^2], \quad (3.4)$$

where  $D_i W = \partial_i W + (\partial_i \mathcal{K}) W$  is the covariant derivative of the superpotential and  $\mathcal{K}$  is the Kähler potential for  $T_i$ . In this chapter we will concentrate in the kind of type IIB models presented in [44, 43, 128, 48] in which the  $\alpha'$  corrections to the potential are taken into account. For these type IIB models the expression for the  $\alpha'$ -corrected Kähler potential is given by [118]

$$\mathcal{K}_{\alpha'} = -2 \ln \left( \mathcal{V} + \frac{\xi}{2} \right), \quad (3.5)$$

where  $\mathcal{V}$  denotes the overall volume of the Calabi-Yau manifold in string units and  $\xi = -\frac{\zeta(3)\chi(M)}{2(2\pi)^3}$  is proportional to  $\zeta(3) \approx 1.2$ . The Euler characteristic of the compactification manifold  $M$  is given by  $\chi(M) = 2(h^{(1,1)} - h^{(1,2)})$  where  $h^{(1,1)}$  and  $h^{(1,2)}$  are the Hodge numbers of the Calabi-Yau. We will concentrate on models for which  $\xi > 0$  (or equivalently with more complex structure moduli than Kähler moduli,  $h^{(1,2)} > h^{(1,1)}$ ). As was explained in [119, 44], the reason for this is that, in order to have the non-supersymmetric minimum at large volume the, leading contribution to the scalar potential coming from the  $\alpha'$  correction should be positive.

### 3.3 Kähler moduli inflation

Having introduced the Large volume scenarios of [44, 43, 128, 48] and the notion of String inspired inflationary scenarios such as the  $D3 - \bar{D}3$  brane inflationary model developed out of the KKLТ scenario [31] let us now look at one of the more interesting models to arise in recent years. This is Kähler moduli inflation. As we noted previously the Kähler moduli obtain vacuum expectation values through the non perturbative contributions to the super potential. We showed that these corrections lead to potentials with large volume minimum which are exponentially flat along the direction

of the small moduli fields. It is natural to ask, as was done in [47] whether or not the flatness could drive inflation.

Following [47] we will consider models for which the internal volume of the Calabi-Yau can be written in the form,

$$\mathcal{V} = \frac{\alpha}{2\sqrt{2}} \left[ (T_1 + \bar{T}_1)^{\frac{3}{2}} - \sum_{i=2}^n \lambda_i (T_i + \bar{T}_i)^{\frac{3}{2}} \right] = \alpha \left( \tau_1^{3/2} - \sum_{i=2}^n \lambda_i \tau_i^{3/2} \right), \quad (3.6)$$

where the complex Kähler moduli are given by  $T_i = \tau_i + i\theta_i$ , with  $\tau_i$  describing the volume of the internal four cycles present in the Calabi-Yau and  $\theta_i$  are their corresponding axionic partners. The parameters  $\alpha$  and  $\lambda_i$  are model dependent constants that can be computed once we have identified a particular Calabi-Yau. These models correspond to compactifications for which only the diagonal intersection numbers of the Calabi-Yau are non-vanishing.

Taking into account the form of the Kähler function one can then easily compute the Kähler metric for an arbitrary number of moduli, namely,

$$\begin{aligned} \mathcal{K}_{1\bar{1}} &= \frac{3\alpha^{4/3}(4\mathcal{V} - \xi + 6\alpha \sum_{k=2}^n \lambda_k \tau_k^{3/2})}{4(2\mathcal{V} + \xi)^2(\mathcal{V} + \alpha \sum_{k=2}^n \lambda_k \tau_k^{3/2})^{1/3}}, \\ \mathcal{K}_{i\bar{j}} &= \frac{9\alpha^2 \lambda_i \lambda_j \sqrt{\tau_i} \sqrt{\tau_j}}{2(2\mathcal{V} + \xi)^2}, \\ \mathcal{K}_{1\bar{j}} &= -\frac{9\alpha^{5/3} \lambda_j \sqrt{\tau_j} (\mathcal{V} + \alpha \sum_{k=2}^n \lambda_k \tau_k^{3/2})^{1/3}}{2(2\mathcal{V} + \xi)^2}, \\ \mathcal{K}_{i\bar{i}} &= \frac{3\alpha \lambda_i (2\mathcal{V} + \xi + 6\alpha \lambda_i \tau_i^{3/2})}{4(2\mathcal{V} + \xi)^2 \sqrt{\tau_i}}, \end{aligned} \quad (3.7)$$

which can be inverted to give,

$$\begin{aligned} \mathcal{K}^{1\bar{1}} &= \frac{4(2\mathcal{V} + \xi)(\mathcal{V} + \alpha \sum_{k=2}^n \lambda_k \tau_k^{3/2})^{1/3} (2\mathcal{V} + \xi + 6\alpha (\sum_{k=2}^n \lambda_k \tau_k^{3/2}))}{3\alpha^{4/3} (4\mathcal{V} - \xi)}, \\ \mathcal{K}^{i\bar{j}} &= \frac{8(2\mathcal{V} + \xi) \tau_i \tau_j}{4\mathcal{V} - \xi}, \\ \mathcal{K}^{1\bar{j}} &= \frac{8(2\mathcal{V} + \xi) \tau_j (\mathcal{V} + \alpha \sum_{k=2}^n \lambda_k \tau_k^{3/2})^{2/3}}{\alpha^{2/3} (4\mathcal{V} - \xi)}, \\ \mathcal{K}^{i\bar{i}} &= \frac{4(2\mathcal{V} + \xi) \sqrt{\tau_i} (4\mathcal{V} - \xi + 6\alpha \lambda_i \tau_i^{3/2})}{3\alpha (4\mathcal{V} - \xi) \lambda_i}, \end{aligned} \quad (3.8)$$

where we have rewritten for later convenience  $\tau_1$  in terms of  $\mathcal{V}$  and  $\tau_i$ ,  $i = 2 \dots n$ . With all this information we can use (3.4) to obtain the F-term scalar potential for the

moduli fields which we find to be,

$$\begin{aligned}
V = & \sum_{\substack{i,j=2 \\ i < j}}^n \frac{A_i A_j \cos(a_i \theta_i - a_j \theta_j)}{(4\mathcal{V} - \xi)(2\mathcal{V} + \xi)^2} e^{-(a_i \tau_i + a_j \tau_j)} (32(2\mathcal{V} + \xi)(a_i \tau_i + a_j \tau_j + 2a_i a_j \tau_i \tau_j) + 24\xi) \\
& + \frac{12W_0^2 \xi}{(4\mathcal{V} - \xi)(2\mathcal{V} + \xi)^2} + \sum_{i=2}^n \left[ \frac{12e^{-2a_i \tau_i} \xi A_i^2}{(4\mathcal{V} - \xi)(2\mathcal{V} + \xi)^2} + \frac{16(a_i A_i)^2 \sqrt{\tau_i} e^{-2a_i \tau_i}}{3\alpha \lambda_i (2\mathcal{V} + \xi)} \right. \\
& \left. + \frac{32e^{-2a_i \tau_i} a_i A_i^2 \tau_i (1 + a_i \tau_i)}{(4\mathcal{V} - \xi)(2\mathcal{V} + \xi)} + \frac{8W_0 A_i e^{-a_i \tau_i} \cos(a_i \theta_i)}{(4\mathcal{V} - \xi)(2\mathcal{V} + \xi)} \left( \frac{3\xi}{2\mathcal{V} + \xi} + 4a_i \tau_i \right) \right] + V_{uplift}.
\end{aligned} \tag{3.9}$$

In this expression for the potential we have introduced an additional uplift term of the form  $V_{uplift}$ . As discussed in chapter 2 the purpose of this term is to uplift the minima of the potential from an anti-de Sitter minimum to a nearly Minkowski vacuum. Its origin in model building has been the subject of some debate. It could be achieved by breaking explicitly supersymmetry through the introduction of anti-branes located in a region with strong red-shift, as suggested in [31], or in other alternative ways involving vector multiplets [101, 30]. Also, from a low-energy effective field theory point of view, it can in principle be implemented by using as the uplifting sector any kind of theory leading to spontaneous supersymmetry breaking, provided the supersymmetric sector is appropriately shielded from this uplifting sector [120]. Of course, the different ways that a term of this form can appear in the low energy description of the theory may lead to slightly different dependencies on the internal volume. For simplicity, as well as for the sake of comparison, we will take the same form as was previously assumed in [47], as seen in equation (2.40) of chapter 2,  $V_{uplift} = \frac{\beta}{\mathcal{V}^2}$ , where here we have  $\mathcal{V}$  as the volume modulus. Nevertheless it is interesting to point out that in these Large Volume Models the presence of an uplifting sector is not necessary in order to break supersymmetry as a non-supersymmetric minimum is already present at large volume [44, 43, 128, 48, 119]. This is in fact our case here as well.

### 3.4 Single Field Kähler Moduli Inflation

In ref. [47] the authors argued that the scalar potential given by the expression (3.9) should be able to support a period of slow roll inflation without any fine tuning, making it a natural candidate to realize the idea of modular inflation. In this section we will briefly review their argument, and in the following sections we will proceed to test how

general this argument can be made.

The first thing one should take into account is that the form of the potential (3.9) simplifies substantially in the limit in which  $\mathcal{V} \gg 1$ . In this regime, as can be inferred from (3.6), we can consider there is a well defined limit in which all of the moduli are small except for one combination which maintains the large volume. Therefore in this combination we can have one four-cycle (the one given by  $\tau_1$ ) much bigger than the rest,  $\tau_1 \gg \tau_i, i = 2, \dots, n$ . This limit has become known as a 'Swiss-Cheese' picture, since the Calabi Yau manifolds volume  $\mathcal{V}$  is large with one identified cycle that controls the overall volume whilst the small cycles are internal and so an increase in their volume will decrease the overall size of the volume (these cycles correspond to the 'holes in the cheese') [44]. Taking this into consideration one can approximate the full potential by the expression:

$$V_{LARGE} = \sum_{i=2}^n \frac{8(a_i A_i)^2}{3\alpha\lambda_i\mathcal{V}} \sqrt{\tau_i} e^{-2a_i\tau_i} + \sum_{i=2}^n \frac{4W_0 a_i A_i}{\mathcal{V}^2} \tau_i e^{-a_i\tau_i} \cos(a_i\theta_i) + \frac{3\xi W_0^2}{4\mathcal{V}^3} + \frac{\beta}{\mathcal{V}^2}, \quad (3.10)$$

where we have only included the leading terms up to  $\mathcal{O}(\frac{1}{\mathcal{V}^3})$ .

The basic idea now to have inflation in this model is to look for the possibility of having a flat enough potential by displacing one of the fields from its minimum value while keeping the others fixed at their global minimum values. It is reasonable to expect that this strategy would lead to a successful inflationary period since the potential is exponentially suppressed along the directions  $\tau_i$  ( $i = 2, \dots, n$ ). On the other hand, the authors in [47] also point out correctly that for this idea to work one should show that the whole inflationary evolution occurs along a single  $\tau_i$  direction, otherwise one would not be able to draw conclusions by looking at that particular slice of the potential in field space.

The way they propose to enforce this constraint is the following: let us assume for concreteness that inflation happens along the  $\tau_2$  direction. Then in the limit in which  $a_i\tau_i \gg 1$ , for  $i = 2, \dots, n$ , the authors of [47] claim that by imposing that the parameters appearing in the potential satisfy the condition  $\rho \ll 1$ , where

$$\rho \equiv \frac{\lambda_2}{a_2^{3/2}} : \sum_{i=2}^n \frac{\lambda_i}{a_i^{3/2}}, \quad (3.11)$$

the minimum of the potential along the other field directions remain virtually unchanged even if one displaces  $\tau_2$  from its global minimum value. In other words, for small enough values of  $\rho$ , there exists a valley of the potential very much aligned with the direction of  $\tau_2$  and therefore one can assume that moving along that valley all the fields except  $\tau_2$  would stay in their global minimum.

Assuming that this is the case, one can then proceed to approximate the potential along the inflaton direction  $\tau_2$  as,

$$V_{LARGE} = \frac{BW_0^2}{\mathcal{V}^3} - \frac{4W_0a_2A_2\tau_2e^{-a_2\tau_2}}{\mathcal{V}^2}, \quad (3.12)$$

where  $B$  includes several terms from Eq. (3.10) that depend on the parameters of the potential as well as on the values of the other fields at their minimum. Also note that the axions  $\theta_i$  have been set to their minimum, for which  $\cos(a_i\theta_i) = -1$ . This is needed in order for a minimum for all the fields  $\tau_i$  at finite values to exist. Otherwise one would have a runaway behavior for some of them. This assumption is relaxed in the next chapter.

We can now obtain the values of the slow roll parameters for this potential at large values of  $\tau_2$  by using their conventional definitions in the single field inflation models, namely (we work in Planck units  $M_P = 1$ ),

$$\epsilon = \frac{1}{2} \left( \frac{V'}{V} \right)^2, \quad \eta = \left( \frac{V''}{V} \right), \quad (3.13)$$

where the primes denote derivatives with respect to the canonically normalised field  $\psi$ , defined by normalising the kinetic term for the inflaton. In the single field inflation approximation we discuss here and to leading order in the volume we see that,

$$\psi = \sqrt{\frac{4\alpha\lambda_2}{3\mathcal{V}}} \tau_2^{3/4}, \quad (3.14)$$

which in turn means that the slow roll parameters are given by [47],

$$\epsilon = \frac{32\mathcal{V}^3}{3\alpha B^2\lambda_2 W_0^2} a_2^2 A_2^2 \sqrt{\tau_2} (1 - a_2\tau_2)^2 e^{-2a_2\tau_2}, \quad (3.15)$$

$$\eta = -\frac{4a_2 A_2 \mathcal{V}^2}{3\alpha\lambda_2 \sqrt{\tau_2} B W_0} (1 - 9a_2\tau_2 + 4(a_2\tau_2)^2) e^{-a_2\tau_2}, \quad (3.16)$$

and in the limit of slow roll, the associated scalar spectral index and tensor to scalar ratio  $r$  are given by

$$n_s - 1 = 2\eta - 6\epsilon, \quad (3.17)$$

$$r \sim 12.4\epsilon. \quad (3.18)$$

The number of e-foldings can be computed within this approximate potential by,

$$N_e = \int_{\psi_{end}}^{\psi} \frac{V}{V'} d\psi \approx \frac{-3BW_0\alpha\lambda_2}{16a_2A_2\mathcal{V}^2} \int_{\tau_2^{end}}^{\tau_2} \frac{e^{a_2\tau_2}}{\sqrt{\tau_2}(1-a_2\tau_2)} d\tau_2, \quad (3.19)$$

where  $\tau_2^{end}$  is taken to be the point in field space where the slow roll conditions break down i.e. when  $\epsilon = \eta = \mathcal{O}(1)$ . It is clear from the expressions (3.15)–(3.19) that one can get small enough slow-roll parameters as well as a large number of e-folds, just by starting at large enough values of  $\tau_2$  so that  $\mathcal{V}^2 e^{-a_2\tau_2} \ll 1$ . Taking into account that we are in the slow roll regime, we can then calculate the amplitude of the adiabatic scalar perturbations using the expression,

$$P = \frac{1}{150\pi^2} \left( \frac{V}{\epsilon} \right) \simeq \frac{1}{150\pi^2} \left( \frac{3\alpha B^3 W_0^4 \lambda_2 e^{2a_2\tau_2}}{32\mathcal{V}^6 a_2^2 A_2^2 \sqrt{\tau_2} (1-a_2\tau_2)^2} \right). \quad (3.20)$$

In [47], the authors proposed a ‘footprint’ for their model of Kähler inflation. Normalising the density perturbations to COBE and seeking  $N_e$  efoldings of inflation (typically between 50-60) they obtained the results

$$\eta \simeq -\frac{1}{N_e}, \quad \epsilon < 10^{-12}, \quad (3.21)$$

$$0.960 < n_s < 0.967, \quad 0 < |r| < 10^{-10}. \quad (3.22)$$

Such a small value for  $\epsilon$  at horizon exit implies that the inflationary energy scale is low in Kähler inflation, being of order  $V_{inf} \sim 10^{13} \text{GeV}$ , which in turn implies that tensor modes would be unobservable. A final point that they make is that for the model to work, the internal volume  $\mathcal{V}$  is found numerically to live within a range of values

$$10^5 l_s^6 \leq \mathcal{V} \leq 10^7 l_s^6, \quad (3.23)$$

where  $l_s = (2\pi)\sqrt{\alpha'}$ . It is remarkable how narrow the range of  $n_s$  is in Eq. (3.22) and how relatively restrictive the range of allowed volumes are Eq. (3.23). One of the goals of this work will be to see whether these footprints really do define the model when we allow for the volume modulus and other moduli fields to evolve.

### 3.5 Full Kähler Moduli inflation

The discussion in the previous section suggests that inflation may be naturally realized in a large subset of string compactifications. This is an interesting claim so we would

like to carefully study the validity of the approximations made as well as compare the observable quantities estimated earlier, such as the number of e-folds, the validity of the assumption  $\rho \ll 1$ , the constancy of the volume modulus and the scalar spectral index, with the more accurate results obtained by numerical integration of the full equations of motion using the full potential in (3.9) instead of the approximate large volume one in (3.12). Our approach differs in detail from that adopted by Bond et al. [53] in that we will be allowing for a number of the moduli fields to vary, including the volume modulus. This will allow us to fully explore the validity of the assumption that the volume remains effectively constant during inflation. In their approach, the volume modulus was kept constant and an analysis of the region of parameter space which led to inflation was based upon that assumption.

### 3.5.1 Numerical evolution

The equations of motion for our moduli fields can be obtained by varying the minimal  $N = 1$ ,  $d = 4$  effective SUGRA action of the form (in Planck units),

$$S = - \int d^4x \sqrt{-g} \left( \frac{1}{2} R + \mathcal{K}_{i\bar{j}} \partial_\mu T^i \partial^\mu \bar{T}^{\bar{j}} + V(T^m, \bar{T}^{\bar{m}}) \right), \quad (3.24)$$

where  $\mathcal{K}_{i\bar{j}}$  is the Kähler metric,  $T^i$  and  $\bar{T}^{\bar{j}}$  are the complex chiral fields. Considering a spatially flat FRW spacetime we get,

$$\begin{aligned} \ddot{T}^l + 3H\dot{T}^l + \Gamma_{ij}^l \dot{T}^i \dot{T}^j + \mathcal{K}^{l\bar{k}} \partial_{\bar{k}} V &= 0, \\ 3H^2 &= \left( \mathcal{K}_{i\bar{j}} \dot{T}^i \dot{\bar{T}}^{\bar{j}} + V \right), \end{aligned} \quad (3.25)$$

where we have used the definition of the connections of the Kähler metric  $\Gamma_{ij}^l = \mathcal{K}^{l\bar{k}} \frac{\partial \mathcal{K}_{i\bar{k}}}{\partial T^j}$  and  $H = \frac{\dot{a}}{a}$  is the Hubble parameter. Armed with the full equations of motion we can now explore numerically the evolution of all the fields and find out what regions of moduli space are suitable for inflation.

For carrying out a numerical analysis we developed a number of separate codes using the utilities, Mathematica [132] and Matlab [133]. The codes were both written using an adaptive step size Runge Kutta algorithm, [134] in order to solve the ordinary differential equations given above. Having numerical methods which were independent from each other allowed the confirmation of simulation results. In order to replicate

the results in each code we required significant precision when providing the initial conditions for each simulation. It is with this in mind that the following examples contain highly precise values for the initial conditions.

### 3.5.2 Example 1

Following [47] we first analyze the case where the parameters are such that  $\mathcal{V} \gg 1$  and  $\rho \ll 1$  and we only displace the inflaton ( $\tau_2$ ) from its global minimum value. Our numerical integration confirms the predictions of the previous analytic arguments. We observe that all the other fields remain nearly constant during the whole evolution while  $\tau_2$  slowly rolls down to its minimum, essentially reproducing the single field scenario discussed earlier.

An example with these properties can be obtained by taking the following set of parameters,

$$\begin{aligned} \xi &= 24, & \alpha &= 1, & \lambda_2 &= \frac{1}{100}, & \lambda_3 &= 1, & a_2 &= 20\pi, & a_3 &= \frac{\pi}{2} \\ A_2 &= \frac{1}{300}, & A_3 &= \frac{1}{300}, & \beta &= 1.984002914 \times 10^{-6}, & W_0 &= 2. \end{aligned} \quad (3.26)$$

We have chosen a viable example of this scenario with the minimal number of fields possible, which is three. We first obtain the global minimum of the potential, i.e. the minimum at zero cosmological constant<sup>1</sup>, finding it to be at,

$$\begin{aligned} \tau_1^f &= 35189.343156992, & \tau_2^f &= 0.302053449, & \tau_3^f &= 5.886085128, \\ \mathcal{V}^f &= 6.601 \times 10^6. \end{aligned} \quad (3.27)$$

We see that indeed this is a large volume compactification scenario so we should be well within the regime of applicability of the approximations that we indicated in the previous section. On the other hand, we have chosen these parameters to have

$$\rho \approx 10^{-5}, \quad (3.28)$$

so we expect that the value of the volume at the minimum should remain pretty much unaffected by the displacement of  $\tau_2$ . We choose the initial value of the inflaton to be

---

<sup>1</sup>In all the examples in this paper we have adjusted  $\beta$  so that the overall minimum of the potential is located at vanishing value of the  $4d$  cosmological constant. We tried to be as precise as possible for its value so the model can be explicitly reproduced by other people.

$\tau_2^i = 0.8510534498^2$  and find numerically the new values of the local minima in the  $\tau_1$  and  $\tau_3$  directions for this case to be,

$$\tau_1^i = 35244.7673818281, \quad \tau_3^i = 5.887497350, \quad \mathcal{V}^i = 6.616 \times 10^6. \quad (3.29)$$

Comparing these values to ones obtained in the global minimum one can clearly see that the displacement of  $\tau_2$  does not have a big impact on the position of the local minima for the other fields in agreement with the analytic arguments given above.

We have chosen this particular value of  $\tau_2^i$  to illustrate that it is straightforward to obtain sixty e-folds of inflation with this set of values. Similarly we have normalized the parameters in the potential namely,  $A_2$ ,  $A_3$  and  $W_0$  in (3.26) so that we obtain the correct magnitude of the perturbations for this particular solution.

We can now compute the observational signatures of this model within the analytic approximations described above. Using the expressions given in (3.12), (3.15), (3.16), (3.19) and (3.20) we find,<sup>3</sup>

$$\begin{aligned} N_e &\simeq 61, \quad V_{inf} = 10^{13} \text{ GeV}, \quad P = 4 \times 10^{-10}, \\ \epsilon &= 4 \times 10^{-17}, \quad \eta = -0.0165, \quad n_s = 0.967. \end{aligned} \quad (3.30)$$

Having identified a particular set of parameters that leads to a successful inflationary scenario within the approximations described in [47] we would now like to numerically investigate this example in detail to confirm its analytic predictions. We have evolved the system of equations presented in (3.25) considering the complete potential (3.9), in other words, without using any of the approximations we discussed earlier. This way we check that the fields behave as we expect them to do all the way to their global minimum, even in the region of the potential that is not well approximated by the analytic expressions given above. We show in Fig. 1 the last period of the numerical evolution for  $\tau_2$  that starts at  $(\tau_1^i, \tau_2^i, \tau_3^i)$ . We only show the  $\tau_2$  trajectory since both

<sup>2</sup>The precision of these moduli values is essential since the main point of the analyse in this chapter is to perform a numerical analysis to test the stability of the model of inflation. An additional reason for being precise with the position of the minima and parameters, is to enable the replication of the results given. If the parameters are slightly changed there are changes in the results, but these are quantitative variations and not qualitative ones.

<sup>3</sup>Note that for this set of parameters one should take  $B \approx 0.002$  and  $\tau_2 \approx \tau_2^i$ .

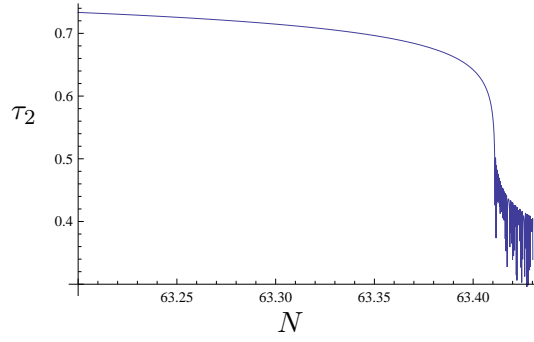


**Figure 3.1:** Evolution of the  $\tau_2$  field in the last few e-folds in Example 1.

$\tau_1$  and  $\tau_3$  stay constant throughout the whole evolution until the inflaton field,  $\tau_2$  rolls rapidly towards its global minimum value given in (3.27). At this point the fields which remain constant during inflation then proceed to evolve towards the global minimum values. This confirms that for these set of parameters we can regard the evolution as effectively a one dimensional problem. The rapid oscillations of the fields at the end of inflation come from their evolution near the overall minimum of the potential. Once the inflationary period ends the cosmological friction does not slow down the fields in their evolution any more and therefore they rapidly oscillate around their minima. The scale of these oscillations is in principle determined by their masses on that minima, although things become more complicated in models with multiple fields and non-minimal kinetic terms, both ingredients that are present in the model being considered. Having found the solution numerically we can now calculate the amplitude of the adiabatic scalar density perturbations directly from the solutions by computing,

$$P(N) = \frac{1}{150\pi^2} \frac{V(N)}{\epsilon(N)}, \quad (3.31)$$

where  $N$  denotes the number of e-foldings along the numerical trajectory and  $\epsilon(N)$  correspond to the slow-roll parameter which in terms of the Kähler metric and the potential takes the form

$$\epsilon(N) = \frac{\mathcal{K}^{i\bar{j}} \nabla_i V \nabla_{\bar{j}} V}{V^2}. \quad (3.32)$$

We can also extract the spectral index  $n_s$  from the expression of the form,

$$n_s = 1 + \frac{d \log P(N)}{dN}. \quad (3.33)$$

Putting all these expressions together we obtain the following results numerically,

$$\begin{aligned} N_e &\simeq 63, \quad V_{inf} = 10^{13} \text{ GeV}, \quad P = 4 \times 10^{-10}, \\ \epsilon &= 4 \times 10^{-17}, \quad n_s = 0.963. \end{aligned} \quad (3.34)$$

which is in very good agreement with current observational data, and also with the analytic prediction of Conlon and Quevedo [47] given in this case by Eqs. (3.30).

### 3.5.3 Example 2

It is interesting to note that we can still find a successful scenario for inflation within these type of models even when some of the approximations used in the previous analytic arguments break down for a particular set of parameters. Let us consider for example what happens when one relaxes the constraint of considering a very large volume. We can accomplish this by just considering a smaller value of  $W_0$ , namely the following parameters,

$$\begin{aligned} \xi &= 24, & \alpha &= 1, & \lambda_2 &= \frac{1}{100}, & \lambda_3 &= 1, & a_2 &= 20\pi, & a_3 &= \frac{\pi}{2} \\ A_2 &= \frac{1}{300}, & A_3 &= \frac{1}{300}, & \beta &= 3.29801836 \times 10^{-9}, & W_0 &= \frac{1}{300} \end{aligned} \quad (3.35)$$

where we have also changed the value of  $\beta$  to be able to set the global minimum at zero cosmological constant. In this case the global minimum becomes,

$$\begin{aligned} \tau_1^f &= 495.4469043856, & \tau_2^f &= 0.302090805, \\ \tau_3^f &= 5.8875322868, & \mathcal{V}^f &= 11013.6. \end{aligned} \quad (3.36)$$

which has a much smaller value of the volume than the one obtained in the previous example and which is not within the range given in (3.23). In fact, one can check that in this case some of the expressions for the large volume limit give a poor approximation for the real values, due to the fact that the volume is not sufficiently large. Nevertheless one can still displace  $\tau_2$  without disturbing the values of the other fields in their minima. In particular, one can show that fixing  $\tau_2^i = 0.747090805$  one changes the values of the local minimum of the potential along the other directions to,

$$\tau_1^i = 496.227462068, \quad \tau_3^i = 5.888944614, \quad \mathcal{V}^i = 11039.2. \quad (3.37)$$

We notice that the change in the volume between these two points in field space is actually much less than 1%. In fact, even if we increase the value of  $\tau_2^i$  considerably the situation will not really change, because the value of the volume or of the local

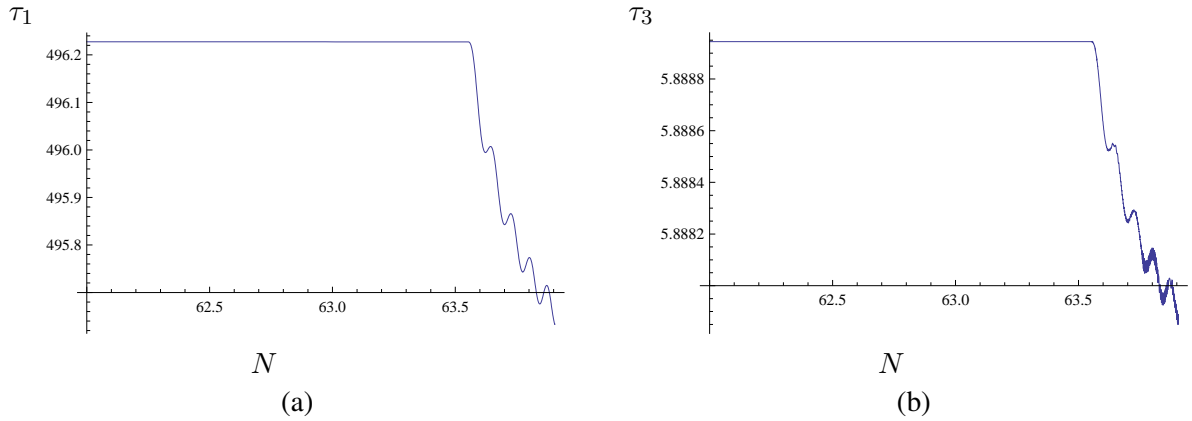


**Figure 3.2:** Evolution of the different moduli fields in the last few e-folds in Example 2. (a) Evolution of the field  $\tau_1$ . (b) Evolution of the field  $\tau_3$ .

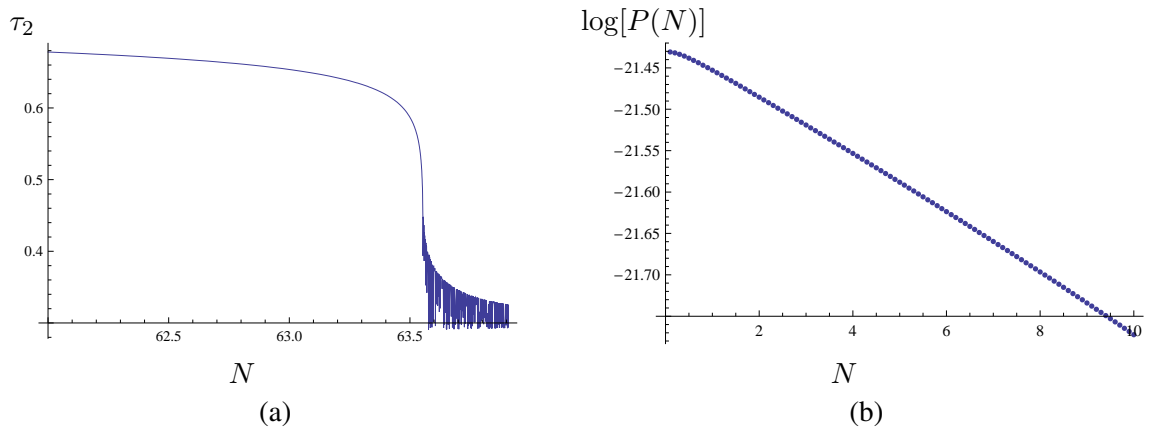


**Figure 3.3:** (a) Evolution of the moduli field  $\tau_2$  (the inflaton) in the last few e-folds in Example 2. (b) Amplitude of the density perturbations in the 10 observationally relevant e-foldings..

minimum in which the fields  $\tau_1^i, \tau_3^i$  sit, remains relatively insensitive to the position of  $\tau_2^i$ .

We show in Figs. 3.2–3.3 the last few e-folds of the numerical evolution that starts at  $(\tau_1^i, \tau_2^i, \tau_3^i)$ . We see that  $\tau_1$  and  $\tau_3$  stay constant through out the whole evolution until the end of inflation where their values drop abruptly to their global minimum values. So effectively our model is still a one dimensional inflationary model.

We can now use the expressions given above in Eqs. (3.31) and (3.33) to get in this case,

$$n_s = 0.965 \quad (3.38)$$

where we have normalized the potential to obtain the correct magnitude of the perturbations within the cosmologically observable region. (See Fig. 3.3).

We conclude from this example that one can extend the region of parameter space where a successful inflationary region can occur even when one can not use some of the large volume approximations presented in the previous section, but rather the expressions computed from the full potential. We will see in the following examples that this also the case for some of the other assumptions made in [47].

### 3.5.4 Example 3

As we explained above, the value of the internal volume in the previous examples remains very much the same during inflation and it is almost exactly the same as the final value of the volume in the overall minimum of the potential. This seems to be a stronger requirement than necessary. In fact, we should only impose that the volume remains constant during the inflationary period but it is otherwise free to change substantially after that in its way to the global minimum. In the following, we will describe one such example where the volume varies by 45% from its value during inflation to the final value.<sup>4</sup> To illustrate this point let us consider an example with the following values of the parameters

$$\begin{aligned} \xi &= 24, & \alpha &= 1, & \lambda_2 &= 1, & \lambda_3 &= 1, & a_2 &= 20\pi, & a_3 &= \frac{\pi}{2} \\ A_2 &= \frac{3}{32}, & A_3 &= \frac{1}{320}, & \beta &= 6.213734280 \times 10^{-9}, & W_0 &= \frac{1}{160} \end{aligned} \quad (3.39)$$

With these values,  $\rho \sim 10^{-3}$ , so we are again working in the regime considered in [47]. For this particular example, we can show that the global minimum of the potential is located at

$$\begin{aligned} \tau_1^f &= 751.9457707162, & \tau_2^f &= 0.2824390994, \\ \tau_3^f &= 5.8472434856, & \mathcal{V}^f &= 20605.289 \end{aligned} \quad (3.40)$$

---

<sup>4</sup>There may be other regions of the parameter space where this change is in fact more drastic, however, we have restricted ourselves to this milder example for simplicity.

while by displacing the value of  $\tau_2^i = 0.6624390994$  we see that the new minimum for the other fields is now found at,

$$\tau_1^i = 970.6098419930, \quad \tau_3^i = 6.0764936267, \quad \mathcal{V}^i = 30170.0176 \quad (3.41)$$

Once again we evolve the system of equations presented in (3.25) using the complete potential (3.9) and check what is the behaviour of the different fields. We plot in Fig. 3.4 and in part a) of Fig.3.5 the results for evolution of the fields for this example. In part b) of Fig. 3.5 we show the evolution of the internal volume in the last few e-folds. We can clearly see there that the volume remains constant for the relevant period of inflation and only changes to its global minimum value within the last e-fold or so.

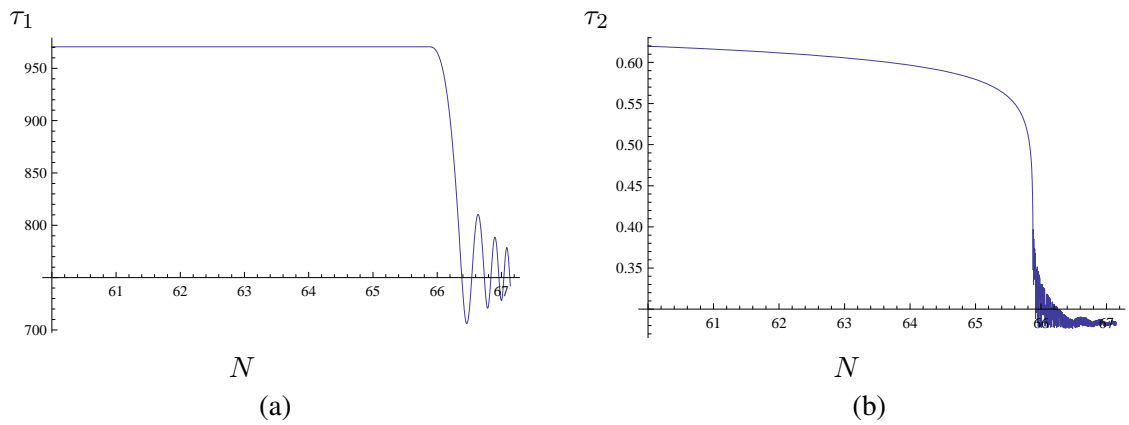


**Figure 3.4:** Evolution of the different moduli fields in the last few e-folds in Example 3. (a) Evolution of the field  $\tau_1$ . (b) Evolution of the field  $\tau_2$ .

What can we conclude from this case compared to the previous examples? It is clear that although the set of parameters that we have used here represents a slightly different behaviour from the one described in [47], in particular the fact that the volume modulus can change quite considerably at the end of inflation, nevertheless, it still represents a perfectly valid inflationary period regarding its observational signatures so once again this example increases the acceptable region of the parameter space within this kind of model. Actually we have again normalized the parameters in the potential so that we obtain the correct magnitude of the perturbations and therefore we can use the expressions (3.33) together with (3.31) to get in this case

$$n_s = 0.967, \quad (3.42)$$

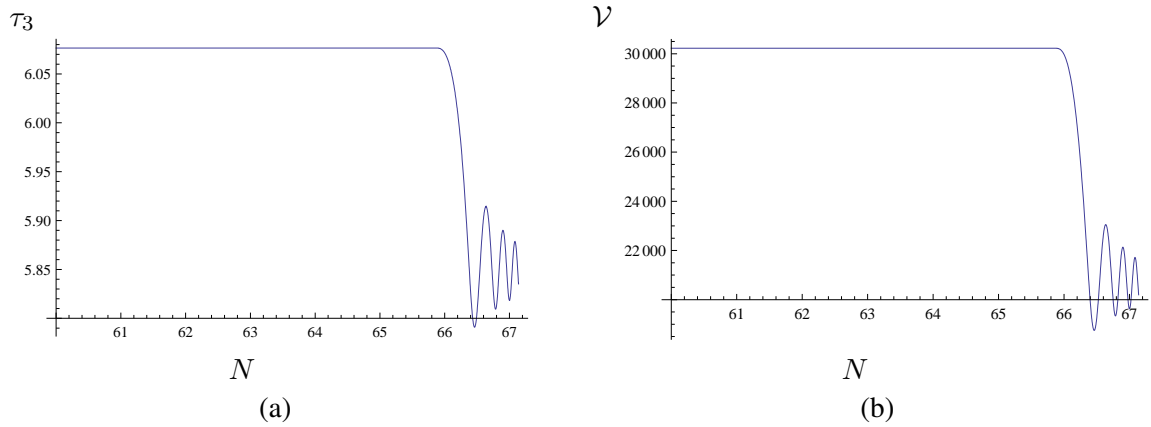


**Figure 3.5:** Evolution of the different moduli fields in the last few e-folds in Example 3. (a) Evolution of the field  $\tau_3$ . (b) Evolution of the field  $\mathcal{V}$ .

once again perfectly consistent with the range predicted in [47].

We can therefore see from this example that the real condition in order for a successful period of inflation to take place is that the volume remains constant during inflation only, but not necessarily during the whole evolution of the fields<sup>5</sup>.

### 3.5.5 Example 4

As we have mentioned, the analytic estimates made in [47] for the spectral index  $n_s$ , are based on the assumption that during inflation  $\rho \ll 1$ . In this final example, we relax that condition, and address whether successful inflation still occurs in that situation (recall we are allowing all the fields to evolve). For this purpose let us consider the following values of the parameters,

$$\begin{aligned} \xi &= \frac{1}{2}, \quad \alpha = \frac{1}{9\sqrt{2}}, \quad \lambda_2 = 10, \quad \lambda_3 = 1, \quad a_2 = \frac{2\pi}{30}, \quad a_3 = \frac{2\pi}{3}, \quad (3.43) \\ A_2 &= \frac{1}{1.7 \times 10^6}, \quad A_3 = \frac{1}{425}, \quad \beta = 6.9468131457 \times 10^{-5}, \quad W_0 = \frac{40}{17}. \end{aligned}$$

which yields,

$$\rho \sim 0.99. \quad (3.44)$$

<sup>5</sup>This does not mean, of course, that there could not be successful models of inflation where the volume can change during the inflationary period but it is clear that in this case there should be another mechanism in play that makes it possible to avoid the  $\eta$  problem.

The global minimum of the potential is now located at

$$\tau_1^f = 2555.95, \quad \tau_2^f = 4.7752, \quad \tau_3^f = 2.6512, \quad \mathcal{V}^f = 10143.94363. \quad (3.45)$$

Displacing the value of  $\tau_2$  to a substantially larger value, namely,  $\tau_2^i = 78.7752067$  we see that the new minimum for the remaining fields is found at,

$$\tau_1^i = 2781.185086997, \quad \tau_3^i = 2.684717126, \quad \mathcal{V}^i = 10973.9. \quad (3.46)$$

As in the previous example we can now evolve again the system of equations presented in (3.25) using the complete potential (3.9) and check what is the behaviour of the different fields. We plot the results in Figs. 3.6 and 3.7. More concretely in Fig. 3.6 and in part (a) of Fig. 3.7 the evolution of the fields  $\tau_i$  and in part (b) of Fig. 3.7 the evolution of the internal volume in the last few e-folds.

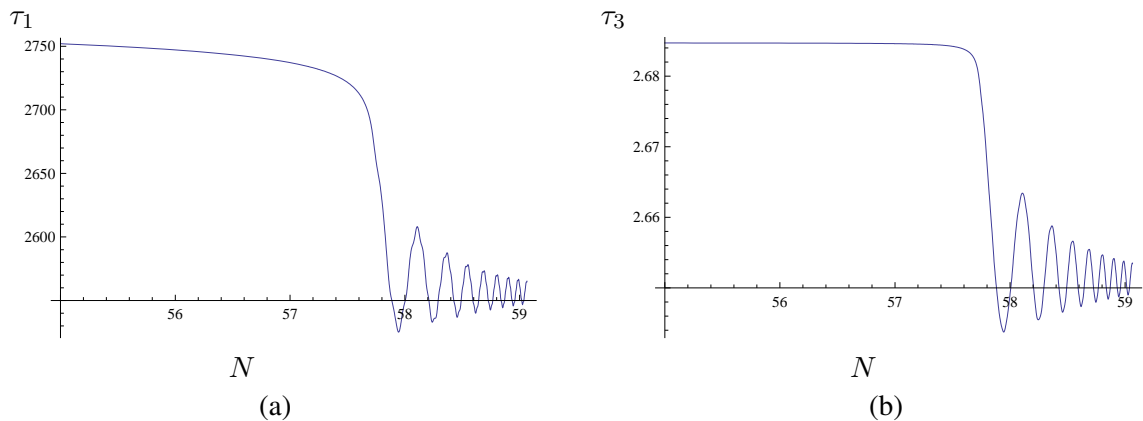


**Figure 3.6:** Evolution of the different moduli fields in the last few e-folds in Example 4. (a) Evolution of the field  $\tau_1$ . (b) Evolution of the field  $\tau_3$ .

As before, we find a successful period of inflation with this new set of parameters, reproducing the correct amplitude of density perturbations and obtaining

$$n_s = 0.960, \quad (3.47)$$

which is very similar to the range predicted in [47].

The reason why this system of parameters works is that the initial value of  $\tau_2$  is large enough so that the exponential dependence of the potential with this field makes a negligible contribution to the calculation of the minima as a function of the other two

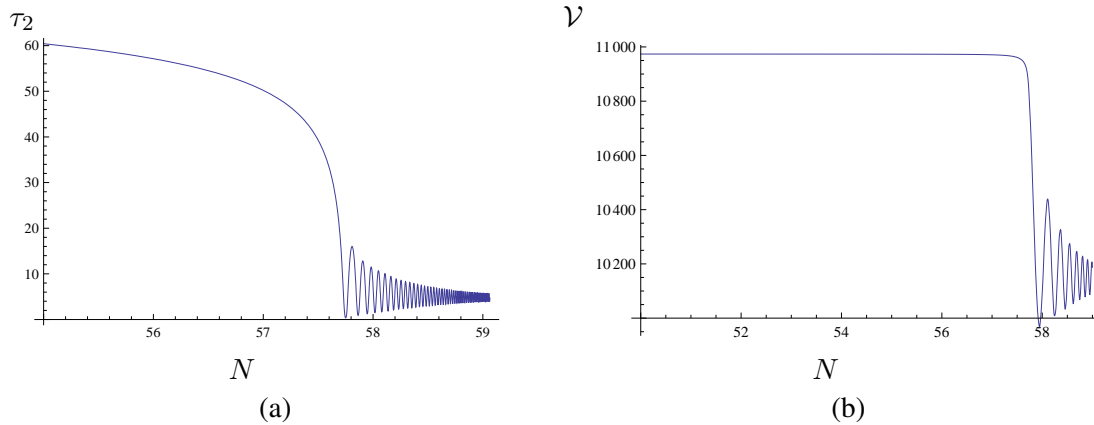


**Figure 3.7:** Evolution of the different moduli fields in the last few e-folds in Example 4. (a) Evolution of the field  $\tau_2$  (the inflaton). (b) Evolution of the field  $\mathcal{V}$ .

degrees of freedom, namely,  $\tau_3$  and  $\mathcal{V}$ . This allows for the possibility of having an inflationary valley sitting at the minimum of the potential along those directions, even in cases where  $\rho \sim 1$ .

In summary, the examples shown above demonstrate the existence of a large region of parameter space within these models with inflationary solutions consistent with current cosmological observations even when one relaxes most of the constraints stated in [47].

### 3.6 Conclusions

Realising inflation in the context of string theory has been played by a number of difficulties from the onset. The former relies on scalar fields slowly evolving in an almost flat potential, whereas the natural scales for parameters in string theory tend to have potentials which are too steep to sustain an extended period of inflation. Moreover, the plethora of moduli fields arising in these models makes it difficult to have just one field evolving (the inflaton) whilst the others remain fixed in their minima. Therefore, when a model is proposed which appears to successfully reconcile these two important disciplines it deserves attention. The model proposed by Conlon and Quevedo [47] is one such example and has been the focus of this chapter.

We have performed a detailed numerical analysis of inflationary solutions in the Kähler moduli sector of the Large Volume Models built in the context of type IIB flux com-

pactifications. Our investigations confirmed the key result of [47], namely that there are inflationary solutions where all but one of the moduli fields, (the inflaton), are stabilised to the local minima of the potential. We have provided explicit examples of these trajectories, and shown how the corresponding tilt of the density perturbations power spectrum leads to a robust prediction of  $n_s \approx 0.96$  for 60 e-folds of inflation, in agreement with the analytic prediction. However, we have gone further and showed that even when all the moduli fields play an important role in the overall shape of the scalar potential, inflationary trajectories still exist. In particular, we have demonstrated that there exists a direction of attraction for the inflationary trajectories that correspond to the constant volume direction. It leads to a basin of attraction which enables the system to have an island of stability in the set of initial conditions leading to inflation.

Furthermore we were able to show, using the numerical evolution of the fields under the influence of the full potential, that there are still successful inflationary trajectories even when one relaxes most of the assumptions made in the analytical approximations of [47]. This is an interesting point that makes the conclusions from these type of models much more robust.

The examples discussed throughout this chapter are not special regions of parameter space in which inflation occurs. We find that the choice of parameters giving the Kähler inflation scenario can be quite general. This has been shown in the example sets of [53] where a number of parameter sets in the  $\rho \ll 1$  regime (similar to the example studied in 3.5.2 where shown to realise inflation. Similarly we found many regions of parameter space in which examples similar to examples 2,3 and 4 of this chapter were realised. The robustness of this model resides in part to the appearance of the basin of attraction which we will study further in the next chapter. We will utilise the broad class of parameter choices and describe the effect particular choices have on the scalar potential (3.4). One however must be careful that the overall volume remains large. If this is the case the inclusion of the  $\alpha'$  corrections is justified and we have the large volume class of vacua of [44]. There must also still exist a minimum for  $\mathcal{V}$ , which becomes easier with the inclusion of additional 'small' Kähler moduli, since these generate a minimum for the overall volume [44].

# Chapter 4

## On the Basin of Attraction, Axionic Inflation and the generation of perturbations

### 4.1 Basin of attraction

In the previous chapter, we considered that the fields  $\tau_1$  and  $\tau_3$  were initially placed at the local minimum, associated with the displacement of  $\tau_2$  from its global minimum, i.e.  $\tau_1^i = \tau_1^{\text{local}}$  and  $\tau_3^i = \tau_3^{\text{local}}$ . In this section, we want to relax this assumption and verify whether the model allows for some freedom in the choice of initial conditions, namely we would like to see whether there is a region in the space of  $\tau_1^i$ ,  $\tau_2^i$  and  $\tau_3^i$  that leads to viable inflationary solutions as good as the ones presented above.

We note that the relative difference between  $\tau_3^{\text{local}}$  and  $\tau_3^f$  as given by Eqns.(3.27), (3.29), (3.36), (3.37), (3.40), (3.41) and (3.45), (3.46), is at the most of only a few percent. Hence, we can consider that for an initial condition in the vicinity of  $\tau_3^{\text{local}}$ ,  $\tau_3$  is nearly constant during inflation. This simplification allows us to illustrate the shape of the scalar potential during inflation, and, in particular, to show that there is a basin of attraction in the  $(\tau_1, \tau_2)$  plane. We show this plane in Figs. 4.1 and 4.2 as well as Fig. 4.3 and 4.4 corresponding to examples 1, 2, 3 and 4, respectively. The dashed line represents the direction of constant volume  $\mathcal{V}$  for fixed  $\tau_3^i = \tau_{\text{local}}$ . We

also show in Figs. 4.1, 4.2, 4.3 and 4.4 (blue lines), the full numerical evolution of the fields with initial conditions slightly away from (3.29), (3.36), (3.41) and (3.46). This choice serves our purpose but initial conditions further away from the local minimum are also allowed and can in fact increase the number of e-folds of inflation as  $\tau_2$  can be displaced to higher values.

We see that the basin of attraction not only stabilises the evolution of the fields directing them towards the global minimum, but also forces them to satisfy the essential condition  $\mathcal{V} \approx \text{constant}$  which is established by the orientation of the basin itself in the  $(\tau_1, \tau_2)$  plane. When inflation terminates, the fields quickly evolve to the global minimum and the evolution departs from the trajectory  $\mathcal{V} \approx \text{constant}$  represented in the figures.

Curiously, this variation of the internal manifold volume  $\mathcal{V}$  leads to the existence of two different scales for the gravitino mass. During inflation  $\mathcal{V} \approx \mathcal{V}_i$  and once it ends, the fields fall to the global minimum where, at least in our examples,  $\mathcal{V} = \mathcal{V}_f < \mathcal{V}_i$ . Given that the gravitino mass is,

$$m_{3/2}^2 \sim e^K |W|^2 \sim W_0^2 / (\mathcal{V} + \xi/2)^2 \sim W_0^2 / \mathcal{V}^2, \quad (4.1)$$

we have  $m_{3/2_{\text{inflation}}}^2 \approx W_0^2 / \mathcal{V}_i^2$  and  $m_{3/2_f}^2 = W_0^2 / \mathcal{V}_f^2$ , leading to a larger gravitino mass after inflation. For the four sets of parameters in our examples, the gravitino masses during inflation are  $m_{3/2} = 3 \times 10^{-7}$ ,  $3 \times 10^{-7}$ ,  $2 \times 10^{-7}$  and  $2 \times 10^{-4}$  in Planck units, for examples 1, 2, 3 and 4, respectively. These scales are rather high and therefore not very appealing phenomenologically. Actually this is typically the case in most of the inflationary models built from string theory. This follows from the fact that, as was argued in [35, 34] and recently in relation to the string vacua of this thesis in [32], the scale of inflation is generically bounded from above by the mass of the gravitino  $H \lesssim m_{3/2}$ . Therefore since these string inflationary models (in order to reproduce the correct amplitude for the density perturbations given by current observational data) predict a high scale of inflation, they also predict as well a high supersymmetry breaking scale. This is sometimes referred to as the gravitino mass problem. This feature is stronger in this class of inflationary models built from the  $\alpha'$ -corrected Kähler potential [123, 124], where the scale of inflation that can be realised within these setups corresponds to  $H \sim m_{3/2} / \mathcal{V}^{1/2}$  or  $H \sim m_{3/2}^{3/2}$  using Eq. (4.1), which will typically rise

to even higher supersymmetry breaking scales. Recall, however, that this mass corresponds to the gravitino mass during inflation, which does not have to be necessarily the same as the gravitino mass in the vacuum. This point has been used for example in [107, 121, 122] to propose a mechanism which can achieve low energy supersymmetry breaking scales, which consists in performing an extra fine-tuning in the models, through the addition of Kähler moduli dependent terms in the Kähler potential so that the gravitino mass during and at the end of inflation are substantially different. [107] used a method first described in Barrerio, de Carlos and Copeland, [80] which used the friction of the background expansion caused by presence of a background baryotropic fluid to stabilise the dilaton by forcing it into an attractor solution an is crucial for the success of [107]. In the context of these models it is interesting to note that the examples mentioned above also display a different gravitino mass during and after inflation. Unfortunately in our examples we have always found  $m_{3/2}^i < m_{3/2}^f$  and therefore the gravitino mass at the vacuum is heavier than the one during inflation which is going in the wrong direction. The question is whether or not there are trajectories of the form described in the previous examples which can lead to the volume increasing immediately after inflation. There is no obvious reason why this can not happen, but it remains a challenge to find an example.

#### 4.1.1 Variation of parameters

The existence of the basin of attraction holds with the relaxation of the constraint (3.11), which requires  $\rho \ll 1$ . This constraint restricts the form of the potential by minimising its variation with the displacement of the moduli field. Relaxation of this constraint whilst considering the full dynamics of the fields allows for a class of inflationary trajectories in which the overall volume has two scales, which could be used to overcome the gravitino mass problem. Resolution of the problem requires the increase in value of the overall volume  $\mathcal{V}$  at the end of the inflationary epoch. This would correspond to a decrease in the gravitino mass at the end of inflation. If the variation in volume was significantly large one could theoretically have high energy inflation whilst predicting a suitably low present day gravitino mass. This mechanism could occur through a number of dynamical situations,

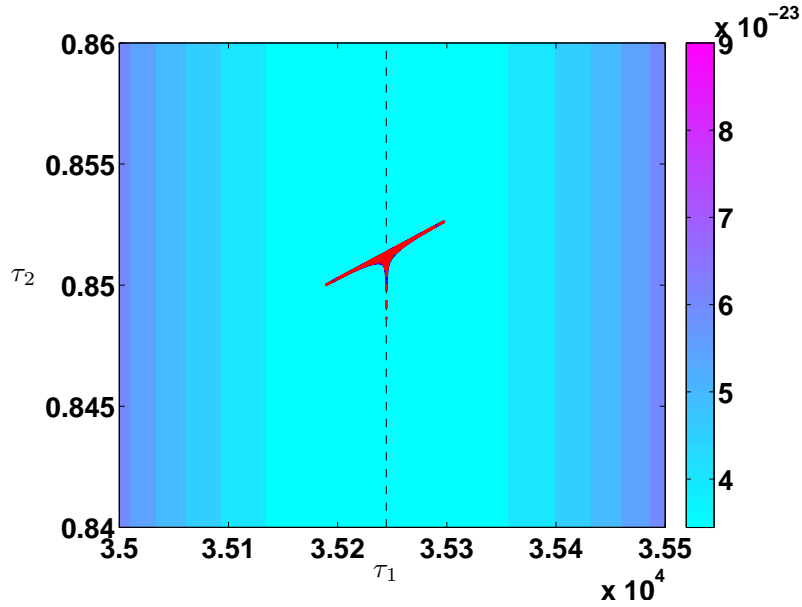


**Figure 4.1:** Contour plot of the scalar potential  $V$  in the  $(\tau_1, \tau_2)$  plane for fixed  $\tau_3 = \tau_3^{\text{local}}$ , for example 1 of chapter 3. The dashed line shows the trajectory which maintains volume  $\mathcal{V}$  constant at this fixed  $\tau_3$ . The trajectories plotted are  $\theta_2^i = \theta_{2_{\min}}$  (blue solid line) and  $\theta_2^i \neq \theta_{2_{\min}}$  (red dashed line).

1. The modulus controlling the overall volume,  $\tau_1$  has a local minimum in the basin of attraction at a smaller value than its global minimum. At the end of inflation the  $\tau_1$  modulus would roll towards its global minimum increasing the overall volume's size. This would require the 'light' blow up cycles,  $\tau_i$ , where  $i = 2, \dots, n$  have negligible contribution as they roll to their global minimum values. Since the  $\tau_1$  modulus appears only in the Kähler potential it is thought that this is only achievable through fine tuning of the model dependant parameter  $\lambda_1$ . This parameter simply rescales the cycle size and we conclude this outcome cannot exist.
2. All or a single 'light' modulus have local minima in the basin at larger values than their global minimum values, as seen in the examples, with  $\rho \geq 1$ . The motion of the field as it rolls towards its minimum would significantly decrease  $\mathcal{V}$  since these moduli describe the blow up cycles, or holes in the internal manifold. Additionally the variation of the  $\tau_1$  field is negligible since any  $\delta\tau_1$  leads to significant variation of  $\mathcal{V}$ .
3. Additional contributions to the Kähler potential [107], following the attractor

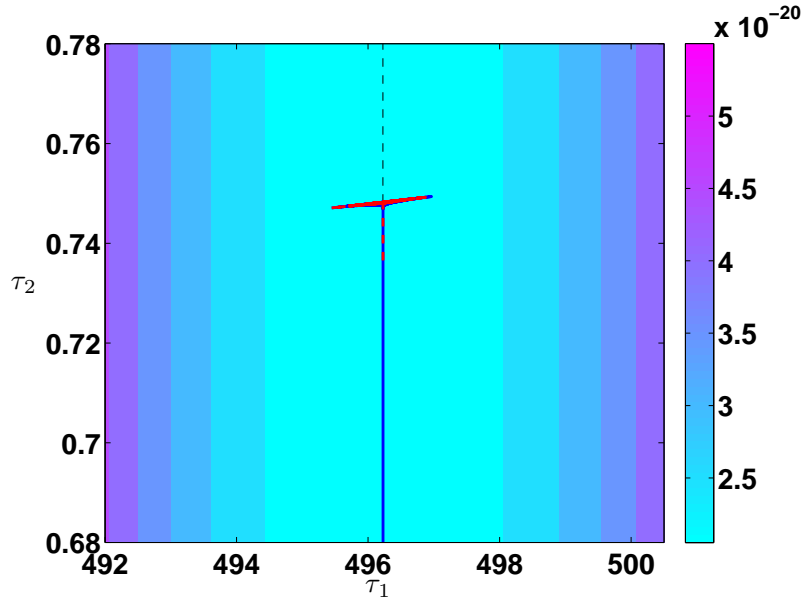


**Figure 4.2:** Contour plot of the scalar potential  $V$  in the  $(\tau_1, \tau_2)$  plane for fixed  $\tau_3 = \tau_3^{\text{local}}$ , for example 2 of chapter 3. The dashed line shows the trajectory which maintains volume  $\mathcal{V}$  constant at this fixed  $\tau_3$ . The trajectories plotted are  $\theta_2^i = \theta_{2_{\min}}$  (blue solid line) and  $\theta_2^i \neq \theta_{2_{\min}}$  (red dashed line).

mechanism idea of [80].

Example 4 in the previous chapter gave the closest example to the second scenario above, with  $\rho \sim 1$  and only a small variation in the overall volume at the end of inflation, whilst the initial  $\tau_2$  was almost 20 times that of its value in the minimum, however this still met with a positive  $\delta\mathcal{V}$ . Investigation into the possibility of finding such methods achieved through the tuning of model parameters could help in locating a region of parameter space which would give a negative  $\delta\mathcal{V}$ .

The volume at its global minimum value is seen via the relation (3.12) to be proportional to  $W_0$  while the values of the rest of the fields are proportional to  $\frac{W_0}{\mathcal{V}}$ . This implies that through a rescaling  $W_0 \rightarrow \alpha W_0$ , the volume of the minimum is rescaled by  $\mathcal{V} \rightarrow \alpha\mathcal{V}$  whilst leaving the rest of the values of the moduli invariant. This is seen as we adjust the value of  $W_0$  and determine the location of the global minimum, Table 4.1. The variation of  $W_0$  alters the minimum of the volume and scale of inflation as expected. Therefore with tuning of the parameters, it is possible to use large  $W_0$  to obtain the large volumes required in order to satisfy phenomenological constraints,

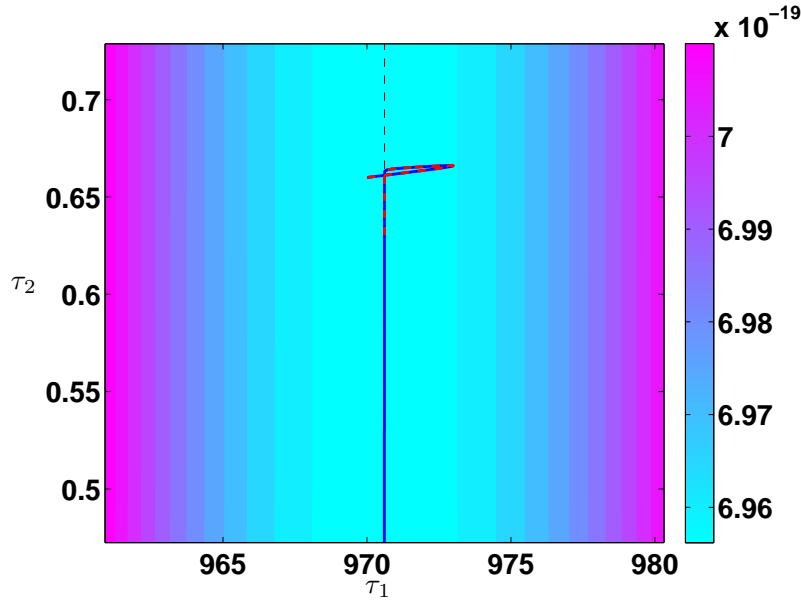


**Figure 4.3:** Contour plot of the scalar potential  $V$  in the  $(\tau_1, \tau_2)$  plane for fixed  $\tau_3 = \tau_3^{\text{local}}$ , for example 3 of chapter 3. The dashed line shows the trajectory which maintains volume  $\mathcal{V}$  constant at this fixed  $\tau_3$ . The trajectories plotted are  $\theta_2^i = \theta_{2_{min}}$  (blue solid line) and  $\theta_2^i \neq \theta_{2_{min}}$  (red dashed line).

$m_{3/2} \sim 1$  TeV (corresponding to  $\mathcal{V} \sim 10^{15}$ ). For the parameters considered this leads to a variation of  $\delta\mathcal{V} \sim -22\%$  post inflation. The percentage change in the overall volume as the system evolves from the basin of attraction to the global minimum is left invariant under variation of  $W_0$ . The final decrease is in contrast to the increase in volume desired, with it appearing evident that any choice of  $W_0$  will not lead to a solution of the gravitino mass problem.

If suitable tuning of the parameters are to yield a solution to this problem, it lies in the parameters characterising the  $\alpha'$  corrections to the Kähler potential or the non perturbative sector. Since we are limited in our choice of the  $\alpha'$  parameters we look to the non-perturbative sector and consider the effect of varying  $a_i, A_i$ .

We find the possibility of generating significant volume variations,  $\delta\mathcal{V}$  through variation of  $A_2$  whilst leaving the global minimum values of the Kähler moduli (Table 4.2) relatively unaltered. It is possible to achieve large variations between the global minimum and inflationary values of  $\mathcal{V}$  with  $A_2 = (1/2, 3/2)$  giving changes of  $\delta\mathcal{V} \sim (20\%, 30\%)$ . This however, similarly to  $W_0$ , lifts the potential's overall scale and the basin is still at a large volume than the global minimum volume,  $\mathcal{V}_{inf} > \mathcal{V}_{min}$ .  $a_i$  is

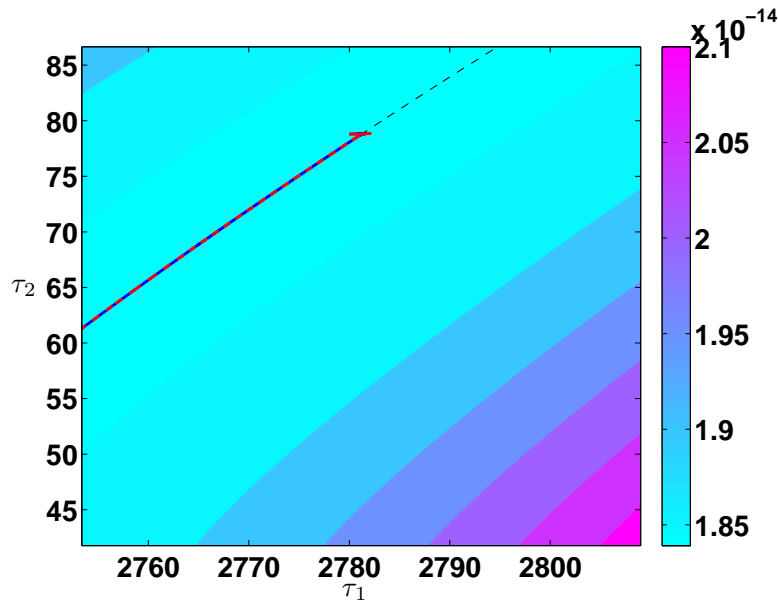


**Figure 4.4:** Contour plot of the scalar potential  $V$  in the  $(\tau_1, \tau_2)$  plane for fixed  $\tau_3 = \tau_3^{\text{local}}$ , for example 4 of chapter 3. The dashed line shows the trajectory which maintains volume  $\mathcal{V}$  constant at this fixed  $\tau_3$ . In this example, the inflationary trajectory is essentially given by a combination of two fields. The trajectories plotted are  $\theta_2^i = \theta_{2_{min}}$  (blue solid line) and  $\theta_2^i \neq \theta_{2_{min}}$  (red dashed line).

a constant that depends on the specific source of the nonperturbative effects. Gaugino condensation gives  $a_i = 1/N$ , where  $N$  is the gauge group of the theory, whilst D3 instantons have  $a_i \sim n$ , where  $n$  is the winding number of the D3 instantons wrapping 4-cycles [16]. If we consider  $W_{np}$  arising from non perturbative effects, considering a smaller gauge group  $N$ , corresponding to a larger  $a_i$  value leads to interesting results which are given in Table 4.3. We find an increase in  $a_2$  decreases the overall scale of the potential whilst reducing the variation between the two gravitino mass scales. This can lead to significant variations in the volume with  $a_2 = 15\pi$  giving a change of  $\delta\mathcal{V} \sim 54\%$ . In the Large volume scenarios the Volume modulus is a function of the Kähler moduli with the minimum of the potential is given approximately by

$$V_{min} \approx -\frac{3}{2} \left[ \sum_{i=2}^k \frac{\alpha\lambda_i}{a_i^{3/2}} (\ln\mathcal{V}_{min} - c_i^{3/2}) - \frac{\xi}{2} \right] + V_{up}, \quad (4.2)$$

where  $\mathcal{V}_{min}$  is the stabilised internal volume of the Calabi Yau and  $c_i = \ln\left(\frac{3\alpha\lambda_i W_2}{4a_i A_i}\right)$ , with the moduli satisfying the equation  $a_i\tau_i \approx \ln\mathcal{V} - c_i$ . We can see that, as  $a_i$  is increased, the exponential suppression of the minimum is decreased and the minimum is lifted. The SUSY minimum is given when  $D_{T_i}W = 0$  which can be solved to give

the position of the fields at the minimum,

$$W_0 = \frac{(\mathcal{V} + \frac{\xi}{2})}{2} a_i A_i (T_i + \bar{T}_i)^{1/2} e^{-a_i T_i} - \sum_j A_j e^{-a_j T_j}. \quad (4.3)$$

Through a basic search of parameter space we have found no choices of  $a_2$  which lead to a decrease in the volume of the potential after inflation, whilst we have seen how tuning of a number of parameters can lead to significant variations in  $\delta\mathcal{V}$ . The possibility that there exists a critical point to these parameters where, for example, decreasing  $a_i$  sufficiently leads to a negative  $\delta\mathcal{V}$  has not been ruled out and it remains interesting that such trajectories could exist.

Due to the attractor nature of the inflationary regime, whereby when  $\tau_2$  is displaced from its global minimum the system evolves towards a region of parameter space where  $\mathcal{V} = \text{constant}$  and the moduli settle in their local minima, it is possible that the system has an associated attractor solution, and a phase plane analysis of the system could well provide a means of understanding the underlying mechanisms of the model. We outline the system of equations that one would study in Appendix A. Such an analysis of cosmologies has been carried out for similar scenarios [76, 78, 79, 80, 81, 77], to determine the stability of models and the nature of their critical points. One could use these techniques to investigate whether any solutions exist which lead to the trajectory increasing in volume at the end of inflation. The addition of a background baryotropic fluid [42, 41] to the models of inflation can, in general, widen the range of initial conditions which lead to successful stabilisation of moduli fields. The presence of a background fluid introduces a regime where the dynamics of the system are dominated by the additional matter source. When this occurs the evolution of the field enters a scaling regime causing the field to 'track' the evolution of the background fluid. This regime is independent of the initial conditions and occurs whenever the background fluid dominates the evolutions. This has been applied to exponential potentials considered too steep to drive a period of inflation with successful results [77], to show the successful stabilisation of the dilaton in a cosmological setting [80], in the KKLT model to stabilise the volume modulus for a large set of initial conditions [79] and, more recently, in [107] to solve the gravitino problem after a period of Large volume Kähler inflation. In the examples studied any significant  $\tau_3$  displacement leads to runaway evolution of the moduli fields, with the volume no longer having a minimum.

This arises since the  $\tau_3$  modulus provides the dominant contribution in the stabilisation of the volume, [44]. Through the addition of a fluid to this model the range of  $\tau_3$  displacements that lead to stabilisation could conceivably be significantly increased. An analysis of the equations derived in Appendix A is a future project.

$W_0$	$\mathcal{O}(V_{min})$	$\tau_{min}$	$\mathcal{V}_{min}$	$\mathcal{O}(V_{basin})$	$\mathcal{V}_{basin}$
1	$10^{-15}$	(482.166 , 0.2305 , 5.863)	10573.2	$10^{-13}$	13029.8
10	$10^{-16}$	(2227.5 , 0.2304 , 5.858)	105115.3	$10^{-14}$	128685.5
100	$10^{-17}$	(10334.3 , 0.2303 , 5.858)	$1.05 \times 10^6$	$10^{-15}$	$1.285 \times 10^6$
1000	$10^{-18}$	(47965.3 , 0.2303 , 5.858)	$1.05 \times 10^7$	$10^{-16}$	$1.285 \times 10^7$
10000	$10^{-19}$	(222634 , 0.2303 , 5.858)	$1.05 \times 10^8$	$10^{-17}$	$1.285 \times 10^8$
$10^{10}$	$10^{-24}$	$(4.7965 \times 10^8 , 0.23039 , 5.8584)$	$1.05 \times 10^{13}$	$10^{-22}$	$1.285 \times 10^{13}$
$10^{12}$	$10^{-26}$	$(1.0334 \times 10^{10} , 0.23039 , 5.8584)$	$1.05 \times 10^{15}$	$10^{-24}$	$1.285 \times 10^{15}$

**Table 4.1:** Location of the global minimum of the scalar potential and the order of the basin of attraction under variation of the flux generated superpotential term,  $W_0$ . Tuning  $W_0$  can lift the scale of the potential. The variation between the two volume scales  $\delta\mathcal{V}$  is left unchanged  $\delta\mathcal{V} \sim 23\%$ , since the overall volume at its minimum  $\mathcal{V}_{min}$  and in the basin  $\mathcal{V}_{basin}$  both scale similarly.

$\xi$	$\beta(\times 10^{-4})$	$V_{min}$	$\tau_i$	$\mathcal{V}_{val}$	$\delta\mathcal{V}$
20	7.98	$1.5355 \times 10^{-14}$	(246.566 , 0.2151 , 5.263)	4671.8	1.21047
23	3.93	$6.2411 \times 10^{-15}$	(408.614 , 0.2267 , 5.714)	10076.6	1.222
24	3.13	$8.7033 \times 10^{-15}$	(482.166 , 0.2305 , 5.863)	13029.8	1.23236
25	2.49	$1.2134 \times 10^{-15}$	(564.095 , 0.2341 , 6.004)	16430.8	1.22775
$A_2$	$\beta$	$V_{min}$	$\tau_i$	$\mathcal{V}_{val}$	$\delta\mathcal{V}$
1/2	3.11	$3.6162 \times 10^{-16}$	(481.239 , 0.2198 , 5.861)	12641	1.199
1	3.13	$8.7033 \times 10^{-15}$	(482.166 , 0.2305 , 5.863)	13029.8	1.23236
3/2	3.14	$1.1944 \times 10^{-14}$	(482.293 , 0.2367 , 5.863)	13264	1.254

**Table 4.2:** Location of the global minimum of the scalar potential (3.4) and the order of the basin of attraction under variation of leading order  $\alpha'$ -correction  $\xi$  and  $A_2$ .

## 4.2 Evolving the Axions

Up to now the axion fields have been set to their local minimum, given by  $\cos a_i \theta_i = -1$ . However this has been for convenience due to the simplification this provides. In reality, in a full analysis, we should let these fields evolve and so we now turn our attention to investigate what happens if we allow the axions  $\theta_i$  to evolve, as well as all the fields  $\tau_i$ . As expected, if the initial conditions for the axions are such that they are placed at their minimum values the examples described above do not change, as the

$a_2$	$V_{min}$	$\tau_{min}$	$\mathcal{V}_{min}$	$\mathcal{O}(V_{basin})$	$\mathcal{V}_{basin}$	$\delta\mathcal{V}$
$15\pi$	$4.3623 \times 10^{-15}$	(473.863 , 0.2980 , 5.84757)	10300.9	$10^{-13}$	15900.5	1.543
$25\pi$	$1.7682 \times 10^{-14}$	(488.695 , 0.1887 , 5.8772)	10788.9	$10^{-14}$	12474.2	1.1562
$200\pi$	$2.1667 \times 10^{-14}$	(501.603 , 0.02846 , 5.898)	11219.8	$10^{-14}$	11301.88	1.0073

**Table 4.3:** Location of the global minimum of the scalar potential (3.4) and the order of the basin of attraction under variation of  $a_2$ . The separation of the inflationary basin and the global minimum can be significantly tuned with the value of  $a_2$ . The uplift parameter  $\beta$  required to obtain a dS vacua is roughly the same in each scenario.

axions do not get displaced from their minimum. However the situation is modified when the initial conditions for the axions are such that they are perturbed from their minimal values. In such a situation a number of different scenarios emerge. In the case in which only the axion corresponding to the inflaton field,  $\theta_2$  is perturbed, we see that the fields evolve in such a way as to roughly reproduce the situation described by Bond et al in [53] (for the case  $\rho \ll 1$ ). In particular, viable inflationary trajectories exist, but the new initial conditions allow for a greater variety of trajectories in which the rolling of the axion can increase the number of e-foldings over those trajectories restricted to lie only in the  $\tau_2$  direction. Such evolutions are the red dashed trajectories in Figs 4.1,4.2, 4.3 and 4.4. The trajectories we observe are similar but within the dynamics there are subtle differences in the evolution arising from the fact we have included full Kähler moduli dynamics, whereas in the analysis of Bond et al [53] all moduli except the displaced inflaton field  $\tau_2$  were fixed at their global minimum values and a constant volume physically imposed.

### 4.2.1 Comparison of Bond and Full Kähler Moduli Analysis

In allowing the evolution and destabilisation of all the moduli we see that the inflation dynamics are altered significantly and differ considerably from [53]. For the initial conditions used in their analysis which they argued lead to rapid stabilisation of the displaced field, we now find that the system evolves towards a basin of attraction with the destabilisation of all the  $\tau_i$  fields. In particular we have analysed the ' $\tau_2$ -valley' where the axions are set to the minimum of their potential. Once here the axions remain fixed and do not contribute to the evolution. Let us now compare the observations of axion displacement in the full model with the roulette model of [53]. It was identified in [53] that full generality would only be achieved through allowing the evolution of

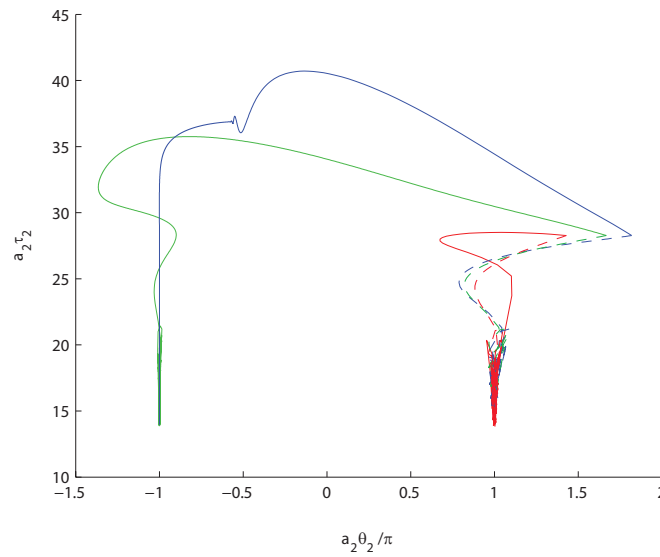


**Figure 4.5:** Comparison of Bond et al. analysis (dashed lines) and Full analysis (solid lines) for  $\tau_{2_i} = 0.45$  and  $\theta_{2_i} = (1/11, 1/12, 1/14)$  for the red, green and blue trajectories respectively. Trajectories using Bond style analysis.  $T_1$  and  $T_3$  fields are not evolved with all fields set to the global minimum values except for the initial displacement of the  $\tau_2$  and  $\theta_2$  fields. Allowing all the moduli fields to evolve in the full analysis we find significantly different trajectories.

all moduli fields and promoting  $\mathcal{V}$  to be a dynamical variable. Following their example and only evolving the equation of motion for the complex field  $T_2 = \tau_2 + i\theta_2$ , whilst fixing the  $T_1$  and  $T_3$  fields one is able to reproduce the roulette inflation results and find the variety of inflationary trajectories seen in [53] arising from parameter set 1 given by,

$$\begin{aligned} \xi &= \frac{1}{2}, & \alpha &= \frac{1}{9\sqrt{2}}, & \lambda_2 &= 1, & \lambda_3 &= 10, & a_2 &= \frac{2\pi}{3}, & a_3 &= \frac{2\pi}{300} \\ A_2 &= \frac{1}{10}, & A_3 &= \frac{1}{200}, & \beta &= 8.5 \times 10^{-6}, & W_0 &= 300. \end{aligned} \quad (4.4)$$

Since  $\rho \ll 1$ , the rolling of  $T_2$  leaves  $\mathcal{V} \sim \text{constant}$ . The dashed line trajectories of Fig.4.5 show some trajectories which correspond to roulette type scenarios using the parameter set given above, these trajectories arise from an initial displacement of  $\tau_2$  and  $\theta_2$ . These simulations show the initially displaced fields simply roll towards the global minimum of the potential. For the displacements shown this results in negligible periods of inflation, however with greater displacement of the  $\tau_2$  field it was shown large periods of inflation could be obtained. We, however, use these trajectories to

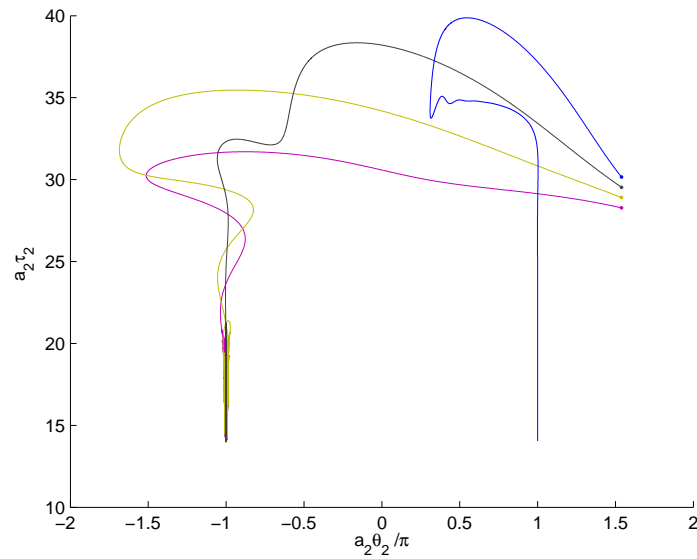


**Figure 4.6:**  $T_2$  plane for simulations using the full dynamical analysis of chapter 3 with an initially non-zero axionic component,  $\theta_{2i} = 1/13$ . Shown are trajectories with a variation of  $\tau_{2i} = (0.45, 0.46, 0.47, 0.48)$ .

highlight the variation in dynamics when all the moduli are allowed to evolve. When these same initial conditions are repeated but allowing all the moduli to evolve as described in chapter 3, the resulting trajectories are significantly different, resulting in basin like inflationary trajectories similar to those studied in chapter 3. These resemble the larger  $\tau_2$  displacements of Bond et al [53], but differ from those obtained using the same initial conditions, these trajectories are given by the solid lines in Figure 4.5. Looking at the  $\theta_{2i} = 1/14$  trajectory, given by the solid blue line in Figure 4.5 we see the trajectory overcomes the axionic ridges of the potential (3.4) in the  $\theta_2$  direction as it evolves towards the basin of attraction. The trajectory oscillates about the basin where it eventually settles. Once the system sits in the basin of attraction the axionic component is minimised and the  $\tau_2$  field evolves along the basin as in the  $\tau$ -valley like solutions given by [53]. The evolution towards the basin of attraction occurs over a short timescale (recall Figure 4.1 where the red trajectory shows a non-minimal  $\theta_2$  component) which has consequences for the perturbation spectrum generated at the end of inflation which we will discuss at the end of this section. As we increase the initial displacement of  $\tau_2$  we find the exploration of the axionic direction is reduced, Figure 4.6. The solid black trajectory in this figure shows the evolution of the fields

in the  $\tau_2 - \theta_2$  plane after an initial displacement of  $\tau_{2_i} = 0.47$ ,  $\theta_{2_i} = 1/13$ . As the system evolves it is 'pulled' towards the basin of attraction, however the field is not sufficiently close to the basin of attraction in the  $\tau_2$  direction and rolls towards the global minimum instead. There then is a critical displacement of  $\tau_{2_{crit}}$  which leads to the system evolving to the basin of attraction resulting in inflationary trajectories. It is clear from the solid blue trajectory of Figure 4.5 corresponding to the initial conditions  $\tau_{2_i} = 0.45$ ,  $\theta_{2_i} = 1/14$  that  $\tau_{2_{crit}}$  is lowered as the axionic component is increased. The solid blue trajectory corresponding to  $\tau_{2_i} = 0.48$ ,  $\theta_{2_i} = 1/13$  has an initial displacement  $\tau_2 > \tau_{2_{crit}}$ . This trajectory evolves to large  $\tau_2$  values before the field then moves towards the basin of attraction. Once in the basin the axionic component is minimised and the  $\tau_2$  field begins slow roll inflation towards its global minimum. Having identified the differences observed between the analysis of [53] and the full analysis of chapter 3 in the  $\tau_2 - \theta_2$  plane, let us look at the effect the full analysis has on the other fields which are no longer set to their global minimum values, but are now allowed to evolve. The initial displacement of the axion  $\theta_2$  also leads to complex evolution in the

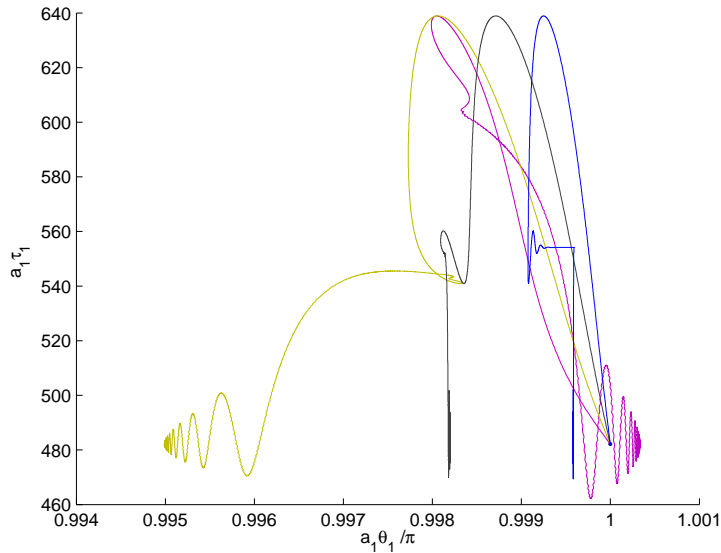


**Figure 4.7:**  $T_1$  plane for a number of simulations with a initially non-zero axionic component,  $\theta_{2_i} = 1/13$ . This shows the variation of the trajectories for  $\tau_{2_i} = (0.45, 0.46, 0.47, 0.48)$

$\tau_1 - \theta_1$  plane, Fig.4.7. There exists no minimum for the  $\theta_1$  axion as it is not stabilised

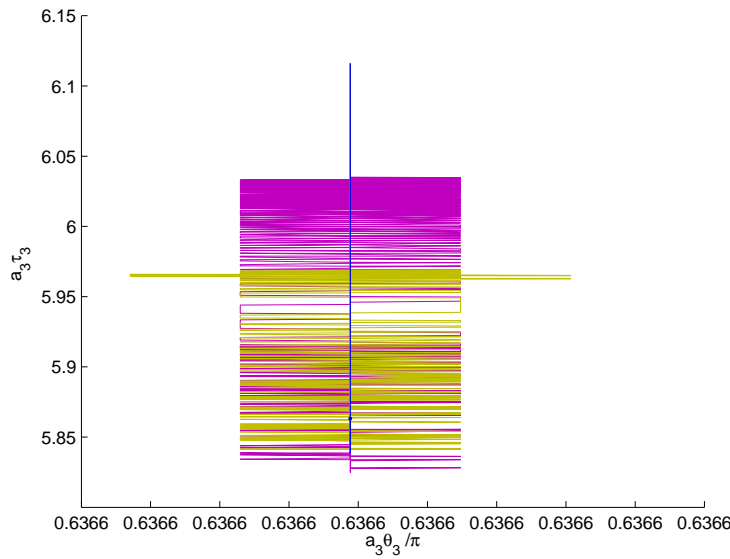


**Figure 4.8:**  $T_3$  plane for a number of simulations with an initially non-zero axionic component,  $\theta_{2i} = 1/13$ . This shows the variation of the trajectories with a variation of  $\tau_{2i} = (0.45, 0.46, 0.47, 0.48)$ .

through the superpotential terms and so corresponds to a flat direction, with its dynamics completely determined by the variation of the other moduli fields. For this reason any initial value of  $\theta_1$  is indistinguishable from any other as far as evolutionary dynamics and stabilisation are concerned. Taking again the initial conditions of  $\tau_{2i} = 0.48$ ,  $\theta_{2i} = 1/13$  corresponding to the solid blue line of Figure 4.7, the evolution towards the basin can clearly be seen.  $\tau_1$  becomes attracted towards and begins to oscillate about the basin, where  $\tau_1 \sim 550$ . The field remains at this roughly constant value for the duration of the inflationary epoch as was shown in chapter 3. Interestingly an initial  $\theta_{2i}$  component has little effect on the trajectories in the  $\tau_3$ - $\theta_3$  plane (Figure 4.8), where the  $\theta_3$  field is seen to oscillate rapidly about its minimum. The  $\tau_3$  field simply evolves towards its basin value as we have previously described in chapter 3. We have so far displaced the axion  $\theta_2$ , the axionic component to the Kähler moduli that plays the dominant role as the inflaton field in the examples of chapter 3. This has revealed a rich class of inflationary scenarios similar to those of [53] in their exploration of the axionic plane, leading in some situations to the stabilisation of all moduli in different minima from the one originally displaced from. Although similar, these highly curved trajectories rapidly explore the axionic plane and reduce to a roughly ' $\tau$ -valley' trajec-

tory. We can find a further class of inflationary scenarios corresponding to perturbing an axion which belongs to the same multiplet as the field which plays the dominant role in the stabilization of the volume, which in our examples would correspond to the field  $\theta_3$ . In this case one can show that the set of viable initial conditions for inflationary trajectories is restricted to small initial perturbations in the position of the axion ( $\delta\theta_3 \ll 1$ ) away from its minimum. Any other significant perturbation of  $\theta_3$  leads to runaway non-inflationary trajectories. Conversely we find  $\theta_1$  displacements have no effect on the evolution of this system. The reason for these different behaviours can be understood as follows: the rolling of the axion field  $\theta_1$  does not have a noticeable impact on the position of the minimum of the volume modulus. On the other hand, a displacement of the axionic field  $\theta_3$  will instead have an effect on the position of the volume modulus, as can be easily read from (3.10). This means that almost any displacement on the field  $\theta_3$  will have the effect of displacing the volume modulus from its minimum and as a consequence of that the fields would tend to roll towards the decompactification limit.

Having found the variety of possible inflationary scenarios through considering the evolution of the axionic fields, let us now return to one of the fundamental differences observed between the analysis of Bond et al [53] and the analysis of chapter 3 when we give an initial displacement to  $\theta_2$ . Interestingly we have seen the axionic exploration arising from a full dynamical consideration occurs on a relatively short time scale and occurs prior to the onset of inflation, shown in the red dashed lines of Figures 4.1, 4.2, 4.3 and 4.4. This is in contrast to the findings of [53] and [51] where the inflationary trajectory has a large axionic component for the majority of time for which the system is inflating [51]. This difference arises through the assumption of a static volume and negligible effect caused by the  $\tau_2$  displacement. It is expected that the rapid minimisation of the axion dynamics will have significant effects on the perturbation spectrum and the generation of isocurvature perturbations in the model. Following the approach in [53] a perturbation analysis of their results found that highly curved trajectories lead to the generation of isocurvature modes. When such modes are present they interact with the adiabatic modes at super horizon scales affecting the evolution of the curvature perturbations [52]. The curvature perturbations sources through isocurvature modes in highly curved trajectories was in fact found to be the major contribution to

the power spectrum after significant periods of inflation [52, 51]. A curved trajectory in field space, in their results corresponding to a large exploration of the axionic plane during the inflationary epoch lead to the sourcing of adiabatic perturbations from isocurvature modes [52] with trajectories with long periods of curving during inflation generating almost all of its power spectrum from isocurvature modes. Such significant isocurvature modes were found to give a large power spectrum which was generally red-tilted and was found to be a general feature of roulette inflation. In contrast to what one would expect from a highly curved field space trajectory the roulette model was found not to give observably large levels of nongaussianity [51]. The coupling of the curvature and isocurvature modes is in general expected to be the cause of a large bispectrum and hence a prediction of nongaussianity. The ' $\tau_2$ -valley' trajectory produced no super horizon nongaussianities for this reason. In the full analysis we see that the axionic component is quickly damped away and the inflationary trajectory is effectively a ' $\tau$ -valley trajectory' of [53, 47]. Since an axionic displacement quickly reduces to the single field case it is expected that the assumption of the previous chapter in which the isocurvature modes were considered negligible still holds. In addition the perturbation spectrum will closely resemble that of the single field ' $\tau$ -valley' in [52, 51] and there will be no nongaussianity generated by the interaction of scalar fields at superhorizon scales. For cases where the constraint  $\rho \ll 1$  is violated, the class of trajectories seen numerically remains roughly consistent with those of the  $\rho \ll 1$  models. For this class of models the separation of the basin of attraction and the global minimum is significant (see examples 3, 4 of chapter 3) however a displacement of the  $\theta_2$  axion although leading to a large exploration of the axionic plane does this in a relatively short period of time and prior to the onset of inflation. This can be seen in Figures 4.1, 4.2, 4.3, 4.4 where the simulations with an initial axionic component are given by the red dashed line. It is then expected that the single field,  $\tau$ -valley predictions for the generation of perturbations and nongaussianities will be a good approximations to those expected here even in the presence of large curved trajectories of the axion,  $\theta_2$ . The key point being that the trajectories are found to be highly curved prior to the period of inflation. Example 4 is a possible exception to this due to the large curved trajectory in the  $\tau_1 - \tau_2$  plane throughout the inflationary epoch, this is shown in Fig.4.4. Although the axionic component  $\theta_2$  is still minimised quickly in this example it is expected that

non trivial perturbation signatures would then arise from the curved trajectory in the  $\tau_1 - \tau_2$  plane. In the two field Kähler moduli inflation model of [111] it was shown that when an additional Kähler modulus is considered to the single field Kähler moduli inflation of [47] the isocurvature mode did not decay rapidly as was found in the  $\tau$ -valley scenario [52]. This lead to a large contribution to the power spectrum from the correlation of the curvature and isocurvature modes. It is expected that there will be similar effects in example 4 of chapter 3 with the curvature perturbation at the end of inflation being significantly sourced by the isocurvature perturbations due to the highly curved trajectory.

### 4.3 Conclusions

We have shown that even when all the moduli fields play an important role in the overall shape of the scalar potential, inflationary trajectories still exist. In particular, we have demonstrated that there exists a direction of attraction for the inflationary trajectories that correspond to the constant volume direction. It leads to a basin of attraction which enables the system to have an island of stability in the set of initial conditions leading to inflation. A large range of inflation  $\tau_2$  directions is found and with suitable tuning of the model parameters we can obtain volume changes  $\delta\mathcal{V} \sim 54\%$ . The variety of inflationary trajectories obtainable through the displacement of other fields was seen to be severely restricted due to the nature of these fields in the model.  $\tau_3$  a stabilising field, present in order to generate a minimum for the volume modulus was limited to displacements  $\delta\theta_3 \ll 1$ . With the introduction of a fluid the option of using stabilising techniques to widen the range of valid initial conditions leading to stabilisation of all dynamical moduli was suggested. An interesting consequence of considering the full Kähler dynamics was the generation of two distinct values of the gravitino mass,  $m_{3/2}$  hinted at a possible mechanism to solve the gravitino mass problem. Through identifying the effects of the parameters on the potential a discussion on the existence of a region of parameter space for which  $\delta\mathcal{V} > 0$  at the end of inflation was presented. The existence of such a solution still evades us, whilst techniques to model attractor solutions in cosmological systems were suggested as a step towards understanding if such a class of models can be ruled out. Using a phase plane analysis the authors of

[77] where able explore the stability of a cosmological model. Through a perturbation analysis they were able to determine the models entered a scaling solution at late times. We were able to show that potentials too steep to drive inflation on their own now could play a possible role of inflation through this scaling regime. Application of similar methods in this model could identify the nature of the basin of attraction and could be used to search for trajectories which would solve the gravitino mass problem. An outline of a future project on this was outlined in appendix A.

Having previously looked at the evolution of the moduli fields with the axion fields restricted to be in their minima in chapter 3, we then in this chapter extended the analysis to allow also for the slight displacement of the axions from their equilibrium position. Whereas a variation of the axion  $\theta_2$  (the partner of the inflaton) still led to a large basin of attraction for the inflationary trajectories (as in [53]), in the case of the axion  $\theta_3$  (the one that lives in the same multiplet as the moduli field responsible for stabilising the volume modulus), a small fluctuation of  $\theta_3$  from its true minimum value is enough to create runaway solutions where all the fields roll towards the decompactification limit. Hence we have a new restriction on these class of models,  $\theta_3$  needs to be very close to its minimum value for inflation to take place. The implications of  $\theta_2$  displacement on the generation of perturbations in Roulette models was discussed [52, 51]. The rapid suppression of the axionic component reducing the inflationary trajectory to the  $\tau$ -valley solution of [53] resulted in the prediction of little (if any) nongaussianity.

# Chapter 5

## Multiple Field Slow Roll Inflation in Supergravity models

### 5.1 Introduction

Achieving a complete implementation of Inflation in a relatively relaxed parameter space takes us one step closer to observationally distinct 'stringy' predictions. After a successful realisation of an inflationary model and the stabilisation of all the moduli, the idea of comparing a string inspired model with cosmological observations seems tantalisingly close. The standard technique used in analysing inflation models is the slow roll approximation [59, 62, 58]. These approximations are, in general, an extremely useful way in which to quantify the predictions of inflation and have become useful since a slow roll analysis can be used to make direct comparisons between models of inflation without having to know the precise form of model, in particular the exact inflationary potential (additionally they bypass the need to find solutions to the equations of motion analytically, which can be done for only a very few simplistic toy models). Using the slow roll parameters it is possible to identify locations on a potential where inflation might occur. Such predictions are found tied onto the back of inflationary models as a 'proof of existence' and it is customary to simplify the analysis in order to make such observational contact. This is an often overlooked yet indispensable area of string cosmology which requires greater care due to the complexities of string inspired models. The standard slow roll formalism however is routed in

the assumption of single scalar field inflaton. As we have seen in chapter 2 string compactifications generally give rise to large numbers of scalar fields, which modern models of inflation, such as that of Kähler moduli inflation studied in chapter 3, utilise as candidate inflaton fields. Additionally the presence of multiple field models can lead to interesting physics such as the generation of isocurvature modes, a feature only associated with models with more than one component. It seems inevitable then that the slow roll formalism must be sufficiently able to describe the inflationary characteristics of the multiple field models.

In this chapter we look at the variety of formalisms and definitions of the slow roll parameters used in contemporary cosmology, with an emphasis on the techniques and methods used in analysing supergravity models of inflation. Such models generally have a number of fields evolving in a complex trajectory on some non-trivial target space metric,  $g_{ab}$ . We argue that considering the slow-roll parameters in a such a way is essential if phenomenological predictions are to be made. These formalisms are then extended so the multiple field definitions in a supergravity setting include  $\xi^2$ , commonly referred to as the third slow roll parameter, and the running of the scalar spectral index  $\frac{dn_s}{dlnk}$ .  $\xi^2$  here differs from the  $\xi$  defined in chapter 2 equation (2.46) corresponding to the leading order  $\alpha'$  correction to the Kähler potential. Since this chapter will focus on the slow roll parameters we will maintain conventions, using  $\xi^2$  as the slow roll parameter and make it clear when the  $\alpha'$  correction  $\xi$  is being used. A comparative study of these formalisms is then carried out for particular models of inflation arising from supergravity. We analyse a chaotic like potential arising in supergravity and a more realistic String inspired inflationary model where a realistic moduli stabilization technique is implemented. We find that, since these models contain many coupled dynamical scalar fields, this results in the different formalisms of slow roll producing different observational predictions. A meaningful analysis of the inflationary model therefore requires consideration of all the subtleties arising and the effect of these fields has on the slow roll predictions of an inflationary model.

We find the eigenvalue analysis used in the literature in the better racetrack inflationary model of [73] gives the most robust predictions of the slow roll parameters in multiple field scenarios, but note that this formalism itself has its short fallings since it makes use of relations derived under the assumption of a single field inflaton when predicting

the scalar spectral index,  $n_s$  and its running  $\frac{dn_s}{d\ln k}$ .

## 5.2 Standard Inflationary Cosmology

The equations of motion for a homogeneous, massive scalar field in a FRW spacetime are given by

$$\ddot{\phi} + 3H\dot{\phi} + V_{,\phi} = 0, \quad 3H^2 \approx M_p^2 \left( \frac{1}{2} \dot{\phi}^2 + V \right). \quad (5.1)$$

We define the slow roll limit as the regime in which the acceleration of the scalar field is negligible compared to the friction term caused by the expanding universe,

$$3H\dot{\phi} + V_{,\phi} \approx 0, \quad 3H^2 \approx M_p^2 V, \quad (5.2)$$

that is, we have the conditions that  $|\dot{\phi}^2| \ll |V|$  and  $|\ddot{\phi}| \ll 3H\dot{\phi}$ , leading to the constraints on the potential and its derivatives,

$$\epsilon \equiv M_p^2/2 \left( \frac{V_{,\phi}}{V} \right)^2 \ll 1, \quad \eta \equiv M_p^2 \frac{V_{,\phi\phi}}{V} \ll 1. \quad (5.3)$$

These slow roll constraints provide the requirement that, in order to be in a slow-rolling regime, the potential must be very flat and have small curvature. There exists another way of defining the requirements of potentials in order for inflation to take place, called the Hamilton-Jacobi formalism. Infact this allows us to rewrite the equations of motion in order to determine inflationary results in an easier fashion. Differentiation of the Friedmann constraint with respect to time and substitution of the scalar field's equation of motion gives,

$$2\dot{H} = -\frac{\dot{\phi}^2}{M_p^2}. \quad (5.4)$$

If we divide through by  $\dot{\phi}$  we obtain a relation between the scalar field and time,  $\dot{\phi} = -2M_p^2 H'(\phi)$ , where the prime is a derivative with respect to  $\phi$ . The Friedmann equation can now be rewritten giving the Hamilton-Jacobi equation

$$H'(\phi)^2 - \frac{3}{2M_p^2} H^2(\phi) = -\frac{1}{2M_p^4} V(\phi). \quad (5.5)$$

It allows us to consider the function  $H(\phi)$  in place of  $V(\phi)$ . This is a more natural quantity to use in describing inflation since once we have specified  $H(\phi)$  the inflationary potential can be reconstructed using this formalism. From this one can then determine  $H(t)$ . Using the new language of inflation we can define the Hamilton-Jacobi slow-roll parameters as

$$\epsilon_H \equiv 2M_p^2 \left( \frac{H'(\phi)}{H(\phi)} \right)^2, \quad (5.6)$$

$$\eta_H \equiv 2M_p^2 \frac{H''(\phi)}{H(\phi)}, \quad (5.7)$$

which in the slow roll limit can be written as

$$\epsilon_H = -\frac{\dot{H}}{H^2}, \quad (5.8)$$

$$\eta_H = \frac{\ddot{\phi}}{H\dot{\phi}} \quad (5.9)$$

These parameters are useful since the slow-roll approximation derived using this formalism does not depend on any assumption or approximation. Inflation is given exactly as  $\ddot{a} > 0$  which occurs when  $\epsilon_H < 1$ . This is a much stronger constraint in contrast to the  $V(\phi)$  slow roll approximations (5.3). To see this recall that inflation is defined as a period of accelerated expansion which gives us the condition,

$$\frac{\ddot{a}}{a} = \dot{H} + H^2 > 0, \quad (5.10)$$

which, for a scalar field, is satisfied when  $\dot{H} < 0$ , leading to the condition

$$\epsilon_H \equiv -\frac{\dot{H}}{H^2} < 1, \quad (5.11)$$

which ensures inflation,  $\ddot{a} > 0$ , is occurring whilst a second condition  $\eta_H \equiv -\frac{\ddot{\phi}}{H\dot{\phi}} < 1$  ensures that inflation lasts sufficiently long.

The two independent definitions of the slow-roll parameters can be shown to be equivalently in the slow-roll limit. First we differentiate the Friedmann equation with respect to time and by application of the slow roll equations (5.2) we get the relation,

$$\begin{aligned} 6H\dot{H} &= M_p^2 V_{,\phi} \dot{\phi}, \\ \dot{H} &= \frac{M_p^2}{2} \frac{V'^2}{(3H)^2}, \\ \frac{\dot{H}}{H^2} &= -\frac{M_p^2}{2} \left( \frac{V'}{V} \right)^2. \end{aligned} \quad (5.12)$$

By use of the slow roll equations once more we find

$$\begin{aligned}\ddot{\phi} &\approx -\frac{\dot{H}\dot{\phi}}{H} - \frac{V_{\phi\phi}\dot{\phi}}{3H}, \\ \frac{-\ddot{\phi}}{H\dot{\phi}} &= M_p^2 \frac{V_{\phi\phi}}{V} - \frac{M_p^2}{2} \left(\frac{V_{\phi}}{V}\right)^2,\end{aligned}$$

from which we find the relations between the two definitions in the slow roll limit given by,

$$\epsilon_H = \epsilon, \quad \eta_H = \eta - \epsilon. \quad (5.13)$$

In addition to the slow roll parameters  $\epsilon$  and  $\eta$ , two more useful observable quantities are the scalar spectral index,  $n_s$  and its running,  $\frac{dn_s}{d\ln k}$ . The 'effective spectral index',  $n_s(k)$ , is defined as the interval of comoving wavenumber  $k$  in which we can consider the variation of the power spectrum as a constant

$$n_s - 1 \equiv \frac{d\ln \mathcal{P}_{\mathcal{R}}}{d\ln k}, \quad (5.14)$$

assuming that  $\mathcal{P}_{\mathcal{R}} \propto k^{n-1}$ , where  $\mathcal{P}_{\mathcal{R}}$  is the spectrum of curvature perturbations generated during inflation,

$$\mathcal{P}_{\mathcal{R}}(k) = \left(\frac{H}{\dot{\phi}}\right)^2 \left(\frac{H}{2\pi}\right)^2 \Big|_{k=aH}. \quad (5.15)$$

The power law relation of the perturbations and wavenumber arises since angular scales cross outside the Horizon rapidly during a period of inflation. As the perturbations amplitude is governed by the physical conditions at this point, we are left with an almost scale invariant spectrum of perturbations since the rapid exit effectively freezes the physical conditions in the state at this exit point.

The power spectrum for a slow rolling scalar field can be written as

$$\mathcal{P}_{\mathcal{R}}(k) = \frac{1}{12\pi^2 M_p^6} \frac{V^3}{V'^2} = \frac{1}{24\pi^2 M_p^4} \frac{V}{\epsilon}, \quad (5.16)$$

and the spectral index can be related to the slow roll parameters by considering that, at horizon crossing,  $k = aH$  if the horizon size is constant. The rate of change of the horizon  $\dot{H}$  is negligible compared to  $\dot{a}$  giving,

$$\frac{d\ln k}{dt} \approx H. \quad (5.17)$$

Now, using the slow roll condition,  $3H\dot{\phi} \approx -V'$  we find

$$\begin{aligned} d \ln k &= -\frac{3H^2}{V'} d\phi, \\ \frac{d}{d \ln k} &= -M_p^2 \frac{V'}{V} \frac{d}{d\phi}. \end{aligned} \quad (5.18)$$

These relations along with (5.14) and (5.16) give us the scalar spectral index in terms of the slow roll parameters<sup>1</sup>,

$$n_s - 1 = -6\epsilon + 2\eta. \quad (5.19)$$

This result is useful as it predicts that in single field inflation it generates very small variations of the curvature spectrum away from the scale invariant case of  $n_s = 1$ , providing an observable able to distinguish between inflationary potentials. In addition the variation of the scalar spectral index with wavenumber, known as the running,  $\frac{dn_s}{d \ln k}$  can provide even more stringent tests of inflationary scenarios. This can also be defined in terms of the slow-roll parameters. Using (5.18) we can find the variation of the slow roll parameters with wavenumber,

$$\begin{aligned} \frac{d\epsilon}{d \ln k} &= -M_p^2 \frac{V'}{V} \frac{d}{d\phi} \left( \frac{M_p^2}{2} \left( \frac{V'}{V} \right)^2 \right) = -\frac{M_p^4}{2} \frac{V'}{V} \left( \frac{2V''V'}{V^2} + \frac{(-2)V'^2V'}{V^3} \right) \\ &= -2\epsilon\eta + 4\epsilon^2 \end{aligned} \quad (5.20)$$

$$\begin{aligned} \frac{d\eta}{d \ln k} &= -M_p^2 \frac{V'}{V} \frac{d}{d\phi} \left( M_p^2 \frac{V''}{V} \right) = -M_p^4 \frac{V'}{V} \left( \frac{V'''}{V} - \frac{V''V'}{V^2} \right) \\ &= +2\epsilon\eta - \xi^2, \end{aligned} \quad (5.21)$$

where we have defined a third slow roll parameter,

$$\xi^2 \equiv M_p^4 \frac{V'V'''}{V^2}. \quad (5.22)$$

Using the relation for the scalar spectral index (5.19) and the variation of the slow roll parameters with wavenumber (5.20), (5.21) and the definition (5.22) we find,

$$\begin{aligned} \frac{dn_s}{d \ln k} &= \frac{d}{d \ln k} (1 - 6\epsilon + 2\eta) = -6 \frac{d\epsilon}{d \ln k} + 2 \frac{d\eta}{d \ln k} \\ &= 16\epsilon\eta - 24\epsilon^2 - 2\xi^2. \end{aligned} \quad (5.23)$$

<sup>1</sup>The Hamilton-Jacobi formalism gives the spectral index as  $n_s - 1 = -4\epsilon_H + 2\eta_H$ , due to the difference between  $\eta_H$  and  $\eta$ .

With this we now have all the required relations in order to define a slow roll footprint of any single field inflationary model. These parameters were first introduced in order to see where inflation might occur in potentials that could not necessarily be solved exactly [59, 62, 63]. They are commonly used as a means of linking theoretical models of inflation to some observational prediction and provide a method of directly comparing models. The derivation of the slow roll formalism considered only a single homogeneous scalar field with a canonical kinetic term. Whilst providing an adequate set equations for determining regions in which inflation is likely to occur, it fundamentally requires the model to contain only one field throughout the duration of inflation. Otherwise the equation of motion and the Friedmann constraint given in (5.1) would contain additional contributions from other fields. Ignoring the contributions from additional fields, and simply calculating the slow roll parameters would provide a poor approximation to the true form of any multiple field inflationary potential. Additionally the assumption of a canonical kinetic term vastly restricts the models that one can study using this standard slow roll formalism. In supergravity models of inflation, with one example being that studied in chapter 3 there exists a field space metric  $K_{i\bar{j}}$ , where  $i, \bar{j}$  run over all the moduli fields. This metric appears in the equation of motion for the fields and can lead to non trivial field dynamics which the formalism derived in this section could not accurately describe unless the model could be reduced to an effectively single field limit.

### 5.3 Supergravity models

Having motivated the need for a multiple field slow roll formalism in the context of modern string inspired inflationary models we now follow the work of [74] and, in parts, [73], presenting two formalisms developed through which multiple field inflationary scenarios can be adequately analysed providing more stringent predictions for the slow roll parameters than those obtained through application of the standard single field slow roll formalism. Recall from chapter 3 that the equations of motion for Kähler moduli fields can be obtained by varying the minimal  $N = 1, d = 4$  effective

supergravity action<sup>2</sup> of the form,

$$S = - \int d^4x \sqrt{-g} \left( \frac{1}{2} R + g_{i\bar{j}} \partial_\mu \phi^i \partial^\mu \bar{\phi}^{\bar{j}} + V \right), \quad (5.24)$$

where  $g_{i\bar{j}}$  is the target-space metric,  $\phi^i$  and  $\bar{\phi}^{\bar{j}}$  are the complex chiral superfields. Considering a spatially flat FRW spacetime we have the equations of motion,

$$\begin{aligned} \ddot{\phi}^l + 3H\dot{\phi}^l + \Gamma_{ij}^l \dot{\phi}^i \dot{\phi}^j + g^{l\bar{k}} \partial_{\bar{k}} V &= 0, \\ 3H^2 &= k_p^2 \left( g_{i\bar{j}} \dot{\phi}^i \dot{\phi}^{\bar{j}} + V \right). \end{aligned} \quad (5.25)$$

The conditions of slow roll in the multi-field case are generalisations of the single field slow roll assumptions  $|\dot{\phi}^2| \ll |V|$  and  $|\ddot{\phi}| \ll 3H\dot{\phi}$  where we now have  $\frac{D}{dt}\dot{\phi}^i = \ddot{\phi}^i + \Gamma_{jk}^i \dot{\phi}^j \dot{\phi}^k$ . This leads us to the multiple field slow roll assumptions,  $|K_{i\bar{j}} \dot{\phi}^i \dot{\phi}^{\bar{j}}| \ll |V|$  and  $|\frac{D}{dt}\dot{\phi}^i| \ll |H\dot{\phi}^i|$ . Under these assumptions the equations of motion reduce to

$$3H\dot{\phi}^i \equiv -K^{i\bar{j}} V_{,\bar{j}} \quad , \quad 3H^2 = M_p^2 V, \quad (5.26)$$

with

$$\begin{aligned} 6H\dot{H} &= M_p^2 (V_{,i} \dot{\phi}^i + V_{,\bar{j}} \dot{\phi}^{\bar{j}}), \\ \dot{H} &= \frac{M_p^2}{6H} \left( -\frac{K^{i\bar{j}} V_{,i} V_{,\bar{j}}}{3H} - \frac{K^{i\bar{j}} V_{,i} V_{,\bar{j}}}{3H} \right) \\ &= -\frac{M_p^2 K^{i\bar{j}} V_{,i} V_{,\bar{j}}}{(3H)^2}, \end{aligned} \quad (5.27)$$

comparing the above equation to (5.12), the presence of the complex field gives twice the previous slow roll parameter<sup>3</sup>,

$$\epsilon_H \equiv -\frac{\dot{H}}{H^2} = \frac{M_p^2 K^{i\bar{j}} V_{,i} V_{,\bar{j}}}{V^2}, \quad (5.28)$$

and the Hamiltonian definition of  $\eta$  is,

<sup>2</sup>In chapter 2 we saw how the low energy 4d description of Type IIb orientifold compactifications [12] was given by  $N = 1$ ,  $d = 4$  effective supergravity.

<sup>3</sup>If the scalar field was not complex the additional factor of 2 would be absent.

$$\eta_H \equiv \sum_a \frac{\ddot{\phi}^a}{H\dot{\phi}^a} = \frac{\ddot{\phi}^i}{H\dot{\phi}^i} + \frac{\ddot{\phi}^{\bar{j}}}{H\dot{\phi}^{\bar{j}}} \quad (5.29)$$

$$\begin{aligned} &= 2\epsilon_H - \eta_l^i \frac{V^{,l}}{V^{,i}} - \eta_l^{\bar{i}} \frac{V^{,\bar{l}}}{V^{,\bar{i}}} - \eta_l^{\bar{i}} \frac{V^{,l}}{V^{,\bar{i}}} - \eta_l^i \frac{V^{,\bar{l}}}{V^{,i}} \\ &= \eta - \epsilon_H, \end{aligned} \quad (5.30)$$

where we have used ; to denote a covariant derivative with respect to  $g_{ij}$ . Looking also at the slow roll assumptions again, we have the new definitions of the slow-roll conditions,

$$\frac{M_p^2 K^{i\bar{j}} V_{,i} V_{,\bar{j}}}{V^2} \ll 1, \quad (5.31)$$

$$-\frac{M_p^2 K^{i\bar{j}} V_{,i} V_{,\bar{j}}}{V^2} - \frac{M_p^2}{V} \left( V_{;l}^i \frac{V^{,l}}{V^{,i}} + V_{;\bar{l}}^{\bar{i}} \frac{V^{,\bar{l}}}{V^{,\bar{i}}} \right) \ll 1, \quad (5.32)$$

which are equivalent to the slow roll constraint

$$\epsilon_H < 1, \quad \eta_H < 1, \quad (5.33)$$

under the additional constraint of

$$\frac{V^{,i}}{V^{,j}} = \frac{K^{i\bar{k}} V_{,\bar{k}}}{K^{j\bar{l}} V_{,\bar{l}}} \sim \mathcal{O}(1). \quad (5.34)$$

This constraint, when multiplied with the slow roll definitions  $\epsilon$ ,  $\eta$ , should be small in order to satisfy the slow roll conditions (5.31). Satisfying this constraint alone is not an indication that a model lies in an inflationary region, but assures that in the slow roll limit we reproduce the relation (5.33) from (5.31). If we define the matrix,

$$\begin{aligned} \eta_a^b &= M_p^2 \frac{g^{cb} \nabla_a \nabla_c V}{V} \\ &= M_p^2 \frac{g^{cb} (V_{,ac} - \Gamma_{ac}^d V_{,d})}{V}, \end{aligned} \quad (5.35)$$

where  $\Gamma_{ac}^d = \frac{1}{2} g^{de} (g_{ae,c} + g_{ce,a} - g_{ac,e})$ , and we contract over the target space metric  $g_{ab}$  so that each direction in the field space is considered, then this gives us the slow roll definitions as used in [73]. Identifying these definitions as the eigenvalue method we have a method by which we can determine the slow roll parameters in a multiple field scenario. Defining the eigenvalue multiple slow-roll parameters as

$$\epsilon_{eig} \equiv \frac{M_p^2 K^{ab} \nabla_a V \nabla_b V}{2 V^2}, \quad (5.36)$$

$$\eta_{eig} \equiv \text{Min Eigenvalue}(\eta_a^b), \quad (5.37)$$

that is  $\eta_a^b \nu_b^{(n)} = \eta_{\text{eig}(n)} \nu_a^{(n)}$ , where the matrix  $\eta_a^b$  takes a similar form to the single field slow roll parameter  $\eta$ . The minimum eigenvalue is chosen since it is the most unstable direction describing the curvature of the potential. A positive eigenvalue here would describe an instability about a local minimum, and so it is not an unstable direction. A negative eigenvalue would suggest that there is a direction in the potential which is negatively curved, which would lead to the field slowly rolling towards some local minimum. It is therefore the largest and most negative eigenvalue of these parameters which is our slow roll parameter.

It appears we have simply promoted the potentials derivatives to covariant derivatives with respect to the target space metric in our definitions of the slow roll parameters, this would lead to  $V'^2 \rightarrow \nabla_a V \nabla_b V$  and  $V'' \rightarrow \nabla_a \nabla_b V$ . To obtain the slow roll parameters we simply contract with the target space metric. Naturally we ask whether there is an analogous slow roll parameter,  $\xi^2$  in the multiple field case. Following the generalisation above we would expect something similar to  $\xi^2 \sim M_p^4 \frac{K^{i\bar{j}} K^{k\bar{l}} \nabla_i V \nabla_{\bar{j}} \nabla_k \nabla_{\bar{l}} V}{V^2}$ , and so we define

$$\begin{aligned} \xi_{cd}^{ab} &= M_p^4 \frac{g^{ae} g^{bf} \nabla_e V \nabla_c \nabla_f \nabla_d V}{V^2} \\ &= M_p^4 \frac{g^{ae} g^{bf} V_{,e}}{V} \left( V_{,cfd} - (\Gamma_{fd}^g)_{,c} V_{,g} - \Gamma_{fd}^g V_{,cg} \right. \\ &\quad \left. - \Gamma_{cf}^h (V_{,hd} - \Gamma_{hd}^g V_{,g}) - \Gamma_{cd}^h (V_{,hf} - \Gamma_{hf}^g V_{,g}) \right), \end{aligned} \quad (5.38)$$

under the impression that  $\xi^2 \equiv \text{Min Eigenvalue}(\xi_{cd}^{ab})$  or something similar. It is easy to see this reduces to the standard definition (5.22) in the single field case, since the connection terms,  $\gamma_{bc}^a$ , all vanish leaving only the first term which for one field is simply the standard definition.

The indices in the definitions (5.35), (5.38) are for general fields, which can be the field or its conjugate (denoted by a bar), where  $a, b \dots = i, \bar{i}$  and  $i = 1, n$  are sums over the fields. We will later be considering complex fields and Kähler metrics, this will lead to simplification of a number of terms, whilst care will be required in consideration of the possible combinations of  $\eta_a^b$  and  $\xi_{cd}^{ab}$ . In general, when using this eigenvalue method, once the slow roll parameters, (5.35) have been determined the scalar spectral index is then found using the single field relation (5.14). This can also be applied to the running of the spectral index, using the result of (5.38) in the single field relation

for the running (5.23). This however is at arms with the reasoning behind developing a slow roll analysis for multiple field scenarios. For a consistent and proper treatment one requires a multiple field relation for the scalar spectral index. The scalar spectral index and its running also require a proper covariant treatment of the field trajectories in Supergravity models, with field interactions all contributing at some level to the generation of density perturbations. Since we have a multi component fluid there is the possibility of isocurvature perturbations. The definition of the curvature spectrum (5.15) in a multiple field system should be written as,

$$\mathcal{P}_{\mathcal{R}}(k) = \left( \frac{H^2}{K_{ij} \dot{\phi}^i \dot{\phi}^j} \right) \left( \frac{H}{2\pi} \right)^2 \Big|_{k=aH}. \quad (5.39)$$

We then find the power spectrum reduces to a similar form as (5.16),

$$\mathcal{P}_{\mathcal{R}}(k) = \frac{1}{12\pi^2 M_p^6} \frac{V^3}{K^{ab} V_{,a} V_{,b}}, \quad (5.40)$$

which then gives the spectral index as,

$$\begin{aligned} n_s - 1 &= \frac{d \ln \mathcal{P}_{\mathcal{R}}}{d \ln k} = -M_p^2 \frac{V_{,c}}{V} \frac{d}{d\phi^c} \left( \ln \frac{V^3}{V_{,b} V_{,b}} \right) \\ &= -M_p^2 \frac{V_{,c} V_{,b} V_{,b}}{V^4} \left[ \frac{3V^2 V_{,c}}{V_{,b} V_{,b}} - 2 \frac{V^3 V_{,c} V_{,b}}{V_{,b} V_{,b} V_{,d} V_{,d}} \right] \\ &= -3 \frac{M_p^2 V_{,c} V_{,c}}{V^2} - 2 \frac{M_p^2 V_{,c} V_{,b}}{V} \frac{V_{,c} V_{,b}}{V_{,d} V_{,d}} \\ &= -6\epsilon + 2\eta_c^b \frac{V_{,c} V_{,b}}{V_{,d} V_{,d}} = -6\epsilon + 2\eta_c^b N_c^b \end{aligned} \quad (5.41)$$

Where in the last line of (5.41) we have defined

$$N_b^a = \frac{V_{,a} V_{,b}}{V_{,d} V_{,d}}. \quad (5.42)$$

We can look at the variation of the new definitions of the slow roll parameters with respect to the comoving wavenumber,  $k$  and find an extended definition of the running of the scalar spectral index,

$$\begin{aligned}
 \frac{d\epsilon}{d\ln k} &= -\frac{M_p^2 V^{,c}}{V} \frac{d}{d\phi^c} \left( \frac{M_p^2 V^{,b} V_{,b}}{2V^2} \right) \\
 &= -\frac{M_p^4 V^{,c}}{2V} \left[ -\frac{2V^{,b} V_{,b} V_{,c}}{V^3} + \frac{2V_{;c}^{;b} V_{,b}}{V^2} \right] \\
 &= \frac{M_p^2 V^{,c} V_{,c}}{V^2} \frac{M_p^2 V^{,b} V_{,b}}{V^2} - \frac{M_p^2 V^{,c} V^{,d} V_{,d} V_{,b}}{V^2 V^{,d} V_{,d}} \frac{M_p^2 V_{;c}^{;b}}{V} \\
 &= 4\epsilon^2 - 2\epsilon \eta_c^b \frac{V^{,c} V_{,b}}{V^{,d} V_{,d}} = 4\epsilon^2 - 2\epsilon \eta_c^b N_b^c, \tag{5.43}
 \end{aligned}$$

and

$$\begin{aligned}
 \frac{d\eta_c^b}{d\ln k} &= -M_p^2 \frac{V^{,a}}{V} \frac{d\eta_c^b}{d\phi^a} \\
 &= -M_p^2 \frac{V^{,a}}{V} \frac{d}{d\phi^a} \left( \frac{M_p^2 V_{;c}^{;b}}{V} \right) \\
 &= \frac{M_p^2 V^{,a} V_{,a}}{V^2} \frac{M_p^2 V_{;c}^{;b}}{V} - \frac{M_p^4 V^{,a} (V_{;c}^{;b})_{;a}}{V^2} \\
 &= 2\epsilon \eta_c^b - \xi_{ca}^{ab}, \tag{5.44}
 \end{aligned}$$

where  $\xi_{ca}^{ab}$  is related to the proposed definition (5.38) by  $\xi_{ca}^{ab} = \xi_{cd}^{ab} \delta_d^a$ ,

$$\xi_{ca}^{ab} \equiv \frac{M_p^4 \nabla^a V \nabla_a \nabla_c \nabla^b V}{V^2} = \frac{M_p^4 V^{,a} (V_{;c}^{;b})_{;a}}{V^2}, \tag{5.45}$$

and, due to the  $N_b^a$  term in (5.41), we also need to consider its variation with wavenumber,

$$\begin{aligned}
 \frac{dN_b^c}{d\ln k} &= -\frac{M_p^2 V^{,a}}{V} \frac{dN_b^c}{d\phi^a} \\
 &= -\frac{M_p^2}{V} \left( \frac{V_{;a}^{;c}}{V} \frac{V^{,a} V_{,b}}{V^{,d} V_{,d}} + \frac{V_{;ba}}{V} \frac{V^{,a} V_{,c}}{V^{,d} V_{,d}} \right) + 2 \frac{M_p^2 V_{;a}^{;d}}{V} \frac{V^{,a} V_{,d} V^{,c} V_{,b}}{V^{,d} V_{,d} V^{,e} V_{,e}} \\
 &= -\left[ \eta_a^c N_b^a + \eta_{ba} N^{ac} - 2\eta_a^d N_d^a N_b^c \right], \tag{5.46}
 \end{aligned}$$

so we have the running to be

$$\begin{aligned}
 \frac{dn_s}{d\ln k} &= \frac{d}{d\ln k} (1 - 6\epsilon + 2\eta_c^b N_b^c) \\
 &= -24\epsilon^2 + [16\epsilon \eta_c^b - 2\xi_{ca}^{ab}] N_b^c - 2\eta_c^b \left[ \eta_a^c N_b^a + \eta_{ba} N^{ac} - 2\eta_a^d N_d^a N_b^c \right]. \tag{5.47}
 \end{aligned}$$

In the supergravity case we find additional contributions to the running of equivalent order to the first three terms in (5.41) which are those seen in the single field definition of the running, (5.23). These additional contributions cancel in the single field case and are a feature of supergravity models<sup>4</sup>. This extended definition provides new non-zero corrections to the running and provides a means to classify, and possibly rule out, particular multi field inflationary models with observations, thus providing a means to tighten constraints on the range of models allowed by current data sets.

The similarity between the single field and multiple field definitions of the spectral index and its running give the impression that  $\eta \sim \eta_b^a N_a^b$ . However this is not the case in general as this chapter will show. Great care and consideration is required in the calculations of these definitions. The parameter  $\xi_{cd}^{ab}$  was defined as an extension of the term arising in the standard slow-roll, usually defined as the third slow-roll parameter  $\xi^2$ , [58]. In fact in the derivation of the running (5.47) there arises a term very similar to  $\xi_{cd}^{ab}$ , multiplied by the  $N_b^c$  potential factor (5.42) with the additional sum over indices  $a, d$  i.e  $\xi_{ca}^{ab} N_b^c$ . We define the multiple field version of the third slow roll parameter  $\xi^2$  in each formalism as follows. Under the eigenvalue formalism identifying the eigenvalues of this parameter will give us the stability of the rate of change of the curvature, therefore a small value would represent a direction that would vary in its curvature negligibly and be a more suitable slow roll direction. We therefore take the eigenvalue closest to zero as the definition of the  $\xi^2$ ,

$$\xi_{eig}^2 \equiv \text{Eigenvalue closest to zero}(\xi_{ca}^{ab}), \quad (5.48)$$

For example if  $a = 1, 2$  we would find the eigenvalues of the matrix  $\xi_c^b = \xi_{c1}^{1b} + \xi_{c2}^{2b}$ . For the extended slow roll formalism of [74] the definition of  $\xi^2$  is made in analogy to that associated with  $\eta$ , giving the definition

$$\xi_H^2 \equiv \xi_{ca}^{ab} \frac{V_{,c}}{V_{,b}} \quad (5.49)$$

$$= \xi_{ja}^{ai} \frac{V_{,j}}{V_{,i}} + \xi_{ja}^{a\bar{i}} \frac{V_{,j}}{V_{,\bar{i}}} + \xi_{ja}^{a\bar{i}} \frac{V_{,\bar{j}}}{V_{,i}} + \xi_{ja}^{a\bar{i}} \frac{V_{,\bar{j}}}{V_{,\bar{i}}}, \quad (5.50)$$

where we use  $a, b, c$  indices to show sums over barred and unbarred indices,  $i, j, \bar{i}, \bar{j} = 1, \dots, n$ .

---

<sup>4</sup>It can be seen that the most significant effect of the multiple field contribution is when we have one direction of the potential rapidly changing with field value whilst the other fields remain constant.

### 5.3.1 Slow roll formalisms

We now have three formalisms in which we can calculate the slow roll footprint of a model.

#### 5.3.1.1 Single field

$$\epsilon \equiv M_p^2/2\left(\frac{V_{,\phi}}{V}\right)^2 \ll 1, \quad \epsilon \ll 1, \quad (5.51)$$

$$\eta \equiv M_p^2 \frac{V_{,\phi\phi}}{V} \ll 1, \quad |\eta| \ll 1, \quad (5.52)$$

$$\xi^2 \equiv M_p^4 \frac{V_{,\phi} V_{,\phi\phi\phi}}{V^2}, \quad (5.53)$$

and the scalar spectral index and its running defined respectively by,

$$n_s = 1 - 6\epsilon + 2\eta, \quad (5.54)$$

$$\frac{dn_s}{d\ln k} = 16\epsilon\eta - 24\epsilon^2 - 2\xi^2. \quad (5.55)$$

#### 5.3.1.2 Eigenvalue

$$\epsilon_{eig} \equiv \frac{M_p^2}{2} \frac{K^{ab} V_{,a} V_{,b}}{V^2}, \quad \epsilon_{eig} \ll 1, \quad (5.56)$$

$$\eta_{eig} \equiv \text{Min Eigenvalue} \left[ \eta_c^b \right], \quad |\eta_{eig}| \ll 1, \quad (5.57)$$

$$\xi_{eig}^2 \equiv \text{Min Eigenvalue} \left[ \xi_{ca}^{ab} \right], \quad (5.58)$$

with the spectral index and its running determined by the single field relations

$$n_{seig} = 1 - 6\epsilon + 2\eta, \quad (5.59)$$

$$\frac{dn_s}{d\ln k_{eig}} = 16\epsilon\eta - 24\epsilon^2 - 2\xi^2. \quad (5.60)$$

### 5.3.1.3 Extended method

$$\epsilon \equiv \frac{M_p^2}{2} \frac{K^{ab} V_{,a} V_{,b}}{V^2}, \quad (5.61)$$

$$\eta \equiv \eta_c^b \frac{V_{,c}}{V_{,b}}, \quad |\eta| \ll 1, \quad (5.62)$$

$$\xi^2 \equiv \xi_{ca}^{ab} \frac{V_{,c}}{V_{,b}}, \quad (5.63)$$

$$\frac{V_{,i}}{V_{,j}} \sim \mathcal{O}(1), \quad (5.64)$$

with the scalar spectral index and its running given respectively as

$$n_s - 1 = -6\epsilon + 2\eta_c^b \frac{V_{,c} V_{,b}}{V_{,d} V_{,d}} = -6\epsilon + 2\eta N^{bc}, \quad (5.65)$$

$$\begin{aligned} \frac{dn_s}{d \ln k} = & -24\epsilon^2 + [16\epsilon \eta_c^b \\ & - 2\xi_{ca}^{ab}] N_b^c - 2\eta_c^b [\eta_a^c N_b^a + \eta_{ba} N^{ac} - 2\eta_a^d N_d^a N_b^c], \end{aligned} \quad (5.66)$$

where the above formalisms use

$$\eta_c^b = M_p^2 \frac{g^{ca} (V_{,bc} - \Gamma_{bc}^d V_{,d})}{V}, \quad (5.67)$$

$$\xi_{ca}^{ab} = M_p^4 \frac{g^{ae} g^{bf} V_{,e}}{V} \left( V_{,cfd} - (\Gamma_{fd}^g)_{,c} V_{,g} - \Gamma_{fd}^g V_{,cg} \right. \quad (5.68)$$

$$\left. - \Gamma_{cf}^h (V_{,hd} - \Gamma_{hd}^g V_{,g}) - \Gamma_{cd}^h (V_{,hf} - \Gamma_{hf}^g V_{,g}) \right) \delta_d^a. \quad (5.69)$$

## 5.4 Comparative study of multiple field methods of slow roll inflation

What has become evident in the development and extension of an extended slow roll formalism of [74, 75] is that there exists a number of methods in the literature by which inflationary models are analysed. The single field approximations [62], the minimum eigenvalue method [73], and the extended formalism [74, 75]. There is also no favoured or standard method used by the Cosmology community for slow roll analysis when analysing string inspired inflationary models with non canonical kinetic terms. Ideally numerical simulations would provide accurate and reliable predictions

of the inflationary footprint for models, however the complexity of multiple field models requires significant periods of time and computing power to obtain such results. For this reason it is desirable obtain a standard method for making robust predictions of non-trivial inflationary scenarios. In this section a comparison of the various slow roll formalisms will be made. Using a variety of supergravity inflationary models we will highlight the inadequacy and pitfalls that can arise in predicting the slow roll observables.

### 5.4.1 Chaotic Inflation in Supergravity

We will first look at a well known model of inflation that can be realised in a supergravity setup and also has a single field equivalent, this will allow us to test the slow roll methods using easily derivable results. One such model is Chaotic inflation<sup>5</sup>, which is an attractive model in that in addition to solving the standard problems of cosmology [59, 60] it is possible to have almost arbitrary initial conditions of the inflaton field. This removes the requirement of the inflationary model builder to define a specific set of initial conditions - for insights into the current status of initial condition debates the reader is directed towards the indispensable textbook [83]. The textbook chaotic inflationary potential is,  $V = \frac{1}{2}m^2\sigma^2$ , where  $\sigma$  is the scalar field that plays the role of a slow rolling inflaton. In order to solve the standard horizon and flatness problems and achieving roughly  $N \sim 60$  e-foldings of inflation requires the initial value of  $\sigma_0 \gtrsim 16$  in Planck units [65]. Under such initial conditions the standard single field slow-roll parameters (5.3), (5.22) can be used to define the slow roll 'footprint' for chaotic inflation ,

$$\begin{aligned}\epsilon &= \frac{2M_p^2}{\sigma^2} \sim 7.81 \times 10^{-3}, \\ \eta &= \frac{2M_p^2}{\sigma^2} \sim 7.81 \times 10^{-3}, \\ \xi &= 0, \\ n_s &\sim 0.96875, \\ \frac{dn_s}{d\ln k} &\sim -4.88 \times 10^{-4}.\end{aligned}\tag{5.70}$$

---

<sup>5</sup>A generic name given to power law inflationary potentials which can have almost arbitrary initial conditions, e.g  $V = \lambda\phi^4$  where  $\lambda$  is a constant.

These predictions arise from approximating the standard equations of motion for an inflaton field in an expanding universe, (5.2), whilst the potential has been constructed solely to meet the conditions of inflation and so the single field slow roll parameters prove to be an excellent tool in analysing the model. However this inflationary scenario is completely separated from any fundamental theory and so is simply a toy model. The original concept of a chaotic inflation model has developed significantly over the years and recent work on inflationary model building has aimed to realise such models in supergravity, [65, 66, 67]. More recently, with the developments in constructing meta-stable de Sitter vacua in string theory as discussed in chapter 2, attention has turned to the embedding of traditional inflationary potentials into a realistic model of moduli stabilization [70, 69]. However since we are simply interested in the observational differences arising from each slow-roll formulation proposed we will not work within these models. Natural chaotic inflation [65, 66] provides a simple realisation of 'mutated' chaotic inflation arising in a supergravity context. Whilst still a toy model it has similarities to the textbook chaotic inflation introduced above, and also retains a relevance to today's cosmology since it has some foundation in a fundamental theory. Additionally since it arises from a supergravity action we are justified in using the multiple field definitions of the slow roll parameters in order to analyse the model and make a comparison between the 3 different approaches to slow roll.

We define the superpotential and Kähler potential for this model as,

$$\mathcal{K} = 1/2(\phi + \bar{\phi})^2 + \chi\bar{\chi}, \quad (5.71)$$

$$W = m\phi\chi, \quad (5.72)$$

where  $\phi$  is the inflaton chiral multiplet and  $\chi$  an additional chiral multiplet present in order to break the shift symmetry,  $\phi \rightarrow \phi + c$  where  $c$  is a constant, in a Kähler potential of this type, lifting the flat direction of the potential.

The resulting Kähler metric is flat and our scalar potential is

$$V(\phi, \chi) = m^2 e^{\mathcal{K}} [|\phi|^2(1 + |\chi|^4) + |\chi|^2(1 - |\phi|^2 + (\phi + \bar{\phi})^2(1 + |\phi|^2))]. \quad (5.73)$$

If we decompose into two real scalars,  $\phi = \frac{1}{\sqrt{2}}(\tau + i\sigma)$  the potential is

$$V(\tau, \sigma, \chi) = m^2 e^{\tau^2 + |\chi|^2} [1/2(\tau^2 + \sigma^2)(1 + |\chi|^4) + |\chi|^2(1 - 1/2(\tau^2 + \sigma^2) + 2\tau^2(1 + 1/2(\tau^2 + \sigma^2)))] \quad (5.74)$$

All the fields, except for  $\sigma$ , appear in the exponential factor and so should be taken to have values of order less than 1 in order to be less than the gravitational scale. On the other hand  $\sigma$  is not limited by this constraint and can take large values and will play the roll of our inflaton field. In this limit the potential takes the form of a Chaotic inflationary potential,

$$V \simeq \frac{1}{2}m^2\sigma^2 + m^2|\chi|^2. \quad (5.75)$$

Using the multi-field slow-roll formalism, and considering the limit in which all fields but  $\sigma$  are zero, we can compare the supergravity chaotic inflation model with a standard toy inflation model. Equation (5.61) reproduces the single field result for the first slow roll parameter,

$$\epsilon = \frac{2M_p^2}{\sigma^2} \quad (5.76)$$

The second slow roll parameter  $\eta$  was defined as the most negative eigenvalue of the matrix  $\eta_a^b$ . In the single field limit the eigenvalues of  $\eta_a^b$  defined by (5.67), gives the eigenvalues,

$$\text{Eigenvalues}[\eta_a^b] = \begin{pmatrix} \frac{2M_p^2}{\sigma^2} \\ M_p^2(-1 + \frac{2}{\sigma^2}) \\ M_p^2(-1 + \frac{2}{\sigma^2}) \\ 2M_p^2(1 + \frac{1}{\sigma^2}) \end{pmatrix} \quad (5.77)$$

Immediately we see the first eigenvalue gives the single field result, however  $\eta$  is defined as the most negative eigenvalue of the matrix  $\eta_a^b$ . This picks out the most unstable direction corresponding to the direction of greatest curvature of the potential. Considering this definition for this model we then find the slow roll parameter (5.57) as,

$$\begin{aligned} \eta_{\text{eig}} &= M_p^2(-1 + \frac{2}{\sigma^2}) \\ &= -0.992188|_{\sigma=16}. \end{aligned} \quad (5.78)$$

This is a significant departure from the standard single field result for  $\eta_{1f}$  given in (5.70) which can be replicated by an alternative choice of eigenvalue from (5.77). Taking the first eigenvalue as,

$$\eta = \frac{2M_p^2}{\sigma^2} = 0.0078125|_{\sigma=16}, \quad (5.79)$$

we find exactly the results of the single field parameters. The deviation from the single field result, even in the single field limit arises since the potential containing additional field directions which contribute to the variation of the potential. These directions define new inflationary directions which are absent in the single field approximation. Using the single field relation for the scalar spectral index at  $\sigma = 16$  and the slow roll estimates from the eigenvalue formalism (5.78) and (5.78) we find,

$$n_{seig} = -1.03474. \quad (5.80)$$

The eigenvalue formalism gives a significant difference in the scalar spectral index prediction from the single field analysis due to the additional inflationary direction. It should be noted though that through an appropriate choice of eigenvalue of  $\eta_a^b$  the single field result can be obtained. Now turning to the extended slow roll formalism we find,

$$\epsilon_H = \frac{2M_p^2}{\sigma^2}, \eta_H = \frac{2M_p^2}{\sigma^2}, \quad (5.81)$$

The scalar spectral index (5.14) has a sum involving derivatives of the potential,  $\eta_a^b N_b^a = \frac{2M_p^2}{\sigma^2}$ , and we recover the single field result,

$$n_s = 1 - 6\frac{2M_p^2}{\sigma^2} + 2\frac{2M_p^2}{\sigma^2} = 1 - \frac{8M_p^2}{\sigma^2}, \quad (5.82)$$

for  $\sigma = 16$  this gives  $n_s = 0.96875$ , which matches the single field result. Using (5.63), we find  $\xi^2 = 0$  in the single field limit, as expected, and the running is then exactly that of the single field chaotic inflationary model,

$$\frac{dn_s}{d\ln\kappa} = -0.000488281. \quad (5.83)$$

These results are hardly surprising as we expect in the limit where the supergravity effects can be ignored they should give the single field result. Importantly, however, we have seen the first discrepancy between the multiple field formalisms and the standard slow roll predictions. The eigenvalue approach was able to pick out additional inflationary directions to those seen through a conventional single field analysis. This lead to the prediction of a highly tilted scalar spectral index  $n_{seig}$  (5.59). With suitable knowledge of the single field result a different  $\eta_{eig}$ , (5.79) can be chosen which reproduces the single field result of  $n_{seig} = 0.96875$ . In contrast, however, the extended formalism gave identical results to the single field approximation. Let us move

onto the case in which there is more than one field contributing to the dynamics. In such a case the inflaton is a combination of a number of fields slowly rolling towards the global minimum. As we have mentioned above, physically we can think of  $\chi$  as being close to but non-zero due to the light mass of the field (this also has consequences on the generation of perturbations after inflation). Expanding the complex field,  $\chi = \frac{1}{\sqrt{2}}(\psi + i\theta)$ , and introducing a small nonzero field value for the imaginary part  $\theta$  generates deviations away from the single field slow roll predictions (5.70). For the initial conditions,

$$\tau = 0, \sigma = 16, \psi = 0, \theta = 0.001, \quad (5.84)$$

we find that the eigenvalue and extended formalisms differ in their estimations of the slow roll parameters and move away from the standard single field approximations. The eigenvalue method, using equations (5.56-5.60) gives,

$$\begin{aligned} \epsilon_{eig} &= 0.00781398, \\ \eta_{eig} &= -0.993927, \\ n_{seig} &= -1.03466, \end{aligned} \quad (5.85)$$

$$\xi^2 = 3.7227 \times 10^{-7}, \quad (5.86)$$

$$\frac{dn_s}{d\ln\kappa} = -0.125662, \quad (5.87)$$

where once again  $\eta_{eig}$  differs to the single field results when the most negative eigenvalue of  $\eta_a^b$  is chosen. This is, as in the single field limit, largely different from the single field approximations (5.70). Taking a similar eigenvalue choice to that done in (5.79) we find  $\eta_{eig} = 0.00781253$  which along with the value for  $\epsilon_{eig}$  gives  $n_{seig} = 0.967235$ . This is very similar to the single field estimate, with the differences attributed to the non minimal  $\theta$  component. However, the system is expected to roll in the direction given by the most negative eigenvalue of  $\eta_a^b$ , as defined in (5.57), and we conclude that the eigenvalue formalism predicts significant deviation from the standard slow roll prediction of  $n_{s_{1f}} = 0.96875$ .

Now using the extended formalism, given by equations (5.61-5.65), we have

$$\epsilon_H = 0.00781398, \quad (5.88)$$

$$\eta_H = -7.94781, \quad (5.89)$$

$$n_s = 0.967235. \quad (5.90)$$

It is worth noting that  $|\eta_H| > 1$ , which violates the slow roll constraint (5.31) whilst  $n_s$  is particularly close to the single field approximation. This arises since the definition of the spectral index contains a summation  $\eta_a^b N_b^a = 0.0070596$  and not  $\eta_H$ . However since the slow roll condition on  $\eta_H$  is not satisfied we must identify and remove the field responsible for violating (5.31). The additional constraint which needs to be satisfied in this model is  $\frac{V_{,i}}{V_{,j}} \sim \mathcal{O}(1)$  in this model, where,

$$\frac{V_{,i}}{V_{,j}} = \begin{pmatrix} \frac{V_{,\Phi}}{V_{,\Phi}} & \frac{V_{,\chi}}{V_{,\Phi}} \\ \frac{V_{,\Phi}}{V_{,\chi}} & \frac{V_{,\chi}}{V_{,\chi}} \end{pmatrix} = \begin{pmatrix} \frac{V_{,\sigma}}{V_{,\sigma}} & \frac{V_{,\theta}}{V_{,\sigma}} \\ \frac{V_{,\sigma}}{V_{,\theta}} & \frac{V_{,\theta}}{V_{,\sigma}} \end{pmatrix}, \quad (5.91)$$

since the complex fields have been expanded as  $\Phi = \frac{1}{\sqrt{2}}(\tau + i\sigma)$ ,  $\chi = \frac{1}{\sqrt{2}}(\psi + i\theta)$  and the real fields set to zero,  $\tau = \phi = 0$ . For the initial conditions,  $\sigma = 16$  and  $\theta = 0.001$  the constraint components are,

$$\begin{pmatrix} 1 & -41.7754 + 0.i \\ -0.0239376 + 0.i & 1 \end{pmatrix}. \quad (5.92)$$

We see the constraint is violated for the  $\frac{V_{,1}}{V_{,2}}$  term. This suggests that  $\chi$  is a heavy field and should be omitted from the calculation of the slow roll parameters. To confirm this and make sure we only included fields which satisfy the slow roll constraint (5.31), we identify the  $\eta_a^b \frac{V_{,a}}{V_{,b}}$  components,

$$\eta_a^b \frac{V_{,a}}{V_{,b}} = \begin{pmatrix} 0.015625 & 0.052466 \\ 9.968801 \times 10^{-6} & -8.01591 \end{pmatrix}. \quad (5.93)$$

Since the  $\eta_\chi^\chi \frac{V_{,\chi}}{V_{,\chi}} \sim \mathcal{O}(1)$  the slow roll condition (5.31) is not satisfied and we conclude that this field is not slow rolling and so should be omitted from the calculations. Including only the  $\sigma$  field gives  $\eta_{H_{inf}} = -0.007811$ , which now satisfies the slow roll conditions, (5.31). Employing the extended summation method we find  $\xi_{ca}^{ab} N_b^a = -0.0000276782$  and using (5.66) we have  $\frac{dn_s}{dln\kappa} = -0.000527427$ . We see then that, through removing the field  $\chi$  from the slow roll calculation, we obtain predictions similar to that of the single field approach. This is not surprising since through removing this field from the calculations, we reduce the analysis to the single field limit, where  $\chi = 0$ , studied previously in this section. This highlights one of the shortcomings of the extended formalism in describing multiple field models of inflation: it does not necessarily consider the entire form of the potential when calculating the slow roll parameters.

Having analysed the natural chaotic inflationary model we have seen that both of the multiple field slow roll formalisms generates deviations away from the standard slow roll parameters. The eigenvalue formalism giving significantly different predictions from the single field approximations whilst the extended formalism agreed remarkably well. One significant result was the prediction of  $|\eta_{eig}| \sim 1$  when using the eigenvalue method, which disagreed with both the single field and extended predictions. However with an appropriate choice of  $\eta_a^b$  eigenvalue the single field predictions could be found, and it was suggested that the original results described another inflationary direction for the potential. Also, interestingly, the extended slow roll method when considering the two field example gave a large  $\eta_H$  when all the fields were included in the calculation whilst the full calculation of the scalar spectral index resulted in only small variation from the single field result. This is thought to have arisen due to the presence of a flat Kähler metric in this model. The diagonal form of the metric would remove contributions to parameters leading to cross terms, e.g.  $\eta_\phi^\chi$  being negligible. This is expected not to be the case when the Kähler metric is no longer diagonal, with the off diagonal contributions possibly giving significant additional contributions to the model parameters.

A fully multi field treatment of this simple case leads to observable constraints of the running of the scalar spectral index and additionally it has pointed to some characteristic flaws within the various approaches, most significantly those in the eigenvalue method. The eigenvalue method predicts a significantly different slow roll footprint from the single field scenario. It was shown that with appropriate choice of  $\eta_{eig}$  a reasonable set of slow roll parameters could be produced. This was not observed in the extended slow roll analysis which agreed remarkably with the single field approximations, giving sensible estimates for all parameters. We therefore conclude in this model of a relatively simple slow roll model that the extended formalism of [74] is favoured significantly over the eigenvalue formalism of [73]. It is clear however that the model of natural chaotic inflation [65] is a simple toy model of supergravity inflation. It has not been embedded in a suitable moduli stabilisation framework such as that outlined in chapter 2. Such extensions to these chaotic models has been considered with successful embedding being achieved in [69] and it is interesting to see how the 3 approaches to slow roll would compare in such settings. However the naturalness

of such models has been questioned and so we move, instead, onto the well motivated model of string inflation of [47] studied previously in chapters 3 and 4 in which we will further test the slow roll formalisms.

### 5.4.2 Comparisons in Kähler Moduli Inflation

The Kähler moduli inflation [47] scenario which has been shown to realise successful inflation by [53] and earlier in chapters 3 and 4, is characterised by a constant volume during inflation with a combination of fields providing this constraint whilst one small Kähler moduli rolls towards its global minimum value. The mechanism for generating inflation here involves a number of moduli and the inflaton is a complex trajectory with a non-trivial Kähler metric. It was shown in chapter 3 though that the single field approximation is well motivated during the inflationary epoch for examples 1, 2 and 3 of chapter 3. Whereas example 4 of chapter 3 was seen to give rise to a inflatary trajectory made from the combination of two Kähler moduli fields. The Kähler moduli inflation model therefore is an ideal scenario by which we can make comparisons between the 3 slow roll approaches introduced in this chapter. Recalling from chapter 3 that the Kähler potential and superpotential are

$$\mathcal{K}_{\alpha'} = -2 \ln \left( \mathcal{V} + \frac{\xi}{2} \right), \quad (5.94)$$

$$W = W_0 + \sum_{i=2}^n A_i e^{-a_i T_i}, \quad (5.95)$$

where  $\xi$  here is the leading order  $\alpha'$  correction and  $\mathcal{V}$  is the internal volume of the compactification manifold

$$\mathcal{V} = \frac{\alpha}{2\sqrt{2}} \left[ (T_1 + \bar{T}_1)^{\frac{3}{2}} - \sum_{i=2}^n \lambda_i (T_i + \bar{T}_i)^{\frac{3}{2}} \right] = \alpha \left( \tau_1^{3/2} - \sum_{i=2}^n \lambda_i \tau_i^{3/2} \right). \quad (5.96)$$

The F-term scalar potential in  $\mathcal{N} = 1$  SUGRA is given by

$$V = e^{\mathcal{K}} [\mathcal{K}^{i\bar{j}} D_i W D_{\bar{j}} \bar{W} - 3|W|^2], \quad (5.97)$$

where  $D_i W = \partial_i W + \partial_i \mathcal{K} W$  is the covariant derivative of the superpotential. Using the Kähler function and the superpotential given above we find the scalar potential to

be,

$$\begin{aligned}
 V = & \frac{12W_0^2\xi}{(4\mathcal{V} - \xi)(2\mathcal{V} + \xi)^2} + \sum_{i=2}^n \frac{12e^{-2a_i\tau_i}\xi A_i^2}{(4\mathcal{V} - \xi)(2\mathcal{V} + \xi)^2} + \frac{16(a_i A_i)^2 \sqrt{\tau_i} e^{-2\alpha\tau_i}}{3\alpha\lambda_i(2\mathcal{V} + \xi)} \\
 & + \frac{32e^{-2\alpha\tau_i} a_i A_i^2 \tau_i (1 + a_i \tau_i)}{(4\mathcal{V} - \xi)(2\mathcal{V} + \xi)} + \frac{8W_0 A_i e^{-a_i\tau_i} \cos(a_i \theta_i)}{(4\mathcal{V} - \xi)(2\mathcal{V} + \xi)} \left( \frac{3\xi}{(2\mathcal{V} + \xi)} + 4a_2\tau_2 \right) \\
 & + \sum_{i<j=2}^n \frac{A_i A_j \cos(a_i \theta_i - a_j \theta_j)}{(4\mathcal{V} - \xi)(2\mathcal{V} + \xi)^2} e^{-(a_i\tau_i + a_j\tau_j)} (32(2\mathcal{V} + \xi)(a_i\tau_i + a_j\tau_j \\
 & + 2a_i a_j \tau_i \tau_j) + 24\xi) + V_{uplift}, \tag{5.98}
 \end{aligned}$$

where we have introduced an additional uplift term of the form  $V_{uplift} = \frac{\beta}{\mathcal{V}^2}$ . This lifts the minima of the potential a de Sitter vacua in place of an anti-de Sitter vacua. The uplift term can be provided by various methods which can have slightly different dependence of the internal volume. For simplicity we will look at the potential in the large volume limit where it takes the form [47],

$$\begin{aligned}
 V_{LARGE} = & \sum_{i=2}^n \frac{8(a_i A_i)^2}{\alpha\lambda_i\mathcal{V}} \sqrt{\tau_i} e^{-2a_i\tau_i} + \sum_{i=2}^n \frac{4W_0 a_i A_i}{\mathcal{V}^2} \tau_i e^{-a_i\tau_i} \cos(a_i \theta_i) + \frac{3\xi W_0^2}{4\mathcal{V}^3} \\
 & + \frac{\beta}{\mathcal{V}^2}. \tag{5.99}
 \end{aligned}$$

During inflation the single field approximation has been shown to be a reasonable approximation [47, 53, 54] and the potential can be approximated as

$$V_{inf} = \frac{BW_0^2}{\mathcal{V}^3} - \frac{4W_0 a_n A_n \tau_n e^{-a_n\tau_n}}{\mathcal{V}^2}, \tag{5.100}$$

where  $\tau_n$  is the inflaton field. From [47, 53, 54] we have the slow roll parameters given by

$$\epsilon = \frac{32\mathcal{V}^3}{3\alpha B^2 \lambda_n W_0^2} a_n^2 A_n^2 \sqrt{\tau_n} (1 - a_n \tau_n)^2 e^{-2a_n\tau_n}, \tag{5.101}$$

$$\eta = -\frac{4a_n A_n \mathcal{V}^2}{3\alpha \lambda_n \sqrt{\tau_n} B W_0} (1 - 9a_n \tau_n + 4(a_n \tau_n)^2) e^{-a_n\tau_n}, \tag{5.102}$$

$$\begin{aligned}
 \xi = & -\frac{16(a_n A_n)^2}{3\sqrt{3} B^2 \tau_n^{1/4}} \left( \frac{\mathcal{V}}{\alpha \lambda_n} \right)^{5/2} (1 + 10a_n \tau_n - 52(a_n \tau_n)^2 \\
 & + 50(a_n \tau_n)^3 - 8(a_n \tau_n)^4) e^{-2a_n\tau_n}. \tag{5.103}
 \end{aligned}$$

Having fully developed this model previously we shall proceed with a comparative study of the slow roll formalisms in this model for the parameter sets studied in chapter 3.

### 5.4.2.1 Example 1

The parameters for example set 1 from chapter 3 are used in the single field slow roll approximations (5.101), (5.102) to give us a basis in which to compare the formalisms,

$$\begin{aligned}
 \epsilon_{1f} &= 1.42 \times 10^{-20}, \\
 \eta_{1f} &= -0.0174074, \\
 \xi_{1f}^2 &= -1.10467 \times 10^{-20}, \\
 n_{s1f} &= 0.965185, \\
 \frac{dn_s}{d\ln\kappa_{1f}} &= 1.8137 \times 10^{-20}.
 \end{aligned} \tag{5.104}$$

Using the formalism developed previously in [73] (eigenvalues) and [75] (extended) and both further in this chapter, the multiple field slow roll parameters can be determined for this model. Using (5.61) we find

$$\epsilon = 2.2421 \times 10^{-4}, \tag{5.105}$$

approximately  $\mathcal{O}(10^{16})$  times larger than the single field prediction. Yet since this still easily satisfies  $\epsilon_H \ll 1$ , we are justified in the use of the eigenvalue method. Taking the most negative eigenvalue of  $\eta_b^a$ , defined by (5.67), provides an estimate for the second slow roll parameter,

$$\eta_{eig} = -0.0173045, \tag{5.106}$$

which we instantly notice gives  $\eta_{eig}$  very close to the single field result (5.104) and the numerics of chapter 3. This is in contrast to the outcome seen in the natural chaotic inflation model comparison (section 5.4.1) where the minimum eigenvalue gave significantly different results from the single field approximation, and one could only reproduce the single field slow roll results through choosing a different eigenvalue for  $\eta_{eig}$ , and therefore different inflationary direction. The eigenvalue which achieved this was that closest to 0 in value, here this corresponds to the eigenvalue of order  $\mathcal{O}(10^{-11})$  which would suggest that the perturbation spectrum is a flat Harrison-Zeldovich spectrum,  $n_s \sim 1$ . This issue is not present in this analysis and suggests the inflationary direction was chosen correctly initially. Taking,  $\eta_{eig} = -0.0173045$  as found through equation (5.57) the spectral index (5.59) is given by

$$n_{seig} = 0.964046, \tag{5.107}$$

which varies only slightly from the single field prediction.

Taking the smallest eigenvalue of the matrix  $\xi_{ca}^{ab}$  gives,  $\xi = 2.45798 \times 10^{-8}$ . This leads to an estimate of the running as

$$\frac{dn_s}{d \ln \kappa} = -4.91596 \times 10^{-8}, \quad (5.108)$$

which is approximately  $\mathcal{O}(10^{11})$  times larger than the single field estimate given in (5.104). We now turn to the second multiple field slow roll formalism we have described in this chapter. When we use this formalism to calculate the spectral index (5.65) we find,

$$\begin{aligned} \epsilon_H &= 4.01207 \times 10^{-16}, \\ \eta_H &= -1.57606 \times 10^{12}, \\ n_{s_{all}} &= 1.57853 \times 10^{12}, \end{aligned} \quad (5.109)$$

the incredibly large  $\eta_H$  and therefore  $n_{s_{all}}$  is clearly inconsistent with the numerical analysis and the single field approximations. Following the methodology of [74, 75] it is possible that such large predictions of  $n_s$  are explained by the presence of non-slow rolling fields. Due to the large size of the  $\epsilon$  and  $\eta$  predictions we propose that these fields must lie along highly curved directions of the potential. Such directions would lead to large  $\eta_a^b$  contributions, which when left in the calculation would contribute to the slow roll calculations through the multiple field relation for the spectral index, (5.65). It was hypothesised in the natural chaotic examples that a non-flat Kähler metric would lead to large contributions, however as we will see this is not the case since the major contribution arises from the  $\eta_3^3 \frac{V^3}{V^3}$  component. This suggests that we should identify and remove the contributions of these directions to the slow roll parameters. In order to do this we look at the constraints (5.34) and (5.31).

The constraint  $\frac{V_{,i}}{V_{,j}} \sim \mathcal{O}(1)$  for the minimum 3 field Kähler moduli inflation model of [47] is written in components as,

$$\frac{V_{,i}}{V_{,j}} = \begin{pmatrix} \frac{V_{,1}}{V_{,1}} & \frac{V_{,1}}{V_{,2}} & \frac{V_{,1}}{V_{,3}} \\ \frac{V_{,2}}{V_{,1}} & \frac{V_{,2}}{V_{,2}} & \frac{V_{,2}}{V_{,3}} \\ \frac{V_{,3}}{V_{,1}} & \frac{V_{,3}}{V_{,2}} & \frac{V_{,3}}{V_{,3}} \end{pmatrix}, \quad (5.110)$$

where the indices  $i, j = 1, \dots, 3$  are the complex fields  $T_i = \frac{1}{2}(\tau_i + i\theta_i)$  in this model.

Violation of this constraint does not explicitly identify the fields as violating slow roll as it simply gives the relative gradients of the potential. Therefore if a component is much greater than of order 1 then the field on the numerator has a much greater gradient than the other field. In such a case one can reason that the field would not be slow-rolling and so should be neglected in the slow-roll calculation. That is we should omit all terms involving that field from calculations of the slow roll parameters.

For this particular example the constraint components are initially,

$$\frac{V_{,a}}{V_{,b}} = \begin{pmatrix} 1 & -7452.57 & 0.018294 \\ -0.000134182 & 1 & -2.45472 \times 10^{-6} \\ 54.6628 & -407378. & 1 \end{pmatrix}. \quad (5.111)$$

The terms  $\frac{V_{,1}}{V_{,2}}$  and  $\frac{V_{,3}}{V_{,2}}$  are both much larger than one suggesting that the  $T_1$  and  $T_3$  field directions are highly curved relative to  $T_2$ , these fields are 'heavy' and should be omitted from the calculations when carrying out the analysis in the extended formalism. This would effectively reduce this to a single (complex) field analysis. In this respect it seems trivial then that this formalism will give results similar to the single field approximations. The necessary condition for slowly rolling fields is that the constraint on the relative gradients on the fields multiplied by the slow-roll parameters is sufficiently small,

$$\epsilon \ll 1, \quad \eta_a^b \frac{V_{,a}}{V_{,b}} \ll 1. \quad (5.112)$$

We already have for this example that the  $\epsilon_H \ll 1$ . We find,

$$\eta_a^b \frac{V_{,a}}{V_{,b}} = \begin{pmatrix} -735882. & -269492. & 5.31404 \times 10^8 \\ 0.00238432 & -0.0338765 & -1.72179 \\ -2.19689 \times 10^9 & -8.04537 \times 10^8 & 1.57853 \times 10^{12} \end{pmatrix}, \quad (5.113)$$

where the only components which satisfy the slow roll conditions are for  $a = 1, b = 2$  and  $a = 2, b = 2$ . When we take into consideration the form of the potential and the results from the numerical simulations we understand that the inflaton direction is in fact  $\tau_2$  with a small contribution coming from the  $\tau_1$  motion, which can be considered roughly as constant and finally the  $\tau_3$  field is frozen at its constant basin value. Now since slow-roll inflation is realized only in the directions where the slow-roll conditions

are satisfied, the scalar fields which do not satisfy the condition may be considered as heavy fields. We can hence omit these fields (or the terms corresponding to their direction) from the calculation of the spectral index. With this reasoning we omit the  $T_1$  and  $T_3$  fields and calculate the slow roll parameters as,

$$\epsilon \rightarrow \frac{M_p^2 K^{2\bar{2}} V_{,2} V_{,\bar{2}}}{V^2}, \quad (5.114)$$

$$\eta \rightarrow \epsilon_H - \eta_2^2 \frac{V_{,2}}{V_{,2}} - \eta_{\bar{2}}^2 \frac{V_{,\bar{2}}}{V_{,\bar{2}}} = \frac{M_p^2 K^{2\bar{2}} (V_{,\bar{2}\bar{2}} - \Gamma_{\bar{2}\bar{2}}^{\bar{2}} V_{,2})}{V}, \quad (5.115)$$

which leads to the predictions,

$$\epsilon_{H_{inf}} = 4.76876 \times 10^{-17}, \quad \eta_{H_{inf}} = 0.0345575, \quad (5.116)$$

where the index  $inf$  represents a sum over the slow roll fields which in this case is only  $T_2$ . The summation with the removal of the heavy fields is then reduced to,

$$\eta_a^b N_{b_{inf}}^a = -0.0172787, \quad (5.117)$$

which leads to a more reasonable prediction for the scalar spectral index,

$$n_{s_{inf}} = 0.965443 \quad (5.118)$$

and with  $\xi^2$  defined by (5.63) and the running of the scalar spectral index (5.66) found to be,

$$\begin{aligned} \xi_{inf}^2 &= 0.00058994, \\ \frac{dn_s}{d \ln \kappa_{inf}} &= -0.00117988. \end{aligned} \quad (5.119)$$

Using the extended slow roll formalism we have carried out an analysis of a complex multiple field inflationary scenario. For an approximately single field example of inflation it has been shown that the inclusion of non inflating fields, which remain at their local minima throughout the inflationary epoch, leads to extremely large slow roll parameter estimations in the extended slow roll formalism of [74]. Those fields which remain approximately constant throughout the duration of inflation have been shown to violate the slow roll conditions. Once these fields are omitted from the calculations this analysis gives a slow roll footprint very close to that found using the standard single field slow roll definitions. Removal of these fields from the analysis reduced the calculation to an effective single field model and so it is thought that this

by definition would give similar results to a standard slow roll analysis. Although the removed fields are known through the analysis of chapter 3 to remain roughly constant throughout inflation, the motivation of obtaining a slow roll formalism which was able to fully describe the nature of multiple field systems appears to be lost if the calculation effectively to that of a single field scenario. In contrast, the eigenvalue formalism has been shown to reproduce the standard field results without the removal of any of the contributions from the calculations, yet still requires a single field relation when calculating the scalar spectral index (5.59) and its running (5.60), with the full multiple field relations given by equations (5.65) and (5.66) respectively. The success of the eigenvalue formalism is somewhat surprising given the conclusions of section 5.4.1 where the formalism gave results not compatible with the single field and extend approaches. In conclusion to this example we find that although both the extended and eigenvalue formalisms give reasonable predictions for the slow roll parameters one would have to favour the eigenvalue formalism since in finding the parameters one does not have to omit any of the fields present in the model<sup>6</sup>.

#### 5.4.2.2 Example 2

Example 2 of Kähler moduli inflation using parameter set 2, (see chapter 3) is an example of effectively single field inflation in a multi-field system. It differs from example 1 through the effect of the inflatons motion on the variation in the local minimum of the potential. This leads to a larger variation in the overall volume at the end of inflation whilst the dynamics during inflation remain similar to example 1. The initial values of the single field slow roll parameter are,

$$\begin{aligned}
 \epsilon_{1f} &= 2.82318 \times 10^{-14}, \\
 \eta_{1f} &= -0.0163843, \\
 \xi_{1f} &= 1.72259 \times 10^{-14}, \\
 n_{s_{1f}} &= 0.967231, \\
 \frac{dn_s}{d\ln\kappa_{inf}} &= -4.18527 \times 10^{-14}.
 \end{aligned} \tag{5.120}$$

<sup>6</sup>Clearly the complex structure moduli and dilaton field have been left out of these calculations as they are considered to remain fixed at their minima. A more complete analysis would also include these fields.

An eigenvalue analysis of this example gives,

$$\epsilon_{eig} = 0.00276022, \quad (5.121)$$

$$\eta_{eig} = -0.0162729, \quad (5.122)$$

$$n_{seig} = 0.950893, \quad (5.123)$$

$$\xi_{eig}^2 = -3.598477 \times 10^{-10}, \quad (5.124)$$

$$\frac{dn_s}{d\ln\kappa_{eig}} = -0.000901519. \quad (5.125)$$

The prediction for  $\epsilon_{eig}$ , (5.121), is relatively large, being approximately  $\mathcal{O}(10^{11})$  larger than  $\epsilon_{1f}$ . However the slow roll condition,  $\epsilon_{eig} \ll 1$  is still satisfied and the evolution of this example is expected still to be determined by the direction of greatest curvature, therefore the eigenvalue formalism is still applicable to this example. The estimate of  $\eta_{eig}$ , (5.122), varies only slightly from  $\eta_{1f}$  with the differences attributed to the multiple field considerations. Although similar to  $n_{s1f}$  the large  $\epsilon_{eig}$  of (5.121) has lead to a noticeably smaller estimate of the scalar spectral index, (5.54), through the eigenvalue approach. This also leads to variations in the prediction of the running (5.60) through the  $\epsilon$  and dependent terms. The prediction of the running (5.125) using the single field relation (5.60) is significantly larger than that of the single field approximation (5.120), this is simply due to the large  $\epsilon_{eig}$  which is  $\mathcal{O}(10^{11})$  times larger than the single field result. Now looking at the extended formalism, naively calculating the slow roll parameters (5.29), (5.61) for this example we find again the slow roll footprint using this method gives extremely large results,

$$\epsilon_H = 0.00276022, \quad (5.126)$$

$$\eta_H = -2.68832 \times 10^9, \quad (5.127)$$

$$n_s = 2.6465 \times 10^9. \quad (5.128)$$

These are in contrast to the inflationary predictions obtained numerically in chapter 3 and once again suggest not a breakdown of the extended slow roll formalism [75] developed in this chapter but the presence of fields which are not slow rolling fields and lead to an incorrect analysis. From the numerical simulation of example 2 in chapter 3 the  $\tau_2$  field played the role of the inflaton with the  $\tau_1$  and  $\tau_3$  fields remaining approximately fixed at their local minimums. Looking at initial values of the constraint (5.110),

$$\frac{V_{,a}}{V_{,b}} = \begin{pmatrix} 1 & 723.061 & 0.155328 \\ 0.00138301 & 1 & 0.00021482 \\ 6.438 & 4655.06 & 1 \end{pmatrix}, \quad (5.129)$$

we find the terms  $\frac{V_{,1}}{V_{,2}}$  and  $\frac{V_{,3}}{V_{,2}}$  are both much larger than 1. When these directions multiply the corresponding  $\eta_a^b$  component, the slow roll condition in this direction is violated, suggesting that only the  $T_2$  contributes to the slow-roll parameters in agreement with the simulations of chapter 3. Confirmation of this is obtained when the slow roll condition (5.31) is calculated,

$$\eta_a^b \frac{V_{,a}}{V_{,b}} = \begin{pmatrix} -738870. & 207295. & 6.37779 \times 10^7 \\ -1.53846 & 0.390275 & 132.797 \\ -3.08217 \times 10^7 & 8.64725 \times 10^6 & 2.64725 \times 10^9 \end{pmatrix}. \quad (5.130)$$

From this we see that the choice of slow roll directions is limited, with only  $\eta_2^2 \frac{V_{,2}}{V_{,2}} < 1$ . The slow roll parameters are now calculated by taking only the  $T_2$  fields contributions as shown in, (5.114) and we have

$$\epsilon_{H_{inf}} = 2.14023 \times 10^{-15}, \quad (5.131)$$

$$\eta_{H_{inf}} = -0.0172072, \quad (5.132)$$

$$n_{s_{inf}} = 1.01721, \quad (5.133)$$

$$\frac{dn_s}{dln\kappa} = 0.00050662. \quad (5.134)$$

These give a slight variation away from the single field estimates, (5.120) with  $\eta_{H_{inf}}$  being reasonably close but also a significant deviation from  $\eta_{1f}$  and  $\eta_{eig}$  which agree excellently. The spectral index produces an unexpected result, which is significantly different from  $n_{s_{inf}}$  predicting a blue tilted perturbation spectrum. This was unexpected since if one uses the values of  $\epsilon$  and  $\eta$  in the single field approximation of the scalar spectral index (5.14) we find  $n_s = 0.965586$  which is still larger than  $n_{s_{1f}}$  and  $n_{s_{eig}}$  but is no longer a positively tilted spectrum. This large  $n_{s_{eig}}$  given in (5.133) arises due to the term  $\eta_a^b N_b^a$  that appears in the definition of the scalar spectral index (5.65) which for this example is given by,

$$\eta_a^b N_b^a = 0.0086036. \quad (5.135)$$

Since this term is positive it leads to a spectral index larger than 1, (5.133). This is obviously a large deviation away from the prediction of the single field and eigenvalue formalisms and is in contrast to the first example where the summation terms gave good agreement with the eigenvalue and single field approaches.

We find then in this example that the large  $\epsilon_{eig}$  lead to a lower estimate of the scalar spectral index of  $n_{seig} \sim 0.95$  and its running  $\frac{dn_s}{d\ln k_{eig}} \sim -9 \times 10^{-4}$  compared to the single field predictions. These deviations from the single field approach can be attributed to the multiple field nature of the eigenvalue formalism, with one expecting the single field results to be an approximation, with additional contributions appearing from the other fields. The large  $\epsilon_{eig}$  is thought to a consequence of the potential in the direction of the basin (chapter 4) adding to this slow roll parameter. The eigenvalue formalism again proves to be a suitable method by which one can determine the slow roll footprint of a model. The same can not be said for the extended formalism, which after reducing the calculation to contributions from a single field,  $\tau_2$  calculates a spectral index  $n_{sinf} \sim 1.02$  which is inconsistent when compared to the results of chapter 4 and the single field approximation. It is unclear why the formalism breaks down for this particular example, since all the required constraints are satisfied within this model.

### 5.4.2.3 Example 3

The method of applying the individual approaches has been outlined in the previous two examples and so here we simply present the results. The single field formalism gives,

$$\begin{aligned}
 \epsilon_{1f} &= 1.02272 \times 10^{-12}, \\
 \eta_{1f} &= -0.0157759, \\
 \xi_{1f} &= 1.12695 \times 10^{-15}, \\
 n_{s1f} &= 0.968448, \\
 \frac{dn_s}{d\ln \kappa_{1f}} &= -2.60403 \times 10^{-13}.
 \end{aligned} \tag{5.136}$$

The small  $\epsilon$  value calculated using (5.61) assures us we can apply the eigenvalue

method which gives,

$$\begin{aligned}
\epsilon_{eig} &= 1.19189 \times 10^{-6}, \\
\eta_{eig} &= -0.0156702, \\
\xi_{eig}^2 &= 2.15921 \times 10^{-14}, \\
n_{seig} &= 0.968652, \\
\frac{dn_s}{d\ln\kappa_{eig}} &= -2.98869 \times 10^{-7}.
\end{aligned} \tag{5.137}$$

The slow roll constraints in the extended slow roll formalism identify only the  $T_2$  field as satisfying the slow roll condition (5.31), giving the estimates for this formalism as,

$$\begin{aligned}
\epsilon_{inf} &= 9.90813 \times 10^{-15}, \\
\eta_{inf} &= -0.0118684, \\
\xi_{inf}^2 &= 0.000554599, \\
n_{sinf} &= 0.976263, \\
\frac{dn_s}{d\ln\kappa_{inf}} &= -0.0011092.
\end{aligned} \tag{5.138}$$

For this example the predictions of both formalisms mirror those outlined in example 1 of this chapter, both approaches predicting similar results to those given by the single field approximations with small deviations arising due to multiple field analysis. The extended formalism so far has been inconsistent in reproducing the single field results as we saw in example 2 whilst the eigenvalue method has provided consistent predictions of the slow roll parameters when compared to the single field approximations. We have so far made comparisons by considering examples for which the evolution is distinctively single field inflation. Let us see if the methods discussed already, i.e. the process of omitting the heavy fields from the extended slow roll formalism of [74] and the so far successful Eigenvalue formalism of [73] hold in a multi-field model with an inflationary trajectory moving in multiple field directions.

#### 5.4.2.4 Example 4

In example 4 of the Kähler moduli inflation chapter the inflaton was a combination of fields, namely  $\tau_1$  and  $\tau_2$ , and so the trajectory in field space was curved in the  $\tau_1 - \tau_2$

plane, Fig.4.4. This is therefore the ideal example to extend this comparative study of the two distinct methods of determining the slow roll parameters for supergravity models of inflation.

The slow roll approximations using (5.101), (5.102) and the initial conditions given in chapter 3 are,

$$\begin{aligned}\epsilon_{1f} &= 2.54153 \times 10^{-8}, \\ \eta_{1f} &= -0.017668, \\ n_{s_{1f}} &= 3.47448 \times 10^{-8}.\end{aligned}\tag{5.139}$$

Numerically using the variation of the time dependent quantities and deducing the spectral index as before we find  $n_s = 0.960$ .

First we work through the eigenvalue formalism. From the simulation data we have the initial value<sup>7</sup> of  $\epsilon_0 = 0.0000914158$ . Since these initial conditions place the fields in a region where  $\epsilon \ll 1$  the condition on the implementation of the eigenvalue method is met. Determining  $\eta_a^b$ , defined by (5.57), and taking the minimum eigenvalue of this matrix yields,

$$\eta_{eig} = -0.0182801.\tag{5.140}$$

Once again this method produces a result consistent with the single field estimate of  $\eta_{1f} = -0.017668$ . The larger  $\eta$  from the eigenvalue method is considered to be a result of the multiple field dynamics, namely the fact the inflaton's trajectory is a combination of field motion including that of the  $\tau_1$  field Fig.4.4. This gives additional contributions to the curvature of the potential along the inflatons trajectory increasing the estimate of  $\eta$ . So it is clear that the eigenvalue method, again in this complex inflaton trajectory gives a convincing prediction for the slow roll parameter  $\eta$  and through the single field definition of the scalar spectral index a well motivated value of  $n_s$  for this model. This method therefore appears to stand up to the complexities involved when there are very complex field dynamics involved. By choosing the most negative eigenvalue here, even though we have a number of steep fields affecting the curvature of the potential,

---

<sup>7</sup>To check that this is representative of the initial value of  $\epsilon$  in the value we average  $\epsilon$  over the first 50 points of simulation data giving  $\epsilon_{mean} = 0.0000846589$  which is consistent with the initial value.

an unstable and negatively curved direction of the potential is identified and a fair estimate of the slow roll footprint made.

$$n_{seig} = 0.962891, \quad (5.141)$$

and  $\xi^2$  and the running of the scalar spectral index are found using (5.58) and (5.60) respectively,

$$\begin{aligned} \xi_{eig}^2 &= 1.99767 \times 10^{-11}, \\ \frac{dn_s}{d\ln\kappa_{eig}} &= -2.6983 \times 10^{-5}. \end{aligned} \quad (5.142)$$

In the previous examples we have seen the complexity associated with determining the slow roll footprint using the extended slow roll formalism. However in section 5.4.2.2 once the appropriate fields had been identified as light slow rolling fields, it was seen that the predictions gave good agreement to those obtained through the eigenvalue and single field approaches. In the examples where the extended formalism provided reliable results, the approach provided a means of determining  $n_s$  through an inherently multiple field definition, (5.65), rather than simply applying a single field relation under the assumptions that it holds in the multiple field scenario. Let us see now look at the extended summation method for this more complex example. First looking at the slow roll footprint obtained using all the fields we find

$$\begin{aligned} \epsilon_H &= 0.0000914158, \\ \eta_H &= -4.73977 \times 10^8, \\ n_s &= -9.479 \times 10^8. \end{aligned} \quad (5.143)$$

Clearly  $\eta_H \gg \mathcal{O}(1)$  in contrast to the numerical simulation data, the single field approximation and the eigenvalue method which all agree on the slow roll parameters up to small deviations. Since this parameter is excessively large we again suspect that the cause is due to the non slow rolling of particular fields which again the characteristically large  $\eta_a^b N_b^a = 2.5017 \times 10^8$  also suggests. Looking first at the ratios of the gradients of the potential(the subsidiary constraint) we can obtain information about the relative curvature of particular fields. These subsidiary constraints are,

$$\begin{pmatrix} 1 & -1.04561 & 0.0124635 \\ -0.956382 & 1 & -0.0119198 \\ 80.2345 & -83.8937 & 1 \end{pmatrix}, \quad (5.144)$$

which suggests that only  $T_3$  is steep and the inflaton is a combination of the directions  $T_1$  and  $T_2$  which is consistent with the numerical simulation findings. As in previous examples we also check to see if the slow roll condition, (5.31) is satisfied for any of the fields,

$$\eta_a^b \frac{V^a}{V^b} = \begin{pmatrix} -5386.21 & -9478.23 & 281009. \\ 145.907 & 256.72 & -7612.23 \\ -9.70289 \times 10^6 & -1.70746 \times 10^7 & 5.00496 \times 10^8 \end{pmatrix}. \quad (5.145)$$

None of the components are found to be small, and all violate the slow roll condition (5.31), indicating that none of the fields are slow rolling in this example. The summation of these terms gives (5.143) where  $\eta_H \gg \mathcal{O}(1)$  in contrast to the numerical simulation results, the single field approximation (which obviously is an approximation for this two field example) and the eigenvalue method which all agree on the slow roll parameters to some degree. Why then is the slow roll condition being violated here for the  $T_1$  and  $T_2$  fields whilst the subsidiary condition identifies the correct fields? Does this suggest yet another weakness of the extended slow roll parameters and its ability to deal with complex trajectories of in field space when the inflaton is a combination of fields? The answer comes from the assumptions under which the extended formalism of [74] was derived. The approach requires that isocurvature modes are negligible so that contributions to the slow roll parameters arise along the inflationary direction only. In this example, as we discussed in chapter 4, the inflaton is a combination of the  $T_1$  and  $T_2$  fields. Through the work of [52, 51] we argued that this would lead to a large isocurvature contribution to the power spectrum and the scalar spectral index,  $n_s$ . If this is the case, this example would violate the conditions in which this formalism can be applied, and hence explain the break down of the approach seen above.

## 5.5 Conclusions

We have investigated the variety of methods used in the literature in order to approximate the slow rolling of fields and obtain observational predictions which can be used to scrutinise models of inflation. The majority of interesting models of inflaton arise

Example	1	2	3	4
$\epsilon_{1f}$	$1.42 \times 10^{-20}$	$2.8232 \times 10^{-14}$	$1.0227 \times 10^{-12}$	$2.5415 \times 10^{-8}$
$\epsilon_{eig}$	0.0002242	0.00276	$1.1919 \times 10^{-6}$	$9.1416 \times 10^{-5}$
$\epsilon_{inf}$	$4.7688 \times 10^{-17}$	$2.14023 \times 10^{-15}$	$9.9081 \times 10^{-13}$	$2.6336 \times 10^{-8}$
$\eta_{1f}$	-0.0174074	-0.0163843	-0.0157759	-0.017668
$\eta_{eigen}$	-0.0173045	-0.0162729	-0.0156702	-0.0181593
$\eta_{inf}$	0.03456	-0.01721	-0.0118684	10.7265
$n_{s1f}$	0.965185	0.967231	0.968448	0.964664
$n_{seigen}$	0.964046	0.950893	0.968652	0.962899
$n_{sinf}$	0.965443	1.01721	0.96263	22.4531
$\xi_{1f}^2$	$-1.1047 \times 10^{-20}$	$1.7220 \times 10^{-14}$	$1.1269 \times 10^{-15}$	-
$\xi_{eig}^2$	$2.45798 \times 10^{-8}$	$-3.5984 \times 10^{-10}$	$2.1592 \times 10^{-14}$	-
$\xi_{inf}^2$	$5.8994 \times 10^{-4}$	$-2.5331 \times 10^{-4}$	$5.5450 \times 10^{-4}$	-
$\frac{dn_s}{dln\kappa}_{1f}$	$1.8137 \times 10^{-20}$	$-4.185 \times 10^{-14}$	$-2.60403 \times 10^{-15}$	-
$\frac{dn_s}{dln\kappa}_{eig}$	$-4.916 \times 10^{-8}$	$-9.01519 \times 10^{-5}$	$-2.98869 \times 10^{-7}$	-
$\frac{dn_s}{dln\kappa}_{inf}$	$-1.1798 \times 10^{-3}$	$5.0662 \times 10^{-4}$	$-1.1092 \times 10^{-3}$	-

**Table 5.1:** Slow roll parameters for Kähler moduli inflation examples of chapter 3 obtained through single field, eigenvalue and extended formalisms. The eigenvalue formalism obtains predictions remarkably similar to the single field approximations for  $\eta$  and  $n_s$  whilst  $\epsilon$  and  $\frac{dn_s}{dln\kappa}$  are consistently larger, the latter resulting from the larger magnitude. The extended formalism gives inconsistent predictions with the requirement of removing 'heavy' fields from the calculations and is found to break down for example 4 for which the inflaton trajectory is highly curved in field space, and so the  $\xi^2$  and  $\frac{dn_s}{dln\kappa}$  terms have not been calculated for this particular example.

from string theory and so, by definition, involve large numbers of candidate inflatons and free scalar fields. Since the dynamics of multiple field inflationary models are quite complex it is common to implement a number of approximations in order to obtain model predictions. These approximations highly simplify the dynamics and in general an inflationary model will be reduced to a single field limit in order to obtain useful predictions. It is clear from the literature that there exists no general consensus as to which method should be used in the calculation of slow roll parameters in the multiple field scenario. In fact it is often assumed that the single field approximations suffice. It was then set out in this chapter to compare the predictions of the 3 slow roll formalisms with the aim of finding a favored formalism when dealing with multiple field inflation models. The three formalisms investigated were the standard single field slow roll formalism [64], which provides an excellent means of directly comparing models of inflation through identifying regions of the inflationary potential which ensure a sufficiently long period of inflation occurs. This approach however was developed to analyse simple toy models of single field inflation and has become outdated with the advent of supergravity inspired models of inflation. Although, as shown in the examples studied, it is possible to find a single field regime, the complexities of

the inflationary potentials often ensure that the single field approximation is not quite enough. This approach however provided the backbone to our analysis through study of the approximately single field limits. The second approach is that of the eigenvalue formalism of [73]. If the parameter space of the model is such that the potential is close to a saddle point, and thus the  $\epsilon$  parameter is negligible then the inflationary trajectory is no longer controlled by the direction of the steepest slope but the direction with the largest curvature. For this limit it is then possible to apply the eigenvalue formalism of [73], which is an ideal candidate for carrying out a slow roll analysis in models arising from supergravity models since it considers the covariant nature of the fields through including a non trivial target space metric in its derivations. It has been coined the "eigenvalue formalism" since for the definition of the slow roll parameter  $\eta_{eig}$  we pick out the most unstable direction along which the field can slow roll towards the minimum of the potential through calculating the eigenvalues of the matrix  $\eta_a^b$ . This parameter contains information about the curvature of the potential in all possible field directions. A similar method is carried out in the calculation of the slow roll parameter  $\xi^2$ . This method however requires the single field slow roll relations for the scalar spectral index and its running in order to obtain a complete slow roll footprint. However, through its consideration of all the fields, this approach is ideal for carrying out a slow roll analysis in multiple field models. The third approach to the slow roll was the extended slow roll formalism of [74]. This is very similar to the eigenvalue method in its derivation however in place of taking the eigenvalues of the matrix of field directions to determine direction of slow roll we identify by hand those directions which are slow rolling, omitting directions which violate the slow roll conditions (5.31). This method is encouraging since it provides multiple field definitions of all the standard slow roll parameter including the scalar spectral index and its running. We have investigated the differences arising from utilising the different approaches to obtaining the slow roll footprint for each formalism in a variety of models. Through these examples it has been shown that the 3 different approaches in some cases can lead to quite large differences in their predictions. First a comparison of the approaches was made using the natural chaotic inflation model of [66]. This simple model, based in a supergravity setting reduces in the single field limit to a textbook chaotic inflation potential. This allowed direct comparison of the approaches to well known and ana-

lytical results. Analysis of the two multiple field approaches here favored the extended formalism of [74], which reproduced the single field results exactly. When the small perturbation to a second field in the model was introduced the extended formalism gave similar results, predicted small deviations away from the single field results as expected. The eigenvalue formalism gave unexpected results for this simple model, finding a  $\eta_{eig}$  roughly an order in magnitude larger than the single field and extended approaches in both examples studied. This was due to the additional slow roll direction arising from the presence of multiple fields, with the eigenvalue approach picking out this direction resulting in a significantly different slow roll footprint. It was noted that with an appropriate choice of eigenvalue the single field chaotic inflation result could be found. The presence of different inflationary directions requires a certain amount of care when calculating the slow roll footprint, however this additional direction was absent from the extended approach suggesting the eigenvalue formalism was slightly more effective in determining the landscape of inflation. The analysis was turned to the model of Kähler moduli inflation studied in chapters 3 and 4 which made use of the moduli stabilisation framework of chapter 2. The Kähler moduli inflation model [47] which has played a central role in this thesis was shown in chapters 3 and 4 to evolve towards an effective single field inflationary model in examples 1, 2 and 3 of chapter 3 and to a two-field inflationary trajectory in example 4<sup>8</sup>. Since the single field approximation was shown to be a good approximation we were able to trust the single field slow roll formalism in these examples. Additionally since this model was shown to give rise to effectively single field inflation, even when all the fields of the model were allowed to evolve (see chapter 4) it was an ideal choice to further compare the slow roll approaches. We found the eigenvalue method of [73] to give remarkably consistent results for the majority of the slow roll parameters. The estimates for  $\epsilon_{eig}$  in this model were significantly larger than the single field predictions. This however was attributed to additional slope of the potential in the basin caused through variation of the volume

---

<sup>8</sup>We considered here the case where the axions are set to their local minimum. It was shown in chapter 4 that the trajectories can be significantly altered with the introduction of axionic components, any axionic component is quickly minimised. In general, an initially non minimal axionic field will lead to longer periods of inflation beginning at larger values of  $\tau_{inf}$  in comparison to a sole displacement of  $\tau_{inf}$ . Since this is the case one would expect that the slow roll parameters are much smaller since the potential is well into the exponentially flat region.

with the Kähler moduli. This additional contribution would have not been present in the single field formalism since a constant volume was assumed in this case in the derivation of the single field slow roll parameters given in equations (5.101-5.103). The eigenvalue formalism provided sensible predictions for the slow roll parameters in all the examples considered. Most notable are the results of example 4, in which the inflaton was a combination of  $T_1$  and  $T_2$  fields. The eigenvalue approach predicted small but significant deviations from the single field formalism, even in this complex multiple field trajectory. We conclude then that formalism in the analysis of realistic models of inflation such as Kähler moduli inflation is quite effective and relatively easy to implement in multiple field scenarios. The extended slow roll formalism of [74], on the other hand, seemed to be quite volatile when applied to the Kähler moduli inflation model. A detailed understanding of the field dynamics for each example was required to determine which fields were heavy and violated the slow roll parameters. Once this was done the parameters were to be once again calculated removing these fields. The success in reproducing results similar to the single field and eigenvalue predictions appeared random at best. In some cases most notably example 4 the extended form gave nonsensical predictions for the slow roll parameters, additionally suggesting in this example that none of the directions would lead to slow roll. It was discussed that this could be due to the presence of non negligible isocurvature modes due to the multiple field nature of the inflationary trajectory. The presence of isocurvature modes in multiple field models is not a special case, and a slow roll formalism intended to deal with multi component inflation models incapable of dealing with such

This, "extended" method, at first appeared quite appealing since it allowed simple calculation of the slow roll footprint in supergravity models of inflation, however its effectiveness means it is not favored over the eigenvalue formalism or the single field formalism. The investigation into the effectiveness of slow roll formalisms has revealed that the process of determining the slow roll footprint of a complex inflationary model is plagued with uncertainties. Armed only with a prior knowledge of the inflationary dynamics and the single field approximations were we able to make informed choices on which multiple field formalism gave more convincing results. It is no wonder then that the literature is still undecided on which formalism is best suited to modern models of inflation arising from string theory. Through this analysis however we are inclined

to consider the eigenvalue formalism of [73] a more suitable and robust method for dealing with such models. It would be interesting to apply such a comparative analysis to models similar to that of Kähler moduli inflation, for example the inflationary models of [112] and [111]. The eigenvalue formalisms ability to predict slight deviations from the standard single field prediction of the scalar spectral index, and the extension of this approach in this chapter to include a multiple field definition of the running has consequences in the constraining of cosmological models of inflation. With the next generation of cosmic microwave background experiments

# Chapter 6

## Conclusions and Discussion

We shall conclude by presenting the main results of this thesis and will discuss possible future directions arising from these results. The main issue in this thesis has been the phenomenological aspects of the Kähler moduli fields of TypeIIb string compactifications, with emphasis placed on the need for suitable descriptive frameworks, which encapsulate the complexities associated with the dynamics of these fields. In chapter 2 we provided the background framework which would be used throughout the thesis. We introduced the concept of string compactifications and the supersymmetry preserving motivation behind the use of a particular class of compactification manifolds called Calabi Yaus. Through the ideas of compactification we saw how generic compactifications gave rise to a large number of moduli fields. A large number of these moduli were shown to be stabilised through the use of fluxes in the string theory, whilst the KKLT construction [31] provided a means to stabilise the remaining moduli and construct AdS vacua through the use of non-perturbative corrections. It was argued that this construction is only consistent in a finely tuned regime and that in general perturbative  $\alpha'$  corrections must also be added. This led to the introduction of a class of large volume string vacua [43] which were free of the fine tuning associated with KKLT. These AdS vacua could both be lifted through the introduction of additional sources to obtain examples of dS vacua in string theory. In light of this it was natural to ask whether such controlled constructions could be used to realise string cosmology, using the many moduli of string compactifications as potential inflaton fields. In chapter 3 we introduced a successful model of inflation [47] that made use of the large volume

vacua of chapter 2, where one of the Kähler moduli played the roll of the inflation field by displacing it from its global minimum. Through an investigation of the full dynamics of this model we confirmed the key results of [47] of an approximately single field inflationary regime. We further extended this analysis, allowing for all the Kähler moduli fields to evolve and found the existence of inflationary trajectories corresponding to a constant volume direction. The class of inflationary models was found to be quite general and we could relax the constraint imposed in [47] that the moduli field responsible for inflation must not significantly alter the form of the potential. In chapter 4 we extended the analysis of this inflationary model demonstrating the roll of the moduli fields in the form of the potential. This led to the discovery of a basin of attraction for the inflationary trajectories seen in chapter 3. A feature of allowing all the moduli fields to evolve was the generation of two masses for the gravitino,  $m_{3/2}$  corresponding to the value of the volume in the basin and that taken at the global minimum. It was proposed that through an increase in volume after inflation this could lead to possible solution of the gravitino mass problem [123, 124] which through phenomenological bounds  $m_{3/2}$  constrains the scale of inflation. However through an investigation into the tuning of parameters we found no such examples with all scenarios leading to an overall increase in volume. A further class of inflationary trajectories was found through displacement of the axionic component of the Kähler moduli. This resulted in a variety of inflationary trajectories which lead to large exploration in the axionic directions. However we found the displacement of the axionic field in the same multiplet as the modulus responsible for providing a minimum for the volume was limited to small displacements to avoid runaway trajectories. We were therefore effectively limited to choosing the axionic field in the same multiplet as the displaced Kähler moduli. This class of axionic trajectories were compared with the similar results of [53] where the authors found a large axionic component to the inflaton existed throughout the duration of inflation. This was in contrast to our findings, where a non minimal axionic component was rapidly stabilised before the onset of inflation. Through the findings of [52, 51] and [111] we then argued that this would have significant consequences on the generation of primordial curvature perturbations. A thorough investigation into the evolution of perturbations when all the fields are allowed to evolve would be of great interest and provides a significant area of future research. We also discussed

the application of scaling solution mechanisms introduced in [77] to further study the dynamics of this model. Such methods, outlined in appendix A could be used to possibly increase the allowed range of axionic inflationary solutions. Furthermore these could be applied to investigate the basin of attraction in further detail and the methods are outlined in appendix A as a future project. Having shown a successful model of multiple field inflation we then argued, in chapter 5 the need for sufficient tools to describe and compare string inspired inflationary models. We first introduced the standard formalism of slow roll inflation, which is based on a single scalar field with a canonical kinetic term. We saw that the low energy 4d effective theory arising from the string compactifications of chapter 2 was  $\mathcal{N} = 1$  supergravity, with the generated potential giving rise to inflation it was argued that to obtain meaningful predictions of the slow roll parameters we must obtain a slow roll formalism applicable to supergravity. The slow roll parameters were then generalised to the multiple scalar fields with non-canonical kinetic terms. We arrived at two approaches to multiple field slow roll inflation; the eigenvalue formalism [73] and the extended formalism [74]. A comparative study of the effectiveness of the three approaches (standard single field and two multiple field descriptions) in predicting the slow roll parameters was then carried out. A simple model of chaotic inflation arising in supergravity [65] was initially studied. The single field limit of this model was well known and so it was possible to directly compare the findings of the three approaches. In this limit we found the extended formalism provided predictions in good agreement with the single field results whilst the eigenvalue formalism gave significant deviations from the standard results. However through an appropriate choice of the slow roll parameter  $\eta_{eig}$  we could recover the known single field results. Similar findings were seen when an additional scalar field was introduced, with the extended formalism giving slight deviations from the standard result as expected. It seemed then that the extended formalism was the favoured approach in multiple field scenarios. However when the 3 approaches were compared in the inflationary model studied in chapters 3 and 4, the eigenvalue formalism was found to give predictions in good agreement with the single field predictions, whilst the extended formalism gave inconsistent results. In the four examples studied, three had been shown in chapter 3 to be approximately single field and so the standard single field slow roll approach was considered a good approximation. This suggested that the

extended formalism was an inadequate approach in the study of such complex multiple field models of inflation. This was made more evident in the fourth example considered where the inflaton field was a combination of two moduli fields. The extended formalism gave predictions of the slow roll parameters which could not be justified and was considered to signal the breakdown of the extended formalism. Conversely the eigenvalue approach was found to give a slow roll footprint similar to the single field analysis, with deviations from these predictions being attributed to the inflation trajectory being highly curved in field space. We concluded from this that the eigenvalue formalism provides the necessary framework to study multiple field models of inflation arising from supergravity. The application of this formalism over the single field approach, when studying realistic inflationary models such as the one studied in detail throughout this thesis, is essential in the age of precision cosmology. Deviations of the predicted slow roll parameters arising through the consideration of the complex field dynamics could tighten the constraints on the range of inflationary potentials allowed by observations and would be interesting to pursue further.

# Appendices

# Appendix A

## Finding attractor solutions using a phase plane analysis

In this appendix we outline the system of equations that could be investigated as part of a future project exploring the nature of the attractor mechanism seen in carrying out a full analysis of the Kähler moduli inflation model of [47] and studied in chapters 3 and 4. In Copeland et al [77] a framework for analysing the evolution of scalar fields with exponential potentials, such as the Kähler moduli arising from string compactifications seen in 2. The motivation behind their work was to find cosmological inflation for these scalar fields, which traditionally where had potentials too steep to have cosmological significance. They considered a scalar potential with an exponential potential  $V = V_0 e^{-\lambda\kappa\phi}$  evolving in a FRW spacetime with a background baryotropic fluid with equation of state  $p_b = (1 - \gamma)\rho_\gamma$ , where  $0 \leq \gamma \leq 2$  and the equations of motion are given by [77],

$$\begin{aligned}\dot{H} &= \frac{\kappa^2}{2} (\rho_\gamma + p_\gamma + \dot{\phi}^2), \\ \dot{\rho}_\gamma &= -3H(\rho_\gamma + p_\gamma), \\ \ddot{\phi} &= -3H\dot{\phi} - \frac{dV}{d\phi},\end{aligned}\tag{A.1}$$

where  $H$  is the Hubble parameter, with the additional Friedmann constraint

$$H^2 = \frac{\kappa^2}{3} (\rho_\gamma + \rho_\phi),\tag{A.2}$$

where  $\kappa \equiv 8\pi G$  and  $\rho_\phi = \frac{1}{2}\dot{\phi}^2 + V$  is the total energy density of the scalar field. Rewriting the equations of motion of the system as a phase plane autonomous system

using the definitions

$$x \equiv \frac{\kappa \dot{\phi}}{\sqrt{6}H}, \quad y \equiv \frac{\kappa \sqrt{V}}{\sqrt{3}H}, \quad (\text{A.3})$$

we can rewrite the system of equations (A.1) as a plane autonomous system [77]

$$\begin{aligned} x' &= -3x + \lambda \sqrt{\frac{3}{2}} y^2 + \frac{3}{2} x [2x^2 + \gamma(1 - x^2 - y^2)], \\ y' &= -\lambda \sqrt{32} xy + \frac{3}{2} y [2x^2 + \gamma(1 - x^2 - y^2)]. \end{aligned} \quad (\text{A.4})$$

The evolution of this system is then completely described by trajectories within this plane, which through the Friedmann constraint (A.2) we see is given by a disc

$$\frac{\kappa^2 \rho_b}{3H^2} + x^2 + y^2 = 1. \quad (\text{A.5})$$

Critical points of the equations (A.4) correspond to fixed values of the variables (A.3), and give solutions to the system of equations for which the scalar field is in a scaling solution having a baryotropic effective equation of state given by,

$$\gamma_\phi \equiv \frac{\rho_\phi + p_\phi}{\rho_\phi} = \frac{2x^2}{x^2 + y^2}. \quad (\text{A.6})$$

Perturbations about the critical points (A.4) allows their stability to be determined and it is possible to extract the attractor solutions through such an analysis [77]. We intended to outline the system of equations that one would require to carry out a similar such analysis for the Kähler moduli inflation model of [47].

Consider the  $N = 1$ ,  $d = 4$  effective SUGRA action is of the form (in Planck units),

$$S = - \int d^4x \sqrt{-g} \left( \frac{1}{2} R + \mathcal{K}_{i\bar{j}} \partial_\mu T^i \partial^\mu \bar{T}^{\bar{j}} + V(T^m, \bar{T}^{\bar{m}}) \right), \quad (\text{A.7})$$

where  $\mathcal{K}_{i\bar{j}}$  is the Kähler metric,  $T^i$  and  $\bar{T}^{\bar{j}}$  are the complex chiral fields. Varying this action with respect to the Kähler moduli in a Friedmann Robertson Walker spacetime we obtain the equation of motion

$$T''^i + 3T'^i + \Gamma_{jk}^i T'^j T'^k + \frac{H'}{H} T'^i + \frac{K^{i\bar{j}}}{H^2} V_{\bar{j}} = 0, \quad (\text{A.8})$$

where  $H$  is again the Hubble parameter, with the Friedmann constraint

$$H^2 = \frac{\kappa_p^2}{3} (K_{i\bar{j}} \dot{T}^i \dot{\bar{T}}^{\bar{j}} + V). \quad (\text{A.9})$$

Differentiating this equation with respect to  $N = \ln a$  indicated by a prime, where  $f' = \frac{df}{dN} = H \frac{df}{dt} = H \dot{f}$  we obtain,

$$2HH' = \frac{\kappa_p^2}{3} (2HH'K_{i\bar{j}}T'^i\bar{T}'^{\bar{j}} + H^2K'_{i\bar{j}}T'^i\bar{T}'^{\bar{j}} + H^2K_{i\bar{j}}T''^i\bar{T}''^{\bar{j}} + H^2K_{i\bar{j}}T'^i\bar{T}'^{\bar{j}} + V'). \quad (\text{A.10})$$

Rearranging the equation of motion for the Kähler moduli (A.8) and substituting into (A.10), we obtain

$$\begin{aligned} \frac{2H'}{H} &= \frac{\kappa_p^2}{3} \left( \frac{2H'}{H} K_{i\bar{j}} T'^i \bar{T}'^{\bar{j}} + K'_{i\bar{j}} T'^i \bar{T}'^{\bar{j}} \right. \\ &\quad + K_{i\bar{j}} (-3T'^i + \Gamma_{lm}^i T'^l T'^m - \frac{H'}{H} T'^i - \frac{K^{i\bar{l}}}{H^2} V_{\bar{l}}) \bar{T}'^{\bar{j}} \\ &\quad \left. + K_{i\bar{j}} T'^i (-3\bar{T}'^{\bar{j}} + \Gamma_{\bar{l}\bar{m}}^{\bar{j}} \bar{T}'^{\bar{l}} \bar{T}'^{\bar{m}} - \frac{H'}{H} \bar{T}'^{\bar{j}} - \frac{K^{\bar{l}\bar{j}}}{H^2} V_{\bar{l}}) + \frac{V'}{H^2} \right) \\ &= \frac{\kappa_p^2}{3} \left( \frac{2H'}{H} K_{i\bar{j}} T'^i \bar{T}'^{\bar{j}} + K'_{i\bar{j}} T'^i \bar{T}'^{\bar{j}} - 6K_{i\bar{j}} T'^i \bar{T}'^{\bar{j}} - K_{i\bar{j}} \Gamma_{lm}^i T'^l T'^m \bar{T}'^{\bar{j}} \right. \\ &\quad - K_{i\bar{j}} T'^i \Gamma_{\bar{l}\bar{m}}^{\bar{j}} \bar{T}'^{\bar{l}} \bar{T}'^{\bar{m}} - \frac{2H'}{H} K_{i\bar{j}} T'^i \bar{T}'^{\bar{j}} \\ &\quad \left. - K_{i\bar{j}} \frac{K^{i\bar{l}}}{H^2} V_{\bar{l}} \bar{T}'^{\bar{j}} - K_{i\bar{j}} T'^i \frac{K^{\bar{l}\bar{j}}}{H^2} V_{\bar{l}} + \frac{V'}{H^2} \right), \end{aligned} \quad (\text{A.11})$$

where we have defined

$$K'_{i\bar{j}} T'^i \bar{T}'^{\bar{j}} = \left( \frac{\partial K_{i\bar{j}}}{\partial T^\sigma} \frac{\partial T^\sigma}{\partial N} + \frac{\partial K_{i\bar{j}}}{\partial \bar{T}^{\bar{\sigma}}} \frac{\partial \bar{T}^{\bar{\sigma}}}{\partial N} \right) T'^i \bar{T}'^{\bar{j}} = K_{i\bar{j}\sigma} T'^i \bar{T}'^{\bar{j}} T'^\sigma + K_{i\bar{j}\bar{\sigma}} T'^i \bar{T}'^{\bar{j}} \bar{T}'^{\bar{\sigma}}. \quad (\text{A.12})$$

If we look at the  $\Gamma_{lm}^i$  terms in (A.11) above we have

$$\begin{aligned} &-K_{i\bar{j}} \Gamma_{lm}^i T'^l T'^m \bar{T}'^{\bar{j}} - K_{i\bar{j}} T'^i \Gamma_{\bar{l}\bar{m}}^{\bar{j}} \bar{T}'^{\bar{l}} \bar{T}'^{\bar{m}} \\ &= -K_{i\bar{j}} K^{i\bar{\sigma}} K_{\bar{l}\bar{m}} T'^l T'^m \bar{T}'^{\bar{j}} - K_{i\bar{j}} K^{\sigma\bar{j}} K_{\bar{l}\bar{m}} \bar{T}'^{\bar{l}} \bar{T}'^{\bar{m}} T'^i \\ &= -(K_{i\bar{j}m} T'^l \bar{T}'^{\bar{j}} T'^m + K_{i\bar{l}m} T'^i \bar{T}'^{\bar{l}} \bar{T}'^{\bar{m}}), \end{aligned} \quad (\text{A.13})$$

where the assumption that  $K_{i\bar{j}} K^{i\bar{\sigma}} = \delta_{\bar{j}}^{\bar{\sigma}}$  has been imposed. For this case the indices are sums over all fields the two equations cancel. A similar trick can be achieved if we look at the  $V_{\bar{l}}$  type terms.

$$\begin{aligned} \frac{V'}{H^2} - K_{i\bar{j}} \frac{K^{i\bar{l}}}{H^2} V_{\bar{l}} \bar{T}'^{\bar{j}} - K_{i\bar{j}} T'^i \frac{K^{\bar{l}\bar{j}}}{H^2} V_{\bar{l}} &= \frac{V_\sigma}{H^2} T'^\sigma + \frac{V_{\bar{\sigma}}}{H^2} \bar{T}'^{\bar{\sigma}} \\ &\quad - \frac{V_i}{H^2} T'^i + \frac{V_{\bar{j}}}{H^2} \bar{T}'^{\bar{j}} = 0, \end{aligned} \quad (\text{A.14})$$

which leaves us with a largely simplified expression

$$\frac{2H'}{H} = -\frac{\kappa_p^2}{3} (6K_{i\bar{j}} T'^i \bar{T}'^{\bar{j}}). \quad (\text{A.15})$$

We can also define

$$x_{i\bar{j}}^2 = \frac{\kappa_p^2}{3} K_{i\bar{j}} T'^i \bar{T}'^{\bar{j}} \quad , \quad y^2 = \frac{\kappa_p^2 V}{3H^2}, \quad (\text{A.16})$$

which we see gives the constraint equation as  $1 = \sum_{i,j} x_{i\bar{j}}^2 + y^2$  and  $\frac{H'}{H} = 3x_{i\bar{j}}^2$ . Now let us obtain equations for  $x_{i\bar{j}}^2, y'^2$  and any more required,

$$2x_{i\bar{j}} x'_{i\bar{j}} = \frac{k_p^2}{3} (K'_{i\bar{j}} T'^i \bar{T}'^{\bar{j}} + K_{i\bar{j}} T''^i \bar{T}''^{\bar{j}} + K_{i\bar{j}} T'^i \bar{T}''^{\bar{j}}). \quad (\text{A.17})$$

Now we can substitute in the equations of motion for  $T'^i$  and  $\bar{T}'^{\bar{j}}$ . We must also remember that the indices  $i, j$  in (A.17) - and from now onwards - are specific fields<sup>1</sup> and not sums. We use greek letters when a sum is present, with this in mind our equation becomes,

$$\begin{aligned} 2x_{i\bar{j}} x'_{i\bar{j}} &= \frac{k_p^2}{3} (K'_{i\bar{j}} T'^i \bar{T}'^{\bar{j}} - K_{i\bar{j}} \Gamma_{\sigma\rho}^i T'^\sigma T'^\rho \bar{T}'^{\bar{j}} - K_{i\bar{j}} T'^i \Gamma_{\bar{\sigma}\bar{\rho}}^{\bar{j}} \bar{T}'^{\bar{\sigma}} \bar{T}'^{\bar{\rho}} \\ &- 6K_{i\bar{j}} T'^i \bar{T}'^{\bar{j}} - \frac{2H'}{H} K_{i\bar{j}} T'^i \bar{T}'^{\bar{j}} - K_{i\bar{j}} \frac{K^{i\bar{\sigma}}}{H^2} V_{\bar{\sigma}} \bar{T}'^{\bar{j}} - K_{i\bar{j}} T'^i \frac{K^{\sigma\bar{j}}}{H^2} V_{\sigma}). \end{aligned} \quad (\text{A.18})$$

Now we can simplify this slightly if the previous trick we employed can be used again as below,

$$\begin{aligned} &K'_{i\bar{j}} T'^i \bar{T}'^{\bar{j}} - K_{i\bar{j}} \Gamma_{\sigma\rho}^i T'^\sigma T'^\rho \bar{T}'^{\bar{j}} - K_{i\bar{j}} T'^i \Gamma_{\bar{\sigma}\bar{\rho}}^{\bar{j}} \bar{T}'^{\bar{\sigma}} \bar{T}'^{\bar{\rho}} \\ &= K_{i\bar{j}\sigma} T'^i \bar{T}'^{\bar{j}} T'^\sigma + K_{i\bar{j}\bar{\sigma}} T'^i \bar{T}'^{\bar{j}} T'^{\bar{\sigma}} - K_{i\bar{j}} K^{i\bar{\gamma}} K_{\sigma\bar{\gamma}\rho} T'^\sigma T'^\rho \bar{T}'^{\bar{\gamma}} \\ &- K_{i\bar{j}} K^{\gamma\bar{j}} K_{\bar{\sigma}\gamma\rho} \bar{T}'^{\sigma} \bar{T}'^{\bar{\rho}} T'^i \\ &= -K_{a\bar{j}\rho} T'^a \bar{T}'^{\bar{j}} T'^\rho - K_{i\bar{b}\bar{\rho}} T'^i \bar{T}'^{\bar{b}} T'^{\bar{\rho}} \quad , \quad a \neq i, \quad b \neq \bar{j} \end{aligned} \quad (\text{A.19})$$

The appearance of these terms arises due to the cross-terms of the Kähler metric . In the case of a diagonal  $K_{i\bar{j}}$  these terms would not appear, with the equations reducing to those given in [76]. We define these new terms as

$$\chi_{i\bar{j}} = -K_{a\bar{j}\rho} T'^a \bar{T}'^{\bar{j}} T'^\rho, \quad \bar{\chi}_{i\bar{j}} = -K_{i\bar{b}\bar{\rho}} T'^i \bar{T}'^{\bar{b}} T'^{\bar{\rho}}, \quad a \neq i, \quad b \neq \bar{j}, \quad (\text{A.20})$$

so using our simplifications we find

$$x'_{i\bar{j}} = -3x_{i\bar{j}} - 3x_{i\bar{j}} \sum_{\sigma, \bar{\rho}=1}^n x_{\sigma\bar{\rho}}^2 + \frac{\chi_{i\bar{j}} + \bar{\chi}_{i\bar{j}} + y^2 \lambda}{2x_{i\bar{j}}}, \quad (\text{A.21})$$

<sup>1</sup>Previously the indices have all represented sums over all fields.

where  $\lambda = -\frac{V'}{V}$ . The equation for the variation of  $y$  is found through similar methods,

$$\begin{aligned} 2yy' &= \frac{k_p^2}{3} \left( \frac{V'}{H^2} - \frac{2VH'}{H^3} \right) = \frac{k_p^2 V}{3H^2} \left( \frac{V'}{V} + 6x_{\sigma\bar{\rho}}^2 \right) = y^2 (6x_{\sigma\bar{\rho}}^2 - \lambda), \\ y' &= y \left( 3x_{\sigma\bar{\rho}}^2 - \frac{\lambda}{2} \right), \end{aligned} \quad (\text{A.22})$$

so we find our system of equations to be

$$1 = \sum_{i,j}^n x_{i\bar{j}}^2 + y^2, \quad (\text{A.23})$$

$$x'_{i\bar{j}} = -3x_{i\bar{j}} - 3x_{i\bar{j}} \sum_{\sigma,\bar{\rho}=1}^n x_{\sigma\bar{\rho}}^2 + \frac{\chi_{i\bar{j}} + \bar{\chi}_{i\bar{j}} + y^2 \lambda}{2x_{i\bar{j}}}, \quad (\text{A.24})$$

$$y' = y \left( 3x_{\sigma\bar{\rho}}^2 - \frac{\lambda}{2} \right), \quad (\text{A.25})$$

$$\lambda' = \lambda^2 (1 - \Lambda), \quad (\text{A.26})$$

where  $\Lambda = \frac{VV''}{V'^2}$ . We see in the case where we have one field,  $i = j = 1$  we have again the system of equations given in [76].

# Appendix B

## Extended slow roll conventions for Kähler metrics and complex fields

In this appendix we outline the definitions used in chapter 5 to calculate the slow roll parameters in the extended and eigenvalue formalisms. In particular we outline the simplifications that arise when the target space  $g_{ab}$  is a Kähler metric.

### B.1 Kähler Metrics and Complex fields

The definitions of the extended and eigenvalue slow roll parameters, given by equations (5.56 - 5.60) and (5.61 - 5.66) respectively, form the basis of chapter 5, with the definitions  $\eta_a^b$  given by (5.67) and  $\xi_{cd}^{ab}$  given by (5.68) being used in each formalism. These are general definitions for a general target space metric  $g_{ab}$ . However in the natural chaotic inflation model [66] and in the Large volume class of inflation models, Kähler moduli inflation [47] the target space is a Kähler metric. We now outline the form of the definitions used in chapter 5 when such a metric is consider. When the target space metric is a Kähler metric [8],

$$g_{i\bar{j}} = \partial_i \partial_{\bar{j}} \mathcal{K} = \mathcal{K}_{i\bar{j}}, \quad (\text{B.1})$$

where  $\mathcal{K}$  is the Kähler potential. The simplification arises due to the nature of the holomorphic coordinates  $z^i, \bar{z}^{\bar{j}}$  and only mixed indices metrics,  $K_{i\bar{j}}$  and same type index connection terms  $\Gamma_{jk}^i$  are non zero. That is in a complex field basis,  $\{\phi^i\} =$

$\{\psi^i, \bar{\psi}^{\bar{i}}\}$  for which  $g_{ij} = g_{\bar{i}\bar{j}} = 0$  and  $g_{i\bar{j}} = g_{\bar{i}j} = \partial_i \partial_{\bar{j}} K = K_{i\bar{j}}$ . The only non-zero connection components are those of pure type  $\Gamma_{jk}^i = K^{i\bar{n}} K_{k\bar{n},j}$  and the complex conjugates.

For epsilon we have for a Kähler metric,

$$\epsilon \equiv \frac{M_p^2}{2} \frac{g^{ab} \nabla_a V \nabla_{\bar{b}} V}{V^2} = M_p^2 \frac{K^{i\bar{j}} \nabla_i V \nabla_{\bar{j}} V}{V^2}. \quad (\text{B.2})$$

This results in four components of  $\eta_a^b$  and 16 components of  $\xi_{cd}^{ab}$ , each of these representing a different combination of the fields and are given as,

$$\eta_a^b = \begin{pmatrix} \eta_i^j & \eta_{\bar{i}}^j \\ \eta_i^{\bar{j}} & \eta_{\bar{i}}^{\bar{j}} \end{pmatrix}, \quad (\text{B.3})$$

where  $\eta_a^b = \frac{g^{bc}(V_{,ca} - \Gamma_{ca}^d V_{,d})}{V}$  and since the target space is Kähler we have,

$$\eta_i^j = \frac{K^{j\bar{k}} V_{,\bar{k}i}}{V}, \quad (\text{B.4})$$

$$\eta_{\bar{i}}^{\bar{j}} = \frac{K^{\bar{j}k} (V_{,ki} - \Gamma_{ki}^l V_{,l})}{V}, \quad (\text{B.5})$$

$$\eta_i^{\bar{j}} = \frac{K^{j\bar{k}} (V_{,\bar{k}i} - \Gamma_{\bar{k}i}^{\bar{l}} V_{,\bar{l}})}{V}, \quad (\text{B.6})$$

$$\eta_{\bar{i}}^j = \frac{K^{\bar{j}k} V_{,k\bar{i}}}{V}, \quad (\text{B.7})$$

and

$$\xi_{cd}^{ab} = \begin{pmatrix} \xi_{kl}^{ij} & \xi_{kl}^{i\bar{j}} & \xi_{k\bar{l}}^{ij} & \xi_{k\bar{l}}^{i\bar{j}} \\ \xi_{kl}^{\bar{i}j} & \xi_{kl}^{\bar{i}\bar{j}} & \xi_{k\bar{l}}^{\bar{i}j} & \xi_{k\bar{l}}^{\bar{i}\bar{j}} \\ \xi_{\bar{k}l}^{ij} & \xi_{\bar{k}l}^{i\bar{j}} & \xi_{\bar{k}\bar{l}}^{ij} & \xi_{\bar{k}\bar{l}}^{i\bar{j}} \\ \xi_{\bar{k}l}^{\bar{i}j} & \xi_{\bar{k}l}^{\bar{i}\bar{j}} & \xi_{\bar{k}\bar{l}}^{\bar{i}j} & \xi_{\bar{k}\bar{l}}^{\bar{i}\bar{j}} \end{pmatrix}, \quad (\text{B.8})$$

where  $\xi_{cd}^{ab} = M_p^4 \frac{g^{ae} g^{bf} V_{,e}}{V} \left( V_{,cfd} - (\Gamma_{fd}^g)_{,c} V_{,g} - \Gamma_{fd}^g V_{,cg} - \Gamma_{cf}^h (V_{,hd} - \Gamma_{hd}^g V_{,g}) - \Gamma_{cd}^h (V_{,hf} - \Gamma_{hf}^g V_{,g}) \right)$  giving the components for the Kähler metric as,

$$\xi_{kl}^{ij} = M_p^4 \frac{K^{i\bar{m}} K^{j\bar{n}} V_{,\bar{m}} V_{;k\bar{n}l}}{V^2}, \quad (\text{B.9})$$

$$\bar{\xi}_{kl}^{\bar{i}\bar{j}} = M_p^4 \frac{K^{\bar{i}\bar{m}} K^{\bar{j}\bar{n}} V_{,m} V_{;k\bar{n}l}}{V^2}, \quad (\text{B.10})$$

$$\xi_{kl}^{\bar{i}\bar{j}} = M_p^4 \frac{K^{i\bar{m}} K^{\bar{j}\bar{n}} V_{,\bar{m}} V_{;knl}}{V^2}, \quad (\text{B.11})$$

$$\xi_{\bar{k}l}^{ij} = M_p^4 \frac{K^{i\bar{m}} K^{j\bar{n}} V_{,\bar{m}} V_{;\bar{k}nl}}{V^2}, \quad (\text{B.12})$$

$$\xi_{\bar{k}l}^{\bar{i}\bar{j}} = M_p^4 \frac{K^{\bar{i}\bar{m}} K^{\bar{j}\bar{n}} V_{,\bar{m}} V_{;k\bar{n}\bar{l}}}{V^2}, \quad (\text{B.13})$$

$$\xi_{kl}^{\bar{i}\bar{j}} = M_p^4 \frac{K^{\bar{i}\bar{m}} K^{\bar{j}\bar{n}} V_{,m} V_{;knl}}{V^2}, \quad (\text{B.14})$$

$$\bar{\xi}_{kl}^{\bar{i}\bar{j}} = M_p^4 \frac{K^{\bar{i}\bar{m}} K^{\bar{j}\bar{n}} V_{,m} V_{;\bar{k}nl}}{V^2}, \quad (\text{B.15})$$

$$\bar{\xi}_{\bar{k}l}^{\bar{i}\bar{j}} = M_p^4 \frac{K^{\bar{i}\bar{m}} K^{\bar{j}\bar{n}} V_{,m} V_{;k\bar{n}\bar{l}}}{V^2}, \quad (\text{B.16})$$

$$\xi_{\bar{k}l}^{\bar{i}\bar{j}} = M_p^4 \frac{K^{i\bar{m}} K^{\bar{j}\bar{n}} V_{,\bar{m}} V_{;\bar{k}nl}}{V^2}, \quad (\text{B.17})$$

$$\xi_{kl}^{\bar{i}\bar{j}} = M_p^4 \frac{K^{i\bar{m}} K^{\bar{j}\bar{n}} V_{,\bar{m}} V_{;knl}}{V^2}, \quad (\text{B.18})$$

$$\xi_{\bar{k}l}^{ij} = M_p^4 \frac{K^{i\bar{m}} K^{j\bar{n}} V_{,\bar{m}} V_{;\bar{k}nl}}{V^2}, \quad (\text{B.19})$$

$$\xi_{kl}^{\bar{i}\bar{j}} = M_p^4 \frac{K^{\bar{i}\bar{m}} K^{\bar{j}\bar{n}} V_{,\bar{m}} V_{;\bar{k}nl}}{V^2}, \quad (\text{B.20})$$

$$\bar{\xi}_{\bar{k}l}^{\bar{i}\bar{j}} = M_p^4 \frac{K^{\bar{i}\bar{m}} K^{\bar{j}\bar{n}} V_{,m} V_{;k\bar{n}\bar{l}}}{V^2}, \quad (\text{B.21})$$

$$\xi_{\bar{k}l}^{\bar{i}\bar{j}} = M_p^4 \frac{K^{\bar{i}\bar{m}} K^{\bar{j}\bar{n}} V_{,m} V_{;\bar{k}nl}}{V^2}, \quad (\text{B.22})$$

$$\xi_{kl}^{\bar{i}\bar{j}} = M_p^4 \frac{K^{i\bar{m}} K^{j\bar{n}} V_{,\bar{m}} V_{;\bar{k}nl}}{V^2}, \quad (\text{B.23})$$

$$\bar{\xi}_{\bar{k}l}^{\bar{i}\bar{j}} = M_p^4 \frac{K^{\bar{i}\bar{m}} K^{\bar{j}\bar{n}} V_{,\bar{m}} V_{;k\bar{n}\bar{l}}}{V^2}, \quad (\text{B.24})$$

where the covariant third derivative of the potential are given by,

$$V_{;knl} = V_{,knl} - \Gamma_{nl}^p V_{,pk} - \Gamma_{kn}^p (V_{,pl} - \Gamma_{pl}^q V_{,q}), \quad (\text{B.25})$$

$$V_{;\bar{k}nl} = V_{,\bar{k}nl} - \Gamma_{nl}^p V_{,p\bar{k}} - (\Gamma_{nl}^p)_{,\bar{k}} V_{,p}, \quad (\text{B.26})$$

$$V_{;k\bar{n}l} = V_{,k\bar{n}l} - \Gamma_{kl}^p V_{,p\bar{n}}, \quad (\text{B.27})$$

$$V_{;knl\bar{l}} = V_{,knl\bar{l}} - \Gamma_{kn}^p V_{,p\bar{l}}, \quad (\text{B.28})$$

$$V_{;\bar{k}nl\bar{l}} = V_{,\bar{k}nl\bar{l}} - \Gamma_{\bar{k}\bar{n}}^{\bar{p}} V_{,\bar{p}l}, \quad (\text{B.29})$$

$$V_{;\bar{k}n\bar{l}} = V_{,\bar{k}n\bar{l}} - \Gamma_{\bar{k}l}^{\bar{p}} V_{,\bar{p}n}, \quad (\text{B.30})$$

$$V_{;k\bar{n}l\bar{l}} = V_{,k\bar{n}l\bar{l}} - \Gamma_{\bar{n}l}^{\bar{p}} V_{,k\bar{p}} - (\Gamma_{\bar{n}l}^{\bar{p}})_{,k} V_{,\bar{p}}, \quad (\text{B.31})$$

$$V_{;\bar{k}n\bar{l}\bar{l}} = V_{,\bar{k}n\bar{l}\bar{l}} - \Gamma_{\bar{n}l}^{\bar{p}} V_{,\bar{p}\bar{k}} - \Gamma_{\bar{k}\bar{n}}^{\bar{p}} (V_{,\bar{p}\bar{l}} - \Gamma_{\bar{p}\bar{l}}^{\bar{q}} V_{,\bar{q}}). \quad (\text{B.32})$$

The above definitions are those for which we have a general target space metric and complex scalar fields.

The notation above might be slightly confusing with the appearance of both barred and unbarred indexes. For example in  $\eta_j^i$  we see there is a  $\bar{j}$  on the inverse Kähler metric, this arises due to the presence of the Kronecker deltas in the derivatives of the potential and the restriction  $K_{ij} = K_{\bar{i}\bar{j}} = 0$ , hence the strange notation.

### B.1.1 $\xi^2$

We define the third slow roll parameter as  $\xi^2 = \xi_{cd}^{ab} N_b^c \delta_d^a$ . Since we have a Kähler metric there are simplifications to the  $\xi_{cd}^{ab}$  terms, as was shown in the previous section. Also, since  $\phi^i \neq \bar{\phi}^{\bar{i}}$  we have a number of additional simplifications, leading to

$$\xi_{ca}^{ab} = \begin{pmatrix} \xi_{ci}^{ib} & \xi_{ci}^{\bar{i}\bar{b}} \\ \xi_{\bar{c}\bar{i}}^{ib} & \xi_{\bar{c}\bar{i}}^{\bar{i}\bar{b}} \end{pmatrix}, = \begin{pmatrix} \xi_{ci}^{ib} & 0 \\ 0 & \xi_{\bar{c}\bar{i}}^{\bar{i}\bar{b}} \end{pmatrix} \quad (\text{B.33})$$

where we have used the notation,  $i = 1, n$  where  $n$  is the number of complex fields and  $a, b, c = i, \bar{i}$  indicate the general indexing. We are left with the full expression for  $\xi^2$  as a sum of 8 expressions,

$$\begin{aligned} \xi^2 &= (\xi_{ci}^{ib} + \xi_{\bar{c}\bar{i}}^{\bar{i}\bar{b}}) N_b^c \\ &= (\xi_{ki}^{ij} + \xi_{\bar{k}\bar{i}}^{\bar{i}\bar{j}}) N_k^j + (\xi_{\bar{k}\bar{i}}^{i\bar{j}} + \xi_{k\bar{i}}^{\bar{i}\bar{j}}) N_{\bar{k}}^{\bar{j}} + (\xi_{ki}^{i\bar{j}} + \xi_{\bar{k}\bar{i}}^{\bar{i}j}) N_k^{\bar{j}} + (\xi_{\bar{k}\bar{i}}^{\bar{i}j} + \xi_{k\bar{i}}^{i\bar{j}}) N_{\bar{k}}^j, \end{aligned} \quad (\text{B.34})$$

## B.2 Supergravity models: Spectral index

Here we outline the argument covered by Chiba and Yamaguchi [74]. This gives an identical expression for  $n_s$  to that given in the main text.

In the multi-field scenario the power spectrum is given as [59]

$$\mathcal{P}_{\mathcal{R}}(k) = \left(\frac{H}{2\pi}\right)^2 N_{,a} N^{,a}, \quad (\text{B.35})$$

where  $k$  is the comoving wavenumber at horizon exit ( $k = aH$ ) and  $N(\phi)$  is the number of efoldings defined in the usual way

$$N(\phi) = \int_{t(\phi)}^{t_e} H dt, \quad (\text{B.36})$$

from which we can obtain the slow-roll relation

$$H = -N_{,a} \dot{\phi}^a \approx N_{,a} \frac{V^{,a}}{3H}, \quad (\text{B.37})$$

where, for target space metric  $g_{ab}$ , we have used  $V^{,a} = g^{ab} V_{,b}$ .

Again assuming at horizon crossing,  $k = aH$  and that  $\dot{H}$  is negligible compared to  $\dot{a}$  (considering  $H = \text{constant}$ ) we have a relation between the comoving wavenumber and Hubble radius,  $d \ln k \approx H dt$ . The spectral index of the scalar perturbations can then be defined as

$$n_s - 1 \equiv \frac{d \ln \mathcal{P}_{\mathcal{R}}}{d \ln k} = 2 \frac{\dot{H}}{H^2} - 2 \frac{N_{,a} \dot{N}_{,a}}{H N_{,c} N_{,c}}. \quad (\text{B.38})$$

As we have seen the first term on the RHS is given by the slow roll parameter  $\epsilon$  whilst using the relations,

$$\begin{aligned} \dot{N}_{,a} &= \dot{\phi}^b \nabla_b \nabla_a N \\ &= \nabla_a (\dot{\phi}^b \nabla_b N) - (\nabla_a \dot{\phi}^b) (\nabla_b N) = -H_{,a} - N^{,b} \nabla_a \dot{\phi}^b, \end{aligned} \quad (\text{B.39})$$

$$\nabla_a \dot{\phi}^b \approx -\nabla_a \left( \frac{V_{,b}}{3H} \right) = \frac{H_{,a} V_{,b}}{3H} - \frac{\nabla_a \nabla_b V}{3H}, \quad (\text{B.40})$$

giving

$$\begin{aligned} n_s - 1 &= 2 \frac{\dot{H}}{H^2} - 2 \frac{N_{,a}}{H N_{,c} N_{,c}} (-H_{,a} - N^{,b} \nabla_a \dot{\phi}^b) \\ &\approx \frac{2}{H^2} (-\dot{N}_{,a} \dot{\phi}^a) - 2 \frac{N_{,a}}{H N_{,c} N_{,c}} (-H_{,a} - N^{,b} \nabla_a \dot{\phi}^b) \\ &\approx -2\epsilon + \frac{\eta_{ab} N^{,a} N^{,b}}{N_{,c} N_{,c}}, \end{aligned} \quad (\text{B.41})$$

where here  $\nabla_a \dot{\phi}^b \equiv \frac{\nabla_a \nabla_b V}{\kappa^2 V}$  and since in the slow roll limit we can write  $N_{,a} = \frac{\kappa^2 V V_{,a}}{V_{,c} V_{,c}}$ , we have

$$N^{ab} = \frac{N^{,a} N^{,b}}{N_{,c} N_{,c}} = \frac{V_{,a} V_{,b}}{V_{,c} V_{,c}}, \quad (\text{B.42})$$

and we are led to

$$n_s - 1 = -6\epsilon + 2\eta_{ab} N^{ab}. \quad (\text{B.43})$$

# Bibliography

- [1] T. Kaluza, “On the Problem of Unity in Physics,” *Sitzungsber. Preuss. Akad. Wiss. Berlin (Math. Phys. )* **1921** (1921) 966–972.
- [2] M. J. Duff, “Kaluza-Klein theory in perspective,”  
arXiv:hep-th/9410046.
- [3] R. D. Newman, E. C. Berg, and P. E. Boynton, “Tests of the gravitational inverse square law at short ranges,”.
- [4] K. Becker, M. Becker, and J. H. Schwarz, “String theory and M-theory: A modern introduction,”. Cambridge, UK: Cambridge Univ. Pr. (2007) 739 p.
- [5] S. Gurrieri, “N = 2 and N = 4 supergravities as compactifications from string theories in 10 dimensions,” arXiv:hep-th/0408044.
- [6] M. Vonk, “A mini-course on topological strings,”  
arXiv:hep-th/0504147.
- [7] V. Bouchard, “Lectures on complex geometry, Calabi-Yau manifolds and toric geometry,” arXiv:hep-th/0702063.
- [8] M. Nakahara, “Geometry, topology and physics,”. Bristol, UK: Hilger (1990) 505 p. (Graduate student series in physics).
- [9] S. Gukov, C. Vafa, and E. Witten, “CFT’s from Calabi-Yau four-folds,” *Nucl. Phys.* **B584** (2000) 69–108, arXiv:hep-th/9906070.
- [10] M. R. Douglas and S. Kachru, “Flux compactification,” *Rev. Mod. Phys.* **79** (2007) 733–796, arXiv:hep-th/0610102.
- [11] M. Grana, “Flux compactifications in string theory: A comprehensive review,” *Phys. Rept.* **423** (2006) 91–158, arXiv:hep-th/0509003.
- [12] S. B. Giddings, S. Kachru, and J. Polchinski, “Hierarchies from fluxes in string compactifications,” *Phys. Rev.* **D66** (2002) 106006,  
arXiv:hep-th/0105097.
- [13] A. Sen, “Orientifold limit of F-theory vacua,” *Phys. Rev.* **D55** (1997) 7345–7349, arXiv:hep-th/9702165.
- [14] J. R. Ellis, A. B. Lahanas, D. V. Nanopoulos, and K. Tamvakis, “No-Scale Supersymmetric Standard Model,” *Phys. Lett.* **B134** (1984) 429.

- [15] T. Barreiro, B. de Carlos, and E. J. Copeland, “On non-perturbative corrections to the Kaehler potential,” *Phys. Rev.* **D57** (1998) 7354–7360, arXiv:hep-ph/9712443.
- [16] F. Denef, “Les Houches Lectures on Constructing String Vacua,” arXiv:0803.1194 [hep-th].
- [17] R. Donagi and M. Wijnholt, “Model Building with F-Theory,” arXiv:0802.2969 [hep-th].
- [18] C. Vafa, “Evidence for F-Theory,” *Nucl. Phys.* **B469** (1996) 403–418, arXiv:hep-th/9602022.
- [19] J. M. Maldacena and C. Nunez, “Supergravity description of field theories on curved manifolds and a no go theorem,” *Int. J. Mod. Phys.* **A16** (2001) 822–855, arXiv:hep-th/0007018.
- [20] K. Saririan, “Gaugino condensation, loop corrections, and S-duality constraint,” arXiv:hep-th/9611093.
- [21] F. Quevedo, “Gaugino condensation, duality and supersymmetry breaking,” *Nucl. Phys. Proc. Suppl.* **46** (1996) 187–197, arXiv:hep-th/9511131.
- [22] H. P. Nilles, “Gaugino condensation and SUSY breakdown,” arXiv:hep-th/0402022.
- [23] E. Witten, “Non-Perturbative Superpotentials In String Theory,” *Nucl. Phys.* **B474** (1996) 343–360, arXiv:hep-th/9604030.
- [24] R. Blumenhagen, S. Moster, and E. Plauschinn, “Moduli Stabilisation versus Chirality for MSSM like Type IIB Orientifolds,” *JHEP* **01** (2008) 058, arXiv:0711.3389 [hep-th].
- [25] S. L. Parameswaran and A. Westphal, “Consistent de Sitter string vacua from Kaehler stabilization and D-term uplifting,” *Fortsch. Phys.* **55** (2007) 804–810, arXiv:hep-th/0701215.
- [26] K. Becker, M. Becker, C. Vafa, and J. Walcher, “Moduli stabilization in non-geometric backgrounds,” *Nucl. Phys.* **B770** (2007) 1–46, arXiv:hep-th/0611001.
- [27] A. Micu, E. Palti, and G. Tasinato, “Towards Minkowski Vacua in Type II String Compactifications,” *JHEP* **03** (2007) 104, arXiv:hep-th/0701173.
- [28] E. Dudas, Y. Mambrini, S. Pokorski, and A. Romagnoni, “Moduli stabilization with Fayet-Iliopoulos uplift,” *JHEP* **04** (2008) 015, arXiv:0711.4934 [hep-th].
- [29] S. L. Parameswaran and A. Westphal, “de Sitter string vacua from perturbative Kaehler corrections and consistent D-terms,” *JHEP* **10** (2006) 079, arXiv:hep-th/0602253.

- [30] A. Achucarro, B. de Carlos, J. A. Casas, and L. Doplicher, “de Sitter vacua from uplifting D-terms in effective supergravities from realistic strings,” *JHEP* **06** (2006) 014, arXiv:hep-th/0601190.
- [31] S. Kachru, R. Kallosh, A. Linde, and S. P. Trivedi, “De Sitter vacua in string theory,” *Phys. Rev.* **D68** (2003) 046005, arXiv:hep-th/0301240.
- [32] R. Kallosh and A. Linde, “Landscape, the scale of SUSY breaking, and inflation,” *JHEP* **12** (2004) 004, arXiv:hep-th/0411011.
- [33] O. DeWolfe and S. B. Giddings, “Scales and hierarchies in warped compactifications and brane worlds,” *Phys. Rev.* **D67** (2003) 066008, arXiv:hep-th/0208123.
- [34] J. R. Ellis, C. Kounnas, and D. V. Nanopoulos, “No Scale Supergravity Models with a Planck Mass Gravitino,” *Phys. Lett.* **B143** (1984) 410.
- [35] S. Weinberg, “Cosmological Constraints on the Scale of Supersymmetry Breaking,” *Phys. Rev. Lett.* **48** (1982) 1303.
- [36] L. Susskind, “The anthropic landscape of string theory,” arXiv:hep-th/0302219.
- [37] L. Susskind, “Supersymmetry breaking in the anthropic landscape,” arXiv:hep-th/0405189.
- [38] F. Denef and M. R. Douglas, “Distributions of flux vacua,” *JHEP* **05** (2004) 072, arXiv:hep-th/0404116.
- [39] F. Denef and M. R. Douglas, “Distributions of nonsupersymmetric flux vacua,” *JHEP* **03** (2005) 061, arXiv:hep-th/0411183.
- [40] R. Brustein and P. J. Steinhardt, “Challenges for superstring cosmology,” *Phys. Lett.* **B302** (1993) 196–201, arXiv:hep-th/9212049.
- [41] T. Barreiro, B. de Carlos, E. Copeland, and N. J. Nunes, “Moduli evolution in the presence of flux compactifications,” *Phys. Rev.* **D72** (2005) 106004, arXiv:hep-ph/0506045.
- [42] R. Brustein, S. P. de Alwis, and P. Martens, “Cosmological stabilization of moduli with steep potentials,” *Phys. Rev.* **D70** (2004) 126012, arXiv:hep-th/0408160.
- [43] V. Balasubramanian, P. Berglund, J. P. Conlon, and F. Quevedo, “Systematics of Moduli Stabilisation in Calabi-Yau Flux Compactifications,” *JHEP* **03** (2005) 007, arXiv:hep-th/0502058.
- [44] J. P. Conlon, F. Quevedo, and K. Suruliz, “Large-volume flux compactifications: Moduli spectrum and D3/D7 soft supersymmetry breaking,” *JHEP* **08** (2005) 007, arXiv:hep-th/0505076.
- [45] M. Berg, M. Haack, and E. Pajer, “Jumping Through Loops: On Soft Terms from Large Volume Compactifications,” *JHEP* **09** (2007) 031, arXiv:0704.0737 [hep-th].

- [46] M. Dine and N. Seiberg, “Is the Superstring Weakly Coupled?,” *Phys. Lett.* **B162** (1985) 299.
- [47] J. P. Conlon and F. Quevedo, “Kähler moduli inflation,” *JHEP* **01** (2006) 146, arXiv:hep-th/0509012.
- [48] J. P. Conlon and F. Quevedo, “Astrophysical and Cosmological Implications of Large Volume String Compactifications,” *JCAP* **0708** (2007) 019, arXiv:0705.3460 [hep-ph].
- [49] J. P. Conlon, “Hierarchy problems in string theory and large volume models,” *Mod. Phys. Lett.* **A23** (2008) 1–16.
- [50] M. Cicoli, J. P. Conlon, and F. Quevedo, “General Analysis of LARGE Volume Scenarios with String Loop Moduli Stabilisation,” *JHEP* **10** (2008) 105, arXiv:0805.1029 [hep-th].
- [51] A. C. Vincent and J. M. Cline, “Curvature Spectra and Nongaussianities in the Roulette Inflation Model,” *JHEP* **10** (2008) 093, arXiv:0809.2982 [astro-ph].
- [52] Z. Lalak, D. Langlois, S. Pokorski, and K. Turzynski, “Curvature and isocurvature perturbations in two-field inflation,” *JCAP* **0707** (2007) 014, arXiv:0704.0212 [hep-th].
- [53] J. R. Bond, L. Kofman, S. Prokushkin, and P. M. Vaudrevange, “Roulette inflation with Kähler moduli and their axions,” *Phys. Rev.* **D75** (2007) 123511, arXiv:hep-th/0612197.
- [54] J. J. Blanco-Pillado, D. Buck, E. J. Copeland, M. Gomez-Reino, and N. J. Nunes, “Kähler Moduli Inflation Revisited,” arXiv:0906.3711 [hep-th].
- [55] N. Barnaby, J. R. Bond, Z. Huang, and L. Kofman, “Preheating After Modular Inflation,” arXiv:0909.0503 [hep-th].
- [56] E. R. Harrison, “Fluctuations at the Threshold of Classical Cosmology,” *Phys. Rev. D* **1** (May, 1970) 2726–2730.
- [57] Y. B. Zeldovich, “A Hypothesis, unifying the structure and the entropy of the universe,” *Mon. Not. Roy. Astron. Soc.* **160** (1972) 1P–3P.
- [58] A. D. Linde, “Particle Physics and Inflationary Cosmology,” arXiv:hep-th/0503203.
- [59] A. R. Liddle and D. H. Lyth, “Cosmological inflation and large-scale structure,” ISBN-13-9780521828499.
- [60] D. Baumann, “TASI Lectures on Inflation,” arXiv:0907.5424 [hep-th].
- [61] A. H. Guth, “Eternal inflation and its implications,” *J. Phys.* **A40** (2007) 6811–6826, arXiv:hep-th/0702178.

- [62] A. R. Liddle and D. H. Lyth, “COBE, gravitational waves, inflation and extended inflation,” *Phys. Lett.* **B291** (1992) 391–398, arXiv:astro-ph/9208007.
- [63] A. R. Liddle and D. H. Lyth, “The Cold dark matter density perturbation,” *Phys. Rept.* **231** (1993) 1–105, arXiv:astro-ph/9303019.
- [64] D. H. Lyth, “What would we learn by detecting a gravitational wave signal in the cosmic microwave background anisotropy?,” *Phys. Rev. Lett.* **78** (1997) 1861–1863, arXiv:hep-ph/9606387.
- [65] M. Kawasaki, M. Yamaguchi, and T. Yanagida, “Natural chaotic inflation in supergravity,” *Phys. Rev. Lett.* **85** (2000) 3572–3575, arXiv:hep-ph/0004243.
- [66] M. Kawasaki, M. Yamaguchi, and T. Yanagida, “Natural chaotic inflation in supergravity and leptogenesis,” *Phys. Rev.* **D63** (2001) 103514, arXiv:hep-ph/0011104.
- [67] N. Kaloper and L. Sorbo, “A Natural Framework for Chaotic Inflation,” *Phys. Rev. Lett.* **102** (2009) 121301, arXiv:0811.1989 [hep-th].
- [68] J. P. Hsu, R. Kallosh, and S. Prokushkin, “On Brane Inflation With Volume Stabilization,” *JCAP* **0312** (2003) 009, arXiv:hep-th/0311077.
- [69] P. Brax and J. Martin, “Shift symmetry and inflation in supergravity,” *Phys. Rev.* **D72** (2005) 023518, arXiv:hep-th/0504168.
- [70] S. C. Davis and M. Postma, “SUGRA chaotic inflation and moduli stabilisation,” *JCAP* **0803** (2008) 015, arXiv:0801.4696 [hep-ph].
- [71] M. Yamaguchi, “Natural double inflation in supergravity,” *Phys. Rev.* **D64** (2001) 063502, arXiv:hep-ph/0103045.
- [72] S. Yokoyama, T. Suyama, and T. Tanaka, “Primordial Non-Gaussianity in Multi-Scalar Slow-Roll Inflation,” *JCAP* **0707** (2007) 013, arXiv:0705.3178 [astro-ph].
- [73] J. J. Blanco-Pillado *et al.*, “Inflating in a better racetrack,” *JHEP* **09** (2006) 002, arXiv:hep-th/0603129.
- [74] T. Chiba and M. Yamaguchi, “Extended Slow-Roll Conditions and Rapid-Roll Conditions,” *JCAP* **0810** (2008) 021, arXiv:0807.4965 [astro-ph].
- [75] T. Chiba and M. Yamaguchi, “Extended Slow-Roll Conditions and Primordial Fluctuations: Multiple Scalar Fields and Generalized Gravity,” *JCAP* **0901** (2009) 019, arXiv:0810.5387 [astro-ph].
- [76] S. C. C. Ng, N. J. Nunes, and F. Rosati, “Applications of scalar attractor solutions to cosmology,” *Phys. Rev.* **D64** (2001) 083510, arXiv:astro-ph/0107321.

- [77] E. J. Copeland, A. R. Liddle, and D. Wands, “Exponential potentials and cosmological scaling solutions,” *Phys. Rev.* **D57** (1998) 4686–4690, arXiv:gr-qc/9711068.
- [78] T. Barreiro, B. de Carlos, and N. J. Nunes, “Moduli evolution in heterotic scenarios,” *Phys. Lett.* **B497** (2001) 136–144, arXiv:hep-ph/0010102.
- [79] T. Barreiro, B. de Carlos, E. J. Copeland, and N. J. Nunes, “Moduli evolution in the presence of thermal corrections,” *Phys. Rev.* **D78** (2008) 063502, arXiv:0712.2394 [hep-ph].
- [80] T. Barreiro, B. de Carlos, and E. J. Copeland, “Stabilizing the Dilaton in Superstring Cosmology,” *Phys. Rev.* **D58** (1998) 083513, arXiv:hep-th/9805005.
- [81] E. J. Copeland, M. R. Garousi, M. Sami, and S. Tsujikawa, “What is needed of a tachyon if it is to be the dark energy?,” *Phys. Rev.* **D71** (2005) 043003, arXiv:hep-th/0411192.
- [82] E. J. Copeland, A. Mazumdar, and N. J. Nunes, “Generalized assisted inflation,” *Phys. Rev.* **D60** (1999) 083506, arXiv:astro-ph/9904309.
- [83] V. Mukhanov, “Physical foundations of cosmology,”. Cambridge, UK: Univ. Pr. (2005) 421 p.
- [84] J. E. Lidsey, D. Wands, and E. J. Copeland, “Superstring cosmology,” *Phys. Rept.* **337** (2000) 343–492, arXiv:hep-th/9909061.
- [85] F. Quevedo, “Lectures on string/brane cosmology,” *Class. Quant. Grav.* **19** (2002) 5721–5779, arXiv:hep-th/0210292.
- [86] A. Linde, “Inflation and string cosmology,” *ECONF C040802* (2004) L024, arXiv:hep-th/0503195.
- [87] J. M. Cline, “String cosmology,” arXiv:hep-th/0612129.
- [88] R. Kallosh, “On Inflation in String Theory,” *Lect. Notes Phys.* **738** (2008) 119–156, arXiv:hep-th/0702059.
- [89] C. P. Burgess, “Lectures on Cosmic Inflation and its Potential Stringy Realizations,” *PoS P2GC* (2006) 008, arXiv:0708.2865 [hep-th].
- [90] L. McAllister and E. Silverstein, “String Cosmology: A Review,” *Gen. Rel. Grav.* **40** (2008) 565–605, arXiv:0710.2951 [hep-th].
- [91] S. Kachru *et al.*, “Towards inflation in string theory,” *JCAP* **0310** (2003) 013, arXiv:hep-th/0308055.
- [92] C. P. Burgess, J. M. Cline, H. Stoica, and F. Quevedo, “Inflation in realistic D-brane models,” *JHEP* **09** (2004) 033, arXiv:hep-th/0403119.
- [93] E. Silverstein and D. Tong, “Scalar Speed Limits and Cosmology: Acceleration from D-cceleration,” *Phys. Rev.* **D70** (2004) 103505, arXiv:hep-th/0310221.

- [94] M. Alishahiha, E. Silverstein, and D. Tong, “DBI in the sky,” *Phys. Rev.* **D70** (2004) 123505, arXiv:hep-th/0404084.
- [95] X. Chen, “Inflation from warped space,” *JHEP* **08** (2005) 045, arXiv:hep-th/0501184.
- [96] D. Baumann, A. Dymarsky, I. R. Klebanov, L. McAllister, and P. J. Steinhardt, “A Delicate Universe,” *Phys. Rev. Lett.* **99** (2007) 141601, arXiv:0705.3837 [hep-th].
- [97] D. Baumann, A. Dymarsky, I. R. Klebanov, and L. McAllister, “Towards an Explicit Model of D-brane Inflation,” *JCAP* **0801** (2008) 024, arXiv:0706.0360 [hep-th].
- [98] D. Baumann, A. Dymarsky, S. Kachru, I. R. Klebanov, and L. McAllister, “Holographic Systematics of D-brane Inflation,” *JHEP* **03** (2009) 093, arXiv:0808.2811 [hep-th].
- [99] J. J. Blanco-Pillado *et al.*, “Racetrack inflation,” *JHEP* **11** (2004) 063, arXiv:hep-th/0406230.
- [100] M. Cicoli, C. P. Burgess, and F. Quevedo, “Fibre Inflation: Observable Gravity Waves from IIB String Compactifications,” *JCAP* **0903** (2009) 013, arXiv:0808.0691 [hep-th].
- [101] C. P. Burgess, R. Kallosh, and F. Quevedo, “de Sitter String Vacua from Supersymmetric D-terms,” *JHEP* **10** (2003) 056, arXiv:hep-th/0309187.
- [102] R. Holman and J. A. Hutasoit, “Systematics of moduli stabilization, inflationary dynamics and power spectrum,” *JHEP* **08** (2006) 053, arXiv:hep-th/0606089.
- [103] Z. Lalak, G. G. Ross, and S. Sarkar, “Racetrack inflation and assisted moduli stabilisation,” *Nucl. Phys.* **B766** (2007) 1–20, arXiv:hep-th/0503178.
- [104] B. de Carlos, J. A. Casas, A. Guarino, J. M. Moreno, and O. Seto, “Inflation in uplifted supergravities,” *JCAP* **0705** (2007) 002, arXiv:hep-th/0702103.
- [105] T. W. Grimm, “Axion Inflation in Type II String Theory,” *Phys. Rev.* **D77** (2008) 126007, arXiv:0710.3883 [hep-th].
- [106] A. Linde and A. Westphal, “Accidental Inflation in String Theory,” *JCAP* **0803** (2008) 005, arXiv:0712.1610 [hep-th].
- [107] J. P. Conlon, R. Kallosh, A. Linde, and F. Quevedo, “Volume Modulus Inflation and the Gravitino Mass Problem,” *JCAP* **0809** (2008) 011, arXiv:0806.0809 [hep-th].
- [108] S. Dimopoulos, S. Kachru, J. McGreevy, and J. G. Wacker, “N-flation,” *JCAP* **0808** (2008) 003, arXiv:hep-th/0507205.

- [109] R. Kallosh, N. Sivanandam, and M. Soroush, “Axion Inflation and Gravity Waves in String Theory,” *Phys. Rev.* **D77** (2008) 043501, arXiv:0710.3429 [hep-th].
- [110] V. Balasubramanian, P. Berglund, R. Jimenez, J. Simon, and L. Verde, “Topology from Cosmology,” *JHEP* **06** (2008) 025, arXiv:0712.1815 [hep-th].
- [111] H.-X. Yang and H.-L. Ma, “Two-field Kähler moduli inflation on large volume moduli stabilization,” *JCAP* **0808** (2008) 024, arXiv:0804.3653 [hep-th].
- [112] A. Misra and P. Shukla, “Large Volume Axionic Swiss-Cheese Inflation,” *Nucl. Phys.* **B800** (2008) 384–400, arXiv:0712.1260 [hep-th].
- [113] P. Binetruy and M. K. Gaillard, “Candidates for the Inflaton Field in Superstring Models,” *Phys. Rev.* **D34** (1986) 3069–3083.
- [114] T. Banks, M. Berkooz, S. H. Shenker, G. W. Moore, and P. J. Steinhardt, “Modular cosmology,” *Phys. Rev.* **D52** (1995) 3548–3562, arXiv:hep-th/9503114.
- [115] K. Kadota and E. D. Stewart, “Successful modular cosmology,” *JHEP* **07** (2003) 013, arXiv:hep-ph/0304127.
- [116] E. J. Copeland, A. R. Liddle, D. H. Lyth, E. D. Stewart, and D. Wands, “False vacuum inflation with Einstein gravity,” *Phys. Rev.* **D49** (1994) 6410–6433, arXiv:astro-ph/9401011.
- [117] N. Arkani-Hamed, S. Dimopoulos, and G. R. Dvali, “The hierarchy problem and new dimensions at a millimeter,” *Phys. Lett.* **B429** (1998) 263–272, arXiv:hep-ph/9803315.
- [118] K. Becker, M. Becker, M. Haack, and J. Louis, “Supersymmetry breaking and alpha'-corrections to flux induced potentials,” *JHEP* **06** (2002) 060, arXiv:hep-th/0204254.
- [119] V. Balasubramanian and P. Berglund, “Stringy corrections to Kahler potentials, SUSY breaking, and the cosmological constant problem,” *JHEP* **11** (2004) 085, arXiv:hep-th/0408054.
- [120] M. Gomez-Reino and C. A. Scrucca, “Locally stable non-supersymmetric Minkowski vacua in supergravity,” *JHEP* **05** (2006) 015, arXiv:hep-th/0602246.
- [121] M. Badziak and M. Olechowski, “Volume modulus inflection point inflation and the gravitino mass problem,” *JCAP* **0902** (2009) 010, arXiv:0810.4251 [hep-th].
- [122] M. Badziak and M. Olechowski, “Volume modulus inflation and a low scale of SUSY breaking,” *JCAP* **0807** (2008) 021, arXiv:0802.1014 [hep-th].

- [123] L. Covi *et al.*, “Constraints on modular inflation in supergravity and string theory,” *JHEP* **08** (2008) 055, arXiv:0805.3290 [hep-th].
- [124] L. Covi *et al.*, “de Sitter vacua in no-scale supergravities and Calabi-Yau string models,” *JHEP* **06** (2008) 057, arXiv:0804.1073 [hep-th].
- [125] R. B. Barreiro, “An overview of the current status of CMB observations,” arXiv:0906.0956 [astro-ph.CO].
- [126] A. Challinor and H. Peiris, “Lecture notes on the physics of cosmic microwave background anisotropies,” *AIP Conf. Proc.* **1132** (2009) 86–140, arXiv:0903.5158 [astro-ph.CO].
- [127] J. P. Conlon, S. S. Abdussalam, F. Quevedo, and K. Suruliz, “Soft SUSY breaking terms for chiral matter in IIB string compactifications,” *JHEP* **01** (2007) 032, arXiv:hep-th/0610129.
- [128] J. P. Conlon, “Sparticle spectra from large-volume string compactifications,” *AIP Conf. Proc.* **957** (2007) 201–204.
- [129] D. Langlois, “Brane cosmology: An introduction,” *Prog. Theor. Phys. Suppl.* **148** (2003) 181–212, arXiv:hep-th/0209261.
- [130] J. F. Grivaz, “Status of SUSY searches,” *Czech. J. Phys.* **55** (2005) B173–B184, arXiv:hep-ex/0411002.
- [131] CDF Collaboration, D. Bortoletto, “Searching for SUSY at the Tevatron,” arXiv:hep-ex/0412013.
- [132] Wolfram Research, Inc, “Mathematica Version 6.0,” *Champaign, Illinois* (2007), <http://www.wolfram.com/products/mathematica/>.
- [133] The Mathworks, Inc, “Matlab,” <http://www.mathworks.com/products/matlab/>.
- [134] “Numerical Recipes, Chapter 16 - Integration of ordinary differential equations,” % tt <http://www.fizyka.umk.pl/nrbook/bookcpdf.html>.
- [135] A. Golovnev, V. Mukhanov, and V. Vanchurin, “Vector Inflation,” *JCAP* **0806** (2008) 009, arXiv:0802.2068 [astro-ph].
- [136] C. G. Boehmer, “Dark spinor inflation – theory primer and dynamics,” *Phys. Rev.* **D77** (2008) 123535, arXiv:0804.0616 [astro-ph].
- [137] G. de Berredo-Peixoto and E. A. de Freitas, “On the torsion effects of a relativistic spin fluid in early cosmology,” *Class. Quant. Grav.* **26** (2009) 175015, arXiv:0902.4025 [gr-qc].
- [138] M. Grana, R. Minasian, M. Petrini, and A. Tomasiello, “Supersymmetric backgrounds from generalized Calabi-Yau manifolds,” *JHEP* **08** (2004) 046, arXiv:hep-th/0406137.
- [139] K. Behrndt, M. Cvetič, and P. Gao, “General type IIB fluxes with SU(3) structures,” *Nucl. Phys.* **B721** (2005) 287–308, arXiv:hep-th/0502154.